P-06-212

Forsmark site investigation

The character and kinematics of deformation zones (ductile shear zones, fault zones and fracture zones) at Forsmark – report from phase 1

Øystein Nordgulen, Aline Saintot
Geological Survey of Norway

December 2006

Svensk Kärnbränslehantering AB
Swedish Nuclear Fuel
and Waste Management Co
Box 5864
SE-102 40 Stockholm Sweden
Tel 08-459 84 00
+46 8 459 84 00
Fax 08-661 57 19
+46 8 661 57 19

ISSN 1651-4416
SKB P-06-212

Forsmark site investigation

The character and kinematics of deformation zones (ductile shear zones, fault zones and fracture zones) at Forsmark – report from phase 1

Øystein Nordgulen, Aline Saintot
Geological Survey of Norway

December 2006

Keywords: Forsmark, AP PF 400-05-088, Structural geology, Deformation zone, Shear zone, Fault zone, Fracture zone, Mylonite, Cataclasite, Fault breccia, Kinematics.

Abstract

A study of predominantly brittle structures, i.e. faults and fractures, has been undertaken at Forsmark. The main aim of the work was to document and characterize the geometry and kinematics of the brittle deformation history of the area. Faults and fractures were also investigated in order to improve our understanding of the deformation mechanisms that controlled the local brittle structural history.

Structural data were obtained from outcrops along the Eckardfjärden deformation zone (EDZ), from three other localities close to the power plant at Forsmark, and from selected, previously defined deformation zones of drill cores from 12 boreholes. Polished thin sections from samples collected both in the field and from the drill cores were studied using standard petrographic techniques, and in some cases also SEM (backscatter). Observations from thin sections combined with data from the field and from drill cores form the basis for the conclusions of this study.

The investigated structures include low-grade ductile shear zones, several generations of cataclasite, and some breccias cemented by diagenetic minerals. In most localities and drill cores, there are abundant joints and fracture sets, commonly with minor offset. These are in most cases coated or filled with a range of different minerals reflecting the conditions during successive brittle events. The minerals coating the fault planes exhibit striations and slickensides that were observed on numerous fault planes. Such data were obtained from outcrops and, to a variable extent, from the deformation zones in the drill cores. In total, a considerable amount of new data has been acquired that pertain to the understanding of the structural evolution of faults and fractures on a local and regional scale.

Combining comprehensive data from surface outcrops with observations from deformation zones in drill cores provides valuable input to a kinematic study of the Forsmark site. The studies of drill cores show that the amount and quality of acquired kinematic structural data are quite variable. However, in many cases excellent data were obtained, and in general this manner of obtaining data adds substantially to the value of structural information that can be effectively retrieved from the drill cores.

Sammanfattning

En undersøkelse av i hovedsak sprø strukturer, dvs. forkastninger og sprekker, er gjennomført i Forsmark. Det viktigste målet med undersøkelsen var å dokumentere og karakterisere geometri og kinematikk relatert til sprø deforamsjonshistorien i området. Forkastninger og sprekker ble også undersøkt for å øke forståelsen av hvilke deformasjonsmekanismer som kontrollerte den lokale strukturelle utviklingen.

Strukturdata ble samlet inn på blotninger langs Eckardfjärden deformation zone (EDZ), og fra tre andre lokaliteter nær kraftverket ved Forsmark, samt fra utvalgte, tidligere definerte deformasjonssoner i kjerner fra 12 borehull. Polerte tynnslip fra prøver samlet inn i felt og fra borekjerner ble studert ved hjelp av standard petrografiske teknikker, og i noen tilfeller ved bruk av SEM (backscatter). Observasjoner fra tynnslip sammen med data fra felt og fra borekjerner danner basis for konklusjonene i dette arbeidet.

De undersøkte strukturene omfatter lavgrads duktile skjærsoner, flere generasjoner med kataklasitt, og breksjer som er sementert av diagenetiske mineraler. De fleste lokaliteter og borehull har flere sprekkesett, vanligvis med mindre sprang. Sprekkene er i de fleste tilfeller dekorert eller fylt med ulike mineraler som reflekterer forholdene under flere deformasjonshendelser. Mineralene på forkastningsflatene har i mange tilfeller slickensides. Slike data kommer fra blotninger på overflaten, og i varierende grad fra deformasjonssoner i borehull. Til sammen ble det samlet inn en betydelig mengde nye data som vil ha betydning for forståelsen av den strukturelle utviklingen av forkastninger og sprekker på lokal og regional skala.

Data fra overflaten kan sammen med observasjoner fra borehull gi et viktig bidrag til et studium av den kinematiske utviklingen av strukturene i Forsmark. De undersøkte borekjernene viser betydelig variasjon i mengden og kvaliteten på kinematiske strukturdata. I mange tilfeller ble likevel svært gode datasett innsamlet, og generelt er denne teknikken en effektiv måte å øke verdien av strukturgeologisk informasjon som kan innhentes fra borekjerner.

Contents

1 Introduction

This document reports the results of a study of the character and kinematics of a number of deformation zones at the Forsmark site. This study forms one of the activities performed within the site investigation work at Forsmark (Figure 1-1). The work was carried out in accordance with activity plan AP PF 400-05-088. Controlling documents for performing this activity are listed in Table 1-1. Both activity plan and method descriptions are SKB's internal controlling documents.

Original data from the reported activity are stored in the primary database Sicada, where they are traceable by the Activity Plan number (AP PF 400-05-088). Only data in SKB's databases are accepted for further interpretation and modelling. The data presented in this report are regarded as copies of the original data.Data in the databases may be revised, if needed. Such revisions will not necessarily result in a revision of the P-report, although the normal procedure is that major data revisions entail a revision of the P-report. Minor data revisions are normally presented as supplements, available at www.skb.se.

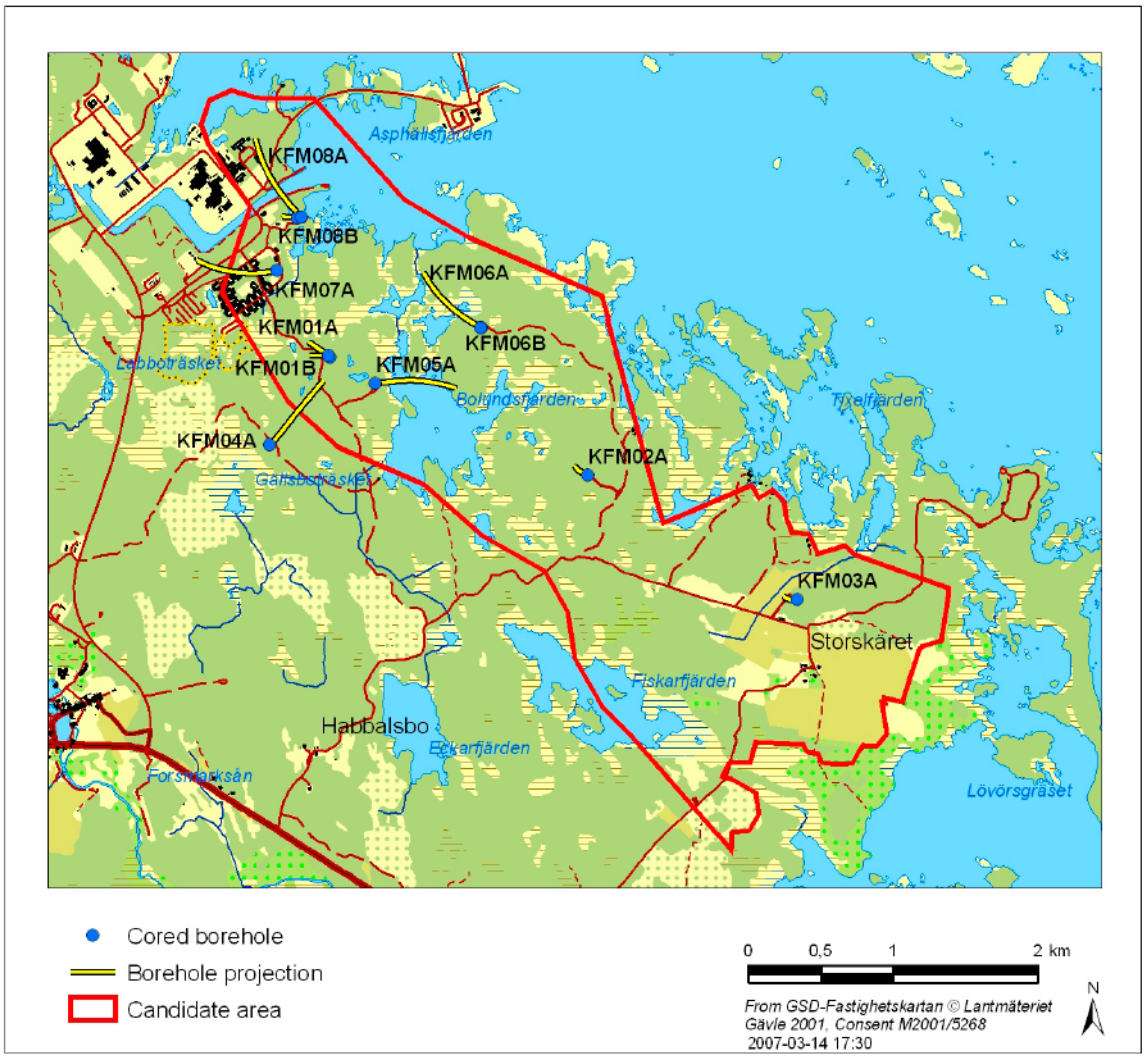

Figure 1-1. *General overview of the Forsmark site investigation area.*

Table 1-1. Controlling documents for the performance of the activity.

Activity plan	Number	Version
Karaktärisering av spröda deformationszoner steg 1	AP PF 400-05-088	1.0
Method descriptions	**Number**	**Version**
/Braathen 1999/	Tectonophysics 302, 99–121.	
/Braathen et al. 2002/	Norwegian Journal of Geology, 82, 225–241.	
/Braathen et al. 2004/	Tectonics, 23, TC4010, doi:10.1029/2003TC001558.	
/Nordgulen et al. 2002/	Norwegian Journal of Geology, 82, 299–316.	
/Osmundsen et al. 2003/	Journal of the Geological Society, London 160, 1–14.	
/Petit 1987/	Journal of Structural Geology 9, 597–608.	
Metodbeskrivning för geologisk enhålstolkning	SKB MD 810.003	3.0

2 Objective and scope

The aim of this study was to describe and document the characteristic properties, including the kinematics, of deformation zones in boreholes, as well as along the Eckarfjärden deformation zone (EDZ) and some other localities on the surface. Fault rocks were investigated in order to improve our understanding of the deformation mechanisms that controlled the local brittle structural history. Observations from thin sections combined with data from the field and from drill cores form the basis for the conclusions of the study. The work was carried out in the context of stage 2 of the single hole interpretation works as described in the method description for this activity.

The fieldwork mainly involved detailed structural studies of several localities along a section of the Eckarfjärden deformation zone (EDZ), which is a major NW-SE-oriented ductile shear and fault zone with a clear geophysical signature /SKB 2004, 2005/. This work expands on the preliminary work carried out in the pilot project in 2005 /Nordgulen and Braathen 2005/. Similar studies were carried out along a NW-SE-oriented fault strand that is parallel to the EDZ. This fault crops out along Linjevägen and Turbinvägen near power plant 3. Further fieldwork was undertaken along a trench that had been dug in the ca. 2 m deep moraine near the location of drill site 7. Finally, outcrops in an open pit prepared for a thermal conductivity experiment were also studied.

A total of 40 deformation zones (see chapter 4.1) from 12 boreholes (KFM01A, KFM01B, KFM02A, KFM03A, KFM03B, KFM04A, KFM05A, KFM06A, KFM06B, KFM07A, KFM08A and KFM08B) were studied with the aim of providing a brief description of the nature of each deformation zone, and to examine faults and fractures searching for features that potentially would have significance for the understanding of the kinematic history of the faults. The deformation zones were selected by SKB based on stage 1 of the single-hole interpretation of individual boreholes. Most zones that were assigned the highest level of confidence (level 3) are included in the study. The boreholes and deformation zones that were inspected are listed in Table 5-1.

3 Equipment

3.1 Description of equipment

During field work and core inspection, the standard equipment for structural investigations was used, including hammer, compass, hand lens, diluted HCl, digital camera, and GPS (Garmin eTrex) for locating observation points according to SKB standards (Swedish Grid). Samples collected in the field and from drill cores were cut in the core laboratory, and selected chips were correctly marked (felt pen) and sent for preparation of polished thin sections. The thin sections were petrographically analysed and some selected sections were analysed using SEM in backscatter mode.

4 Execution

4.1 Nomenclature

Faults occur on all scales in the lithosphere. They control the spatial arrangement of rock units, affect the topography, control the permeability of rocks and sediments and, more importantly, create deformation (strain, plus rotation plus translation) during plate interaction and intraplate movements. The term fault zone is generally used for brittle structures in which loss of continuity and slip occurs on several discrete faults within a band of definable width. Shear zones, on the other hand, are ductile structures, across which a rock body does not lose continuity so that strain is progressively distributed across a band of definable width. Based on this definition, a fault zone or shear zone is a volume of rock where strain is highly localized.

The term Deformation zone (DZ) is generally used by SKB during single-hole interpretation of boreholes. A deformation zone is a general term referring to an essentially 2D structure, along which there is a concentration of brittle, ductile or combined brittle and ductile deformation. The term fracture zone is used to denote a brittle deformation zone without any specification whether there has or has not been a shear sense of movement along the zone. A fracture zone that shows a shear sense of movement is referred to as a fault zone.

Commonly fault zones can be divided into a series of distinctive constituent elements. These are 1) the *undeformed host rock*, 2) the *transition zone* /Munier et al. 2003/ (corresponding to the "damage zone" of /Gudmundsson et al. 2001/) and 3) the proper *fault core* /e.g. Caine et al. 1996, Evans et al. 1997, Braathen and Gabrielsen 2000/. The host rock consists of undisturbed rock with low fracture frequency of < 4 fractures/m /Munier et al. 2003/ (Figure 4-1). The transition zone still contains undeformed rock, but the fracture frequency generally increases up to 9 fractures/m (Figure 4-1). Narrow zones or bands of fault rock may occur, especially closer to the transition to the fault core. The width of the transition zone varies with the size of the fault zone and the style of deformation, and can range from a few meters to tens of meters. The fault core is identified by the occurrence of fault rock or intensively fractured rock (Figure 4-1, Figure 4-2). Fault rocks may occur in lenses alternating with pods of relatively undeformed rock /Caine et al. 1996, Braathen and Gabrielsen 2000/. The width of the fault core may vary from cm to m /Braathen and Gabrielsen 2000/.

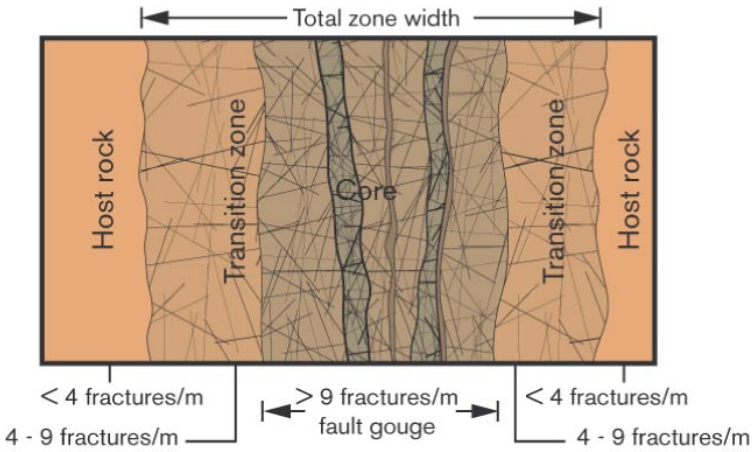

Figure 4-1. *Schematic illustration of a brittle deformation zone according to SKB definition /after Munier et al. 2003/*

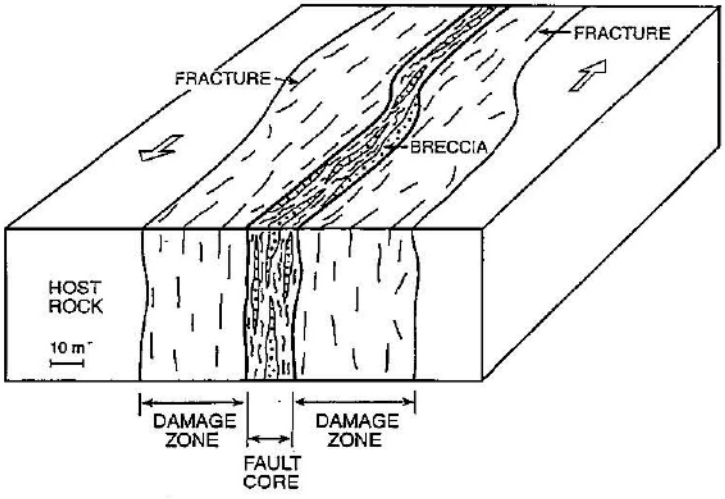

Figure 4-2. *Schematic illustration of the architecture of an idealized fault zone /Gudmundsson et al. 2001/. Note that the term "damage zone" corresponds conceptually to the term "transition zone" of Figure 4-1.*

Rocks that occur within fault zones provide primary evidence for the processes that occur there. It is therefore of great importance to characterize fault rock occurrences so as to better understand faulting processes at all scales. Fault rocks form in response to strain localization within fault and shear zones and reflect the interplay of a variety of physical and environmental parameters such as the finite amount of strain, lithology, style of deformation (i.e. frictional or plastic flow), presence or absence of fluids, strain rate, temperature, pressure and so on. Figure 4-3 shows the classification scheme suggested by /Braathen et al. 2004/ that we will use in this study to classify fault rock occurrences.

Brittle ← *Deformation style* → **Ductile**										
Frictional flow ← *Dominant deformation mechanism* → **Plastic flow**										
Non-cohesive			Secondary cohesion		Primary cohesion					
			Cemented HB	Indurated HB			*> 50% phyllosilicate*	*< 50% phyllosilicate*		*% matrix and grain-size*
Hydraulic breccia (HB)	Breccia series	Proto-breccia	Cemented proto-breccia	Indurated proto-breccia	Cataclasite series	Proto-cataclasite	Proto-phyllonite	Proto-mylonite	Blastomylonite	*0-50% matrix*
		Breccia	Cemented breccia	Indurated breccia		Cataclasite	Phyllonite	Mylonite		*50-90% matrix*
		Ultra-breccia	Cemented ultra-breccia	Indurated ultra-breccia		Ultra-cataclasite	Ultra-phyllonite	Ultra-mylonite		*90-100% matrix*
		Gouge	Cemented gouge	Indurated gouge						*Sub-microscopic matrix*
			Pseudotachylyte							

Figure 4-3. *Fault rock classification scheme proposed by /Braathen et al. 2004/. A brief explanation of some of the terms is given in Table 4-1.*

Table 4-1. Schematic description of different types of fault rocks classified according to /Braathen et al. 2004/.

Term	Description	Note
Fault rocks or fault-related rocks	Commonly formed through strain concentration within a tabular or planar zone that experiences shear stress.	1
Frictional flow	Pressure, subordinate temperature and fluid controlled deformation mechanisms which have a brittle style: granulation of grains by inter, intra and transgranular micro fracturing, and intra or intergranular frictional sliding with abrasion of fracture walls and grain margins	2
Plastic flow	Mainly thermally activated, continuous deformation without rupture, with a ductile style of deformation: dislocation creep and glide, solid state diffusion creep, diffusional mass transfer, and viscous grain boundary sliding	
Non-cohesive	Not consolidated	3
Secondary cohesion	Consolidated after formation, either through cementation of the matrix, or through compaction, recrystallisation or neo-mineralisation (see indurated)	
Primary cohesion	Cohesion preserved during formation	3
Hydraulic fracturing	Fracturing caused by fluid pressure: commonly random orientation of fractures and rough fracture surfaces. The resulting hydraulic breccia may not be tabular or planar, however, it is tectonically induced and frequently fault-related.	4
Cemented	Consolidated through mineral precipitation in pores of the matrix	
Indurated	Consolidated basically by compaction due to directed pressure, annealing by recrystallisation of grains, or neomineralisation (e.g., muscovitisation, silicification, albitisation, epidotisation, saussuritisation). The term disregards cementation unless related to general neomineralisation	
Phyllosilicate content	Content of sheet-minerals (characterised by weak '001' bonds) of the phyllosilicate group	5
Matrix	Fine-grained material in a fault rock formed by granulation or dynamic recrystallisation of grains, filling the interstices between larger clasts of original rock	
Breccia	Mainly chaotic, non-cohesive fault rock, generated by frictional flow	3
Cataclasite	Mainly chaotic fault rock that developed with cohesion, which is generated by mainly frictional flow	6
Phyllonite	Phyllosilicate-rich fault rock with distinct mineral fabric, and dominated plastic flow	7
Mylonite	Fault rock with distinct mineral fabric, and dominated by plastic flow	8
Blasto-mylonite	Fault rock in which dynamic recrystallisation and/or neomineralisation causing grain-size increase of clasts, outpace grain-size reduction	8

1. For classification of fault rocks, see: *Higgins* [1971], *Bell & Etheridge* [1973], *Zeck* [1974], *Sibson* [1977a], *Wise et al.,* [1984], *Schmid & Handy* [1991].
2. Term introduced by *Schmid & Handy* [1991]. See also description of *Bell & Etheridge* [1973].
3. Concept introduced by *Higgins* [1971].
4. For hydraulic breccias, see e.g., *Clark & James* [2003]
5. Clay content as factor in classification of faults rocks in sedimentary units, e.g., *Fisher & Knipe* [1998].
6. Possible application of phyllosilicate content in the sub-division of fault rocks in sedimentary rocks, e.g., *Fisher & Knipe* [1998].
7. Definitions following *Knopf* [1931], however, adding a limit to the phyllosilicate content.
8. See definitions of *Sibson* [1977a].

This study deals not only with faults, but also with brittle structures in general. It is therefore appropriate that the terminology that is used is clarified.

Fractures are all planar brittle structures.

Joints are extensional fractures (with the minimum stress axis perpendicular to the surface) along which no displacement can be observed with unaided eyes. The term is unfortunately not well constrained and the above definition is according to /Twiss and Moores 1992/: 'Most outcrops of rocks exhibit many fractures that show very small displacement normal to their surfaces and no, or very little, displacement parallel to their surfaces. We called such fractures joints.' The authors also noted at this point: 'Unfortunately, there is no universally accepted definition of the term joint. The definition set down here is conservative in that fractures satisfying this definition would be called joints by every other definition of the term'.

Note that the term '***shear joints***' is also used when two sets of joints are at 60 degrees from each other. It implies that the maximum stress axis is the bisector of the acute angle, the minimum stress axis the bisector of the obtuse angle, and the intermediate stress axis is parallel to the intersection of the joints. Here also, it is stipulated that no displacement can be observed with unaided eyes.

The term '***vein***' is descriptive and used for a body larger than wider in a given host rock. A vein can be rock-filled, like a granitic vein, or mineral-filled, like a calcite vein.

The term ***tension gash*** is genetic and interpretative. The tension gashes are inferred to be extensional fractures with a clear displacement normal to their sides (i.e. the minimum stress axis is roughly perpendicular to their sides, or there is little or no evidence of shearing acting along their sides). They are generally mineral-filled and commonly have mineral fibres that grew parallel to the tension axis. In this study, this term has therefore been used only if mineral fibres have been observed in the fracture, allowing for an estimate of the orientation of the minimum stress axis.

Mineral-filled fracture is a very general term that is used to describe fractures with at least some displacement normal to their sides (allowing mineral growth to take place). Provided that a shear component is documented, this would be a fault coated with minerals. This term is descriptive and non-genetic. It is used to describe a fracture with mineral coating on which the orientation of mineral fibres cannot be observed with the unaided eye, i.e. the orientation of the minimum stress axis remains uncertain. With the aided eye, it may be possible to distinguish between a tension gash (with the minimum stress axis roughly perpendicular and fibres parallel to the minimum stress axis) and a fault (shear fracture, with fibres very oblique to the fractures).

4.2 Working procedure

The project was carried out in conformity with the accepted activity plan AP PF 400-05-088. Field investigations were carried out at Forsmark October 10–12, 2005. Investigation of drill cores was conducted during two periods: November 14–18, 2005 and January 23–27, 2006.

The standard procedure for obtaining the true orientation of linear structures (slickensides, striations, etc.) on fault surfaces in drill cores with known orientation is as follows:

1. Fractures of potential interest were identified by visual inspection of drill cores from selected deformation zones, as defined previously by SKB.
2. Individual fractures were identified on the BIPS image of the borehole wall, which provided a mirror image of the core itself. Care had to be taken to ensure that the fracture selected on the image matched the one from the drill core. In some cases this was challenging, particularly where abundant fractures cut the core at different angles. Independent checks

that the correct fracture was picked could be carried out using data in the drill core database. These included the properties of the fracture itself, the acute angle α between the fracture and the core axis, and the angle β, which is the angle (measured counter-clockwise) from the lower intersection of the fracture with the core wall, to the top of the drill core.

3. Having identified the fracture of interest, the top of the drill core was marked based on visual inspection of the BIPS image and on the angle β. For each fracture, its orientation (strike and dip) was obtained using the information contained in the drill core database.
4. The core was positioned the right way up and at the true inclination using a core holder supplied by SKB. This device allowed the accurate adjustment of the core inclination as given in the database.
5. The orientation of the linear structure was determined by measuring its plunge direction (azimuth) and plunge.
6. When the sense of slip could be determined with confidence, the true movement of the hanging wall with respect to the footwall of the fault was established.
7. Relevant data were recorded in a database.

Samples for thin section preparation were collected both in the field and from the drill cores. A total of 33 polished sections, adding to the 17 sections obtained during the pilot study in 2005, were studied at the Geological Survey of Norway (Trondheim) using standard petrographic techniques, and in some cases also SEM (backscatter).

At the Geological Survey of Norway (NGU) in Trondheim, structural data were analysed and plotted using standard techniques. The thin sections were analysed in several steps:

1) Scanning at high resolution of the entire section using a standard slide scanner.
2) Printing of the scanned jpg-images as A4 colour prints that greatly aid in establishing general relationships and locating critical features for detailed study.
3) Petrographic analysis and documentation of textural and micro-structural relations using a digital camera attached to the microscope (Leitz).
4) Detailed studies of specific mineralogical and textural details using SEM in backscatter mode.

4.3 Analysis and interpretation

The methods employed from fieldwork through structural data analysis and petrographic work are based on those described in /Braathen 1999, Braathen et al. 2002, Nordgulen et al. 2002, Osmundsen et al. 2003/. In this report, definition of fault rocks is according to the classification in /Braathen et al. 2004/. Criteria for identifying the slip-direction on slickenside surfaces is presented in /Petit 1987/.

A systematic analysis of fault slip data at the micro- and meso-scale has been made, aiming towards an improved understanding of the kinematic pattern in the area of interest. It consists of the analysis of strike and dip of fault planes and of azimuth and plunge of their striae. It also provides the basis for paleo-stress inversion calculations that can aim at the reconstruction of the stress field evolution through time. Figure 4-4 provides the key to read stereoplots used throughout this report to represent the orientation and the kinematics of individual fault plane/striation pairs.

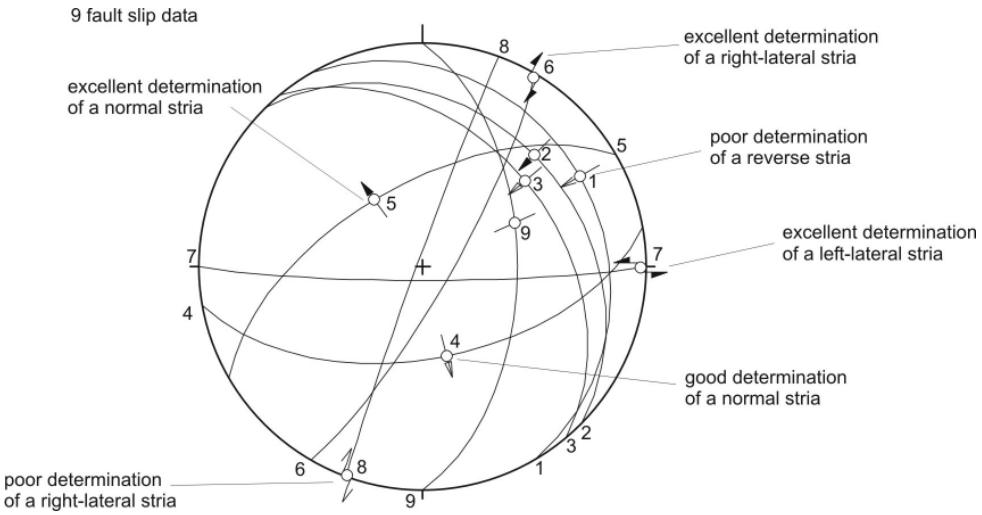

Figure 4-4. *Example of a stereoplot used for plotting kinematic information obtained from striated fault planes, Schmidt's projection, lower hemisphere. Keys for striae: outward directed arrow: normal striae (numbers 4 and 5 on stereoplot); inward directed arrow: reverse striae (numbers 1, 2 and 3); couple of arrows: strike-slip striae (numbers 6, 7 and 8); full black arrow: excellent constraints on the sense of shear (numbers 2, 5, 6 and 7); empty arrow: good constraints on the sense of shear (numbers 3 and 4); simple arrow: poor constraints on the sense of shear (numbers 1 and 8); thin line without any arrowhead: no constraints on the sense of shear (number 9).*

4.4 Data handling and processing

The data obtained in the study are transferred to SKB in a specified format that allows for transfer of the data to the internal database structure at SKB (SICADA).

4.5 Nonconformities

No nonconformities have been noted.

5 Results

5.1 Field investigations

Most of the fieldwork was carried out along the EDZ (10 localities). Three additional localities close to the Forsmark nuclear power plant were also studied. The localities are shown in Figure 5-1, and are listed in Appendix 1. The data are displayed and analysed by site in the following sub-sections, and a summary of the results of this work is also presented.

5.1.1 Eckardfjärden Deformation Zone (EDZ)

The field work mainly involved detailed structural studies of a number of localities along the Eckarfjärden deformation zone (EDZ), which is a major NW-SE-oriented ductile shear and fault zone with a clear geophysical signature /SKB 2004/. This study expands on the preliminary work carried out in the pilot project in 2005 /Nordgulen and Braathen 2005/. The EDZ is a regionally important low-grade mylonite zone that has been repeatedly reactivated in a brittle manner. This has resulted in a complex pattern of brittle deformation commonly observed on large fault zones.

10 localities has been studied along the zone: PFM007086, PFM007087, PFM007088, PFM007089, PFM007090, PFM007091, PFM007092, PFM007093, PFM007094 and PFM007095 (Figure 5-1). In the following these are described. These localities are described in the text which follows.

PFM007086

At site PFM007086, fine-grained, reddish pink metagranite and some amphibolites are present. Planar fractures and faults with epidote (< 2 cm wide) are sub-parallel to the ductile fabric in the rocks. Younger than these are several different fracture sets that in general are oriented at a high angle to the main EDZ trend. Mineralized fractures are filled with epidote, in some cases quartz, and rarely by laumontite. Fault slip data were obtained from four surfaces (Figure 5-2), but the sense of displacement could not be determined. Three steep fault planes trending N-S to NNE-SSW are characterized by striae plunging about 30 degrees southward (Figure 5-2), suggesting conspicuous strike-slip component of displacement. A large fault plane dipping gently to the SSE exhibits dip-slip striae.

The relative displacement along some of the fractures has been identified by the offset of pre-existing structures. An example of this is given on Figure 5-3 showing a clear sinistral component of along a N067 trending fracture.

Observations of numerous cross-cutting relationships have allowed us to determine the relative chronology between some of the mineral-filled fracture sets. A laumontite-filled fracture cuts across a set of NE-SW epidote-filled fractures (stereonet A on Figure 5-4a). NW-SE to NE-SW trending fractures without epidote infill, and sometimes with a pale green mineral infill, cut across two older faults (stereonet B and C on Figure 5-4a). Therefore, the earlier structures at this site include these old fault trends which are the epidote ± chlorite-striated gently SSE-dipping fault plane (see Figure 5-2) and the NW-SE trend of the vertical EDZ fault, but also a set of NE-SW veins filled with epidote. More specifically, the NNE-SSW to NE-SW set of fractures filled with pale green mineral offset, in a dextral way, NW-SE laumontite-filled fractures (stereonet D on Figure 5-4a). Fractures trending ca. ENE-WSW offset earlier structures in a sinistral manner (Figure 5-3 and stereonet D on Figure 5-4a). The NNE-SSW to NE-SW dextral faults and the ENE-WSW sinistral faults probably form a conjugate system of strike-slip faults (Figure 5-4b) that developed under a strike-slip stress regime at a late stage in the deformation history.

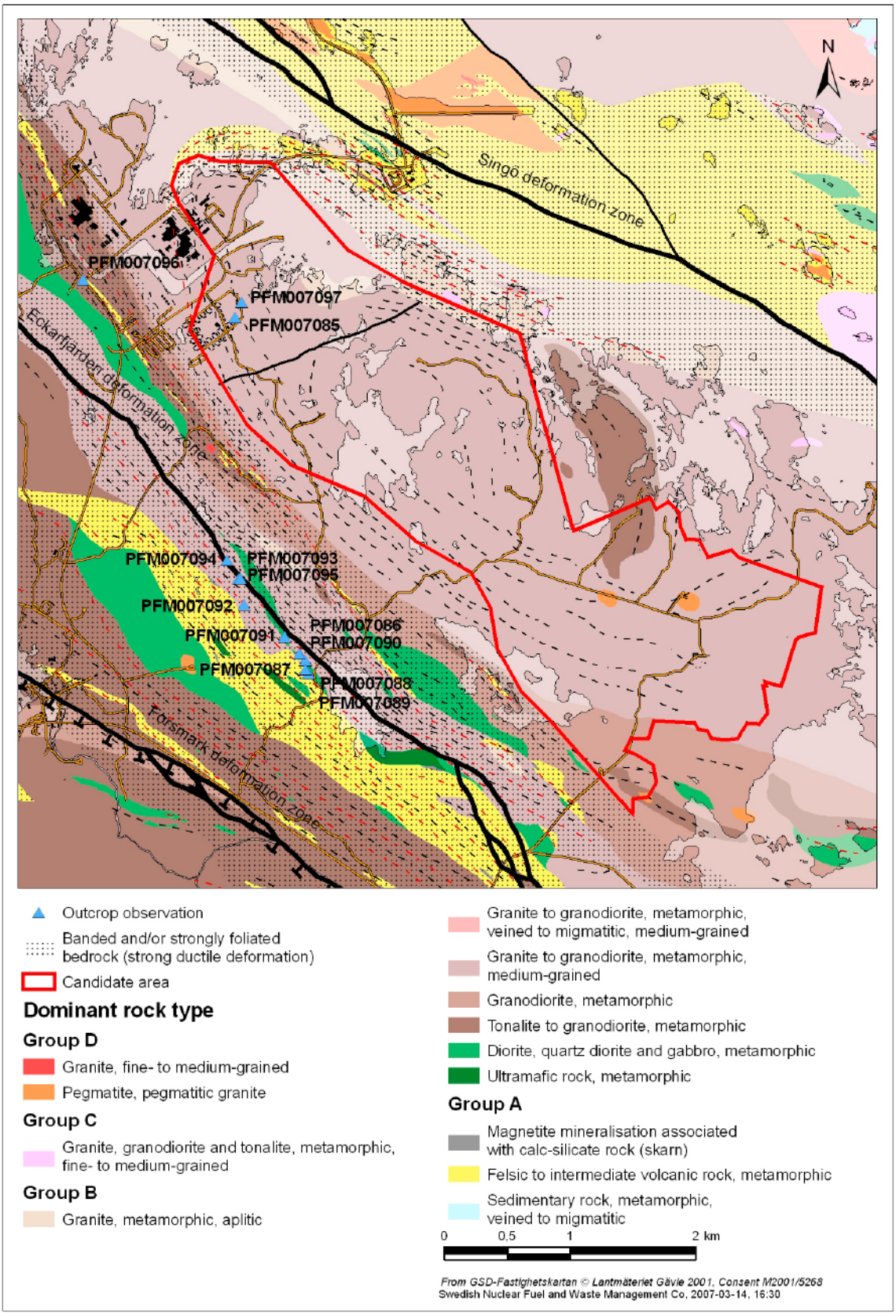

Figure 5-1. *Overview of the Forsmark area showing the locations where fieldwork was conducted in October 2005.*

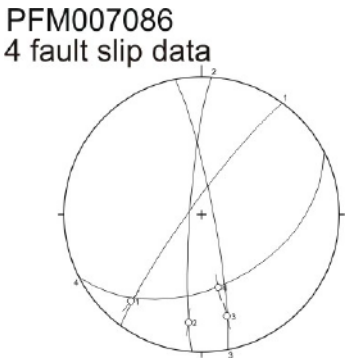

Figure 5-2. *Stereoplot of the 4 fault slip data obtained at site PFM007086.*

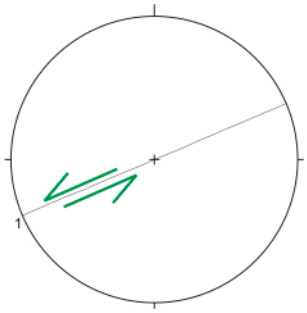

Figure 5-3. *Sinistral component of displacement (shown by arrows) along a N067 trending fracture as determined by the offset of pre-existing ductile fabric (site PFM007086).*

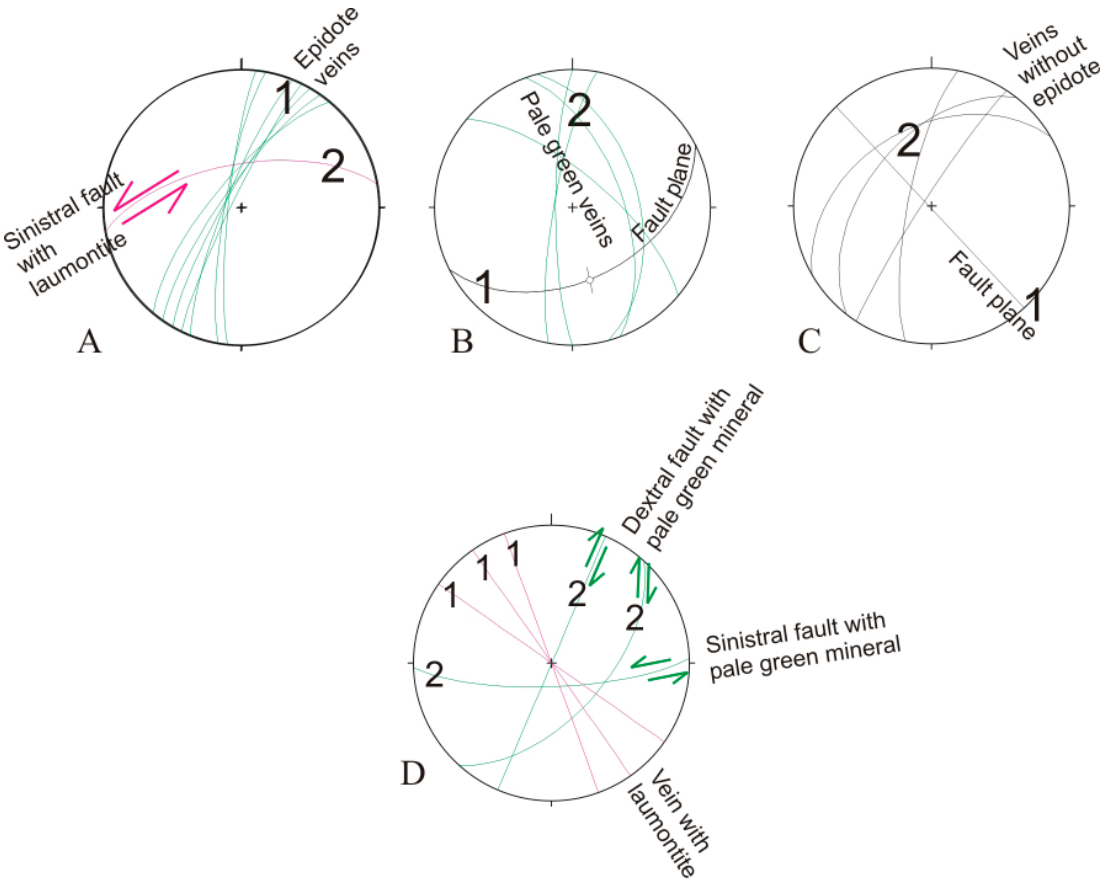

Figure 5-4a. *Examples of relative chronologies between different sets of fractures observed at site PFM007086. (In each case, 1 is the oldest fracture).*

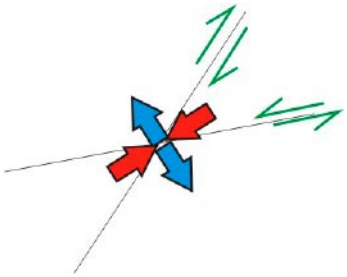

Figure 5-4b. *Young sets of NNE-SSW to NE-SW dextral faults and ENE-WSW sinistral faults as a conjugate system of late strike-slip faults (PFM007086). Couple of blue arrows as inferred extensional trend and couple of red arrows as inferred compressional trend in a strike-slip stress regime.*

PFM007087

At this site the host rock is a coarse-grained, white pegmatite with an epidote-coated fault (115/60) which is cut by a variety of fractures. The orientation of 21 fractures (Figure 5-5) shows that two sets are present: a predominant set of steep NE-SW- to ENE-WSW-trending fractures, and a set of NW-SE steep fractures (parallel to the EDZ) which are filled by white-yellow minerals. No kinematic indicators were observed on the planes. The chronology between the two sets is inconsistent as the ENE-WSW fractures pre-and post-date the NW-SE-trending fractures.

PFM007088

At this site, shear zones and associated fractures developed in a hornblende-bearing, strongly foliated intermediate to mafic meta-igneous rock that occurs at several closely spaced outcrops along the EDZ. Epidote is a common mineral occurring along faults and shear zones, and has been deformed during re-activation of the structures (see below). Reddish alteration has occurred along most shear zones and fractures. A total of 26 fractures and 3 fault slip data have been obtained at the site (Figure 5-6a and b). NW-SE-oriented fractures are steep and quite abundant. NNW-SSE to NNE-SSW, mostly steep fractures, and E-W fractures generally dipping 60 degrees to the south are the two other main sets. On three surfaces of the latter set, strike-slip striae have been identified without giving a sense of shear (Figure 5-6b).

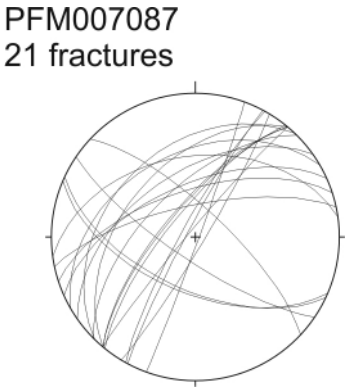

Figure 5-5. *Stereoplot of the 21 fractures observed at site PFM007087.*

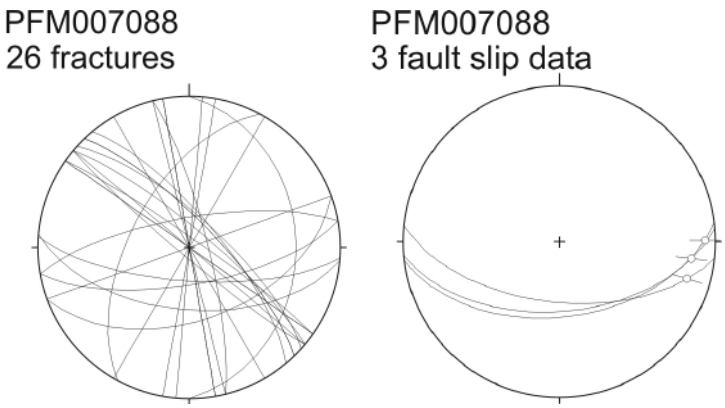

Figure 5-6. *Stereoplots of the 26 fractures (A), and 3 fault slip data (B) obtained at site PFM007088.*

Sinistral offsets of pre-existing fabrics have been observed on outcrops along the N-S to NNW-SSE fractures (Figures 5-7 and 5-8). Also, the development of an echelon tension gashes along a N170 fault zone confirms its sinistral displacement (Figure 5-8 and 5-9a).

The N-S to NNW-SSE faults intersects NW-SE-oriented fractures and faults that also have epidote fill and strong red stain of the wall rock. Relative displacement between the sets could not be determined, however, some dextral displacement has occurred on the NW-SE faults. Together with the sinistral set they may define a conjugate system of strike-slip faults (Figure 5-9b).

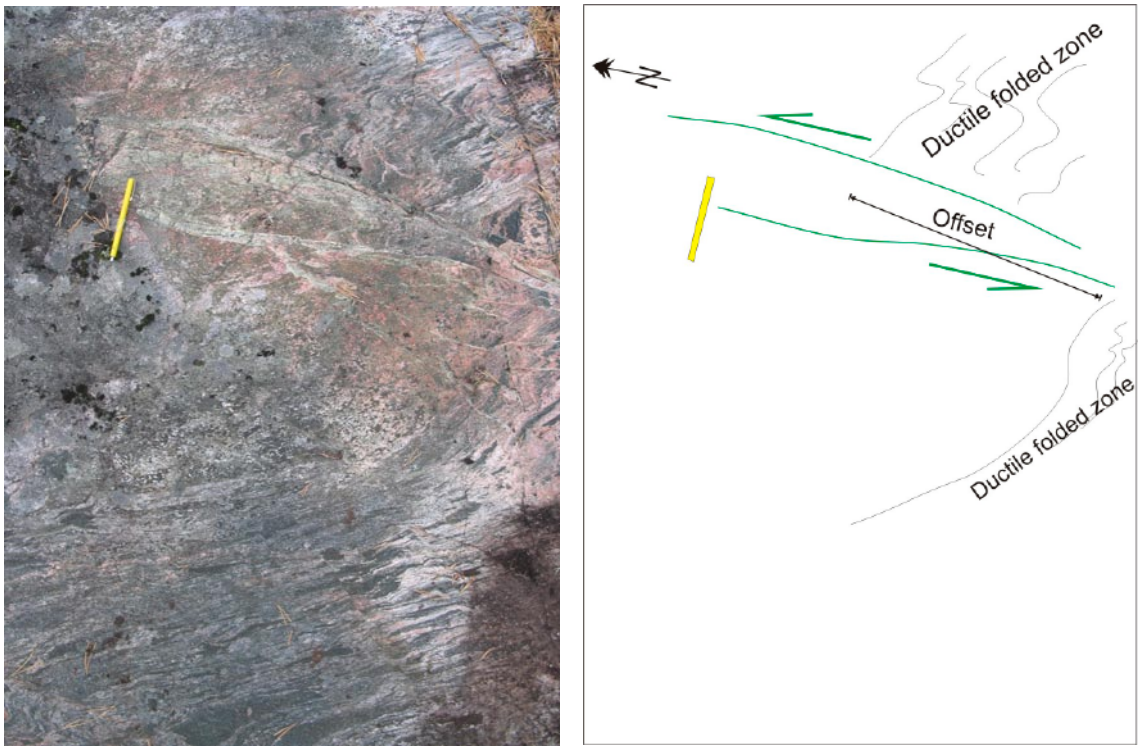

Figure 5-7. *Coarse-grained hornblende-bearing meta-igneous rock with pale lenses of metagranite. The ductile fabric in the rock is folded and subsequently cut by a N-S to NNW-SSE sinistral fault with pale green epidote. Reddish stain of the host rock is indicative of oxidation along the zone affected by brittle deformation. Site PFM007088.*

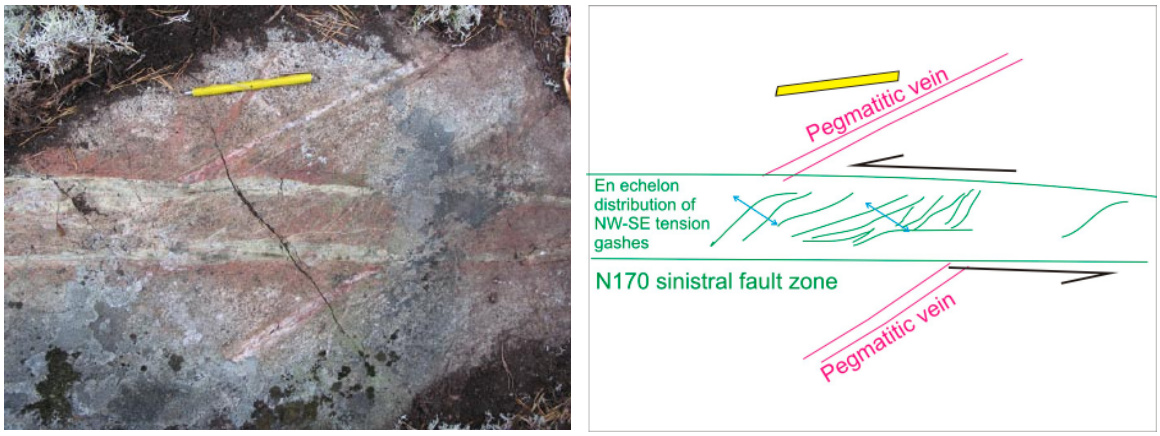

Figure 5-8. *Photograph from outcrop and line-drawing (right) showing epidote-filled faults in reddish metagranite. Sinistral movement along the NNW-SSE fault zone is indicated by (1) sinistral offset of a feldspar-rich pegmatitic vein and (2) en echelon distribution of NW-SE tension gashes within the fault zone (extension direction indicated by the blue arrows). PFM007088.*

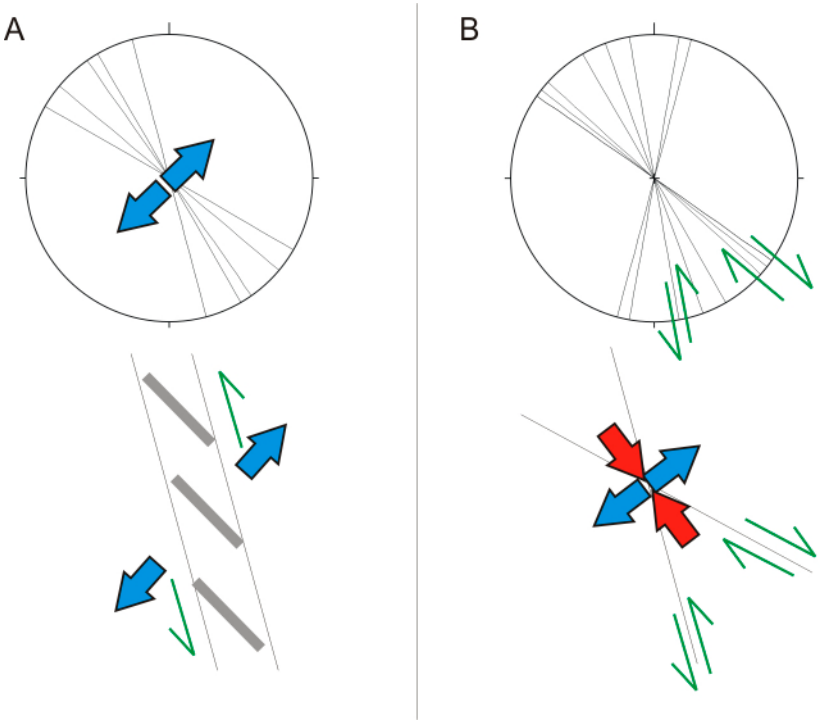

Figure 5-9. *A) Stereoplot of five en echelon tension gashes into a NNW-SSE sinistral fault zone. B) Stereoplot of N-S to NW-SE fractures showing dextral or sinistral components of displacement that are consistent with a conjugate system of strike-slip faults (couple of blue arrows: extension; couple of red arrows: compression). PFM007088.*

A sample for thin section analysis was collected to investigate the mineralogy and texture of the fault rocks. A scanned image of the section (Figure 5-10) shows a sequence of development starting with the development of cataclasites in an amphibole-rich host rock. Early formed angular fragments of fine-grained cataclasites that contain plagioclase, amphibole, epidote and clinozoisite are embedded in a very fine-grained cataclasite developed at a later stage. The cataclasites are cut by thin veinlets of quartz and brownish epidote + laumontite that formed during subsequent events.

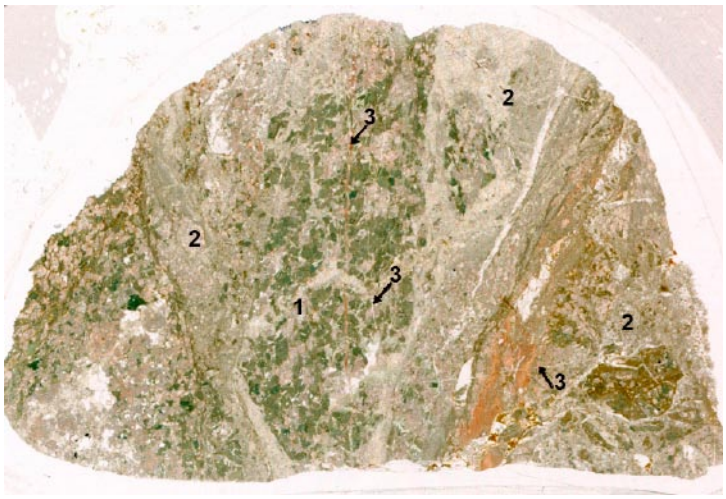

Figure 5-10. *Scanned thin section (sample PFM007088) showing a multi-generation cataclasite developed in amphibolite (1). A variety of fine-grained cataclasites containing plagioclase, amphibole, epidote and clinozoisite (2) are shown. An angular clast of an older generation of cataclasite is present as a dark fragment to the right. The fault rocks are cut by thin veinlets of quartz and brownish epidote+laumontite (3). The field of view is 35 mm wide.*

PFM007089

This is a fairly minor site where only a few data were obtained from a limited (excavated) outcrop with fine-grained metagranite containing some scattered, elongate, rounded inclusions of amphibolite. The metagranite is cut by a fault trending ca. 325/80. The fault rock is a dark green, fine-grained cataclasite with abundant epidote and some quartz (Figure 5-11). The measurements obtained at this site are consistent and show a NNW-SSE-trending fracture set, dipping ca. 60 degrees to the east. Striations on two surfaces plunge gently to the SSE (Figure 5-12), once again indicating a conspicuous strike-slip component of movement.

Figure 5-11. *Epidote-rich cataclasite along steep fault (325/80) in granitoid gneiss. PFM007089.*

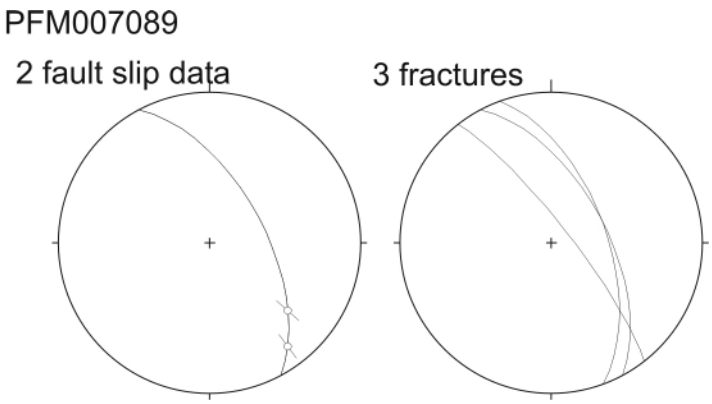

Figure 5-12. *Stereoplots showing data from site PFM007089.*

PFM007090

At this site there is a several metres wide zone of steeply dipping proto-mylonite, mylonite and ultramylonite (Figure 5-13) with foliation-parallel, epidote-filled semi-ductile shear zones and faults with cataclastic textures. The mylonites are low-grade and consist of feldspar, quartz, chlorite, epidote and mica. The cataclasite clearly post-dates the ductile fabric (Figure 5-13).

Figure 5-14 summarizes the measurements of brittle structures and some of their characteristics from field investigations at site PFM007090. Three fault slip data were obtained from oblique SE-plunging striae on NW-SE-oriented steep fault surfaces (Figure 5-14). Given that the NW-SE trend is that of the EDZ, and of the metamorphic foliation (Figure 5-14), the data confirm the brittle reactivation of the ductile fabrics as seen in Figure 5-13.

Figure 5-13. *From left to right the figure shows: 1) Outcrop of mylonite to ultramylonite along the EDZ; 2) part of scanned thin section showing the high-strain planar ductile fabric in ultramylonite. At the right-hand side of the figure, the ductile fabric has been broken apart forming a fine-grained cataclastic texture. The field of view is ca. 20 mm wide. 3) Photomicrograph showing details from the upper right-hand part of the scanned thin section. The ductile fabric is completely disrupted in the cataclasite. A layering due to variation in average clast size is apparent in the cataclasite. The fine-grained, dark grey material cut by thin veins (upper right) is an ultra-cataclasite devoid of microscopically visible mineral grains. The field of view is ca. 8 mm wide. Sample from PFM007090.*

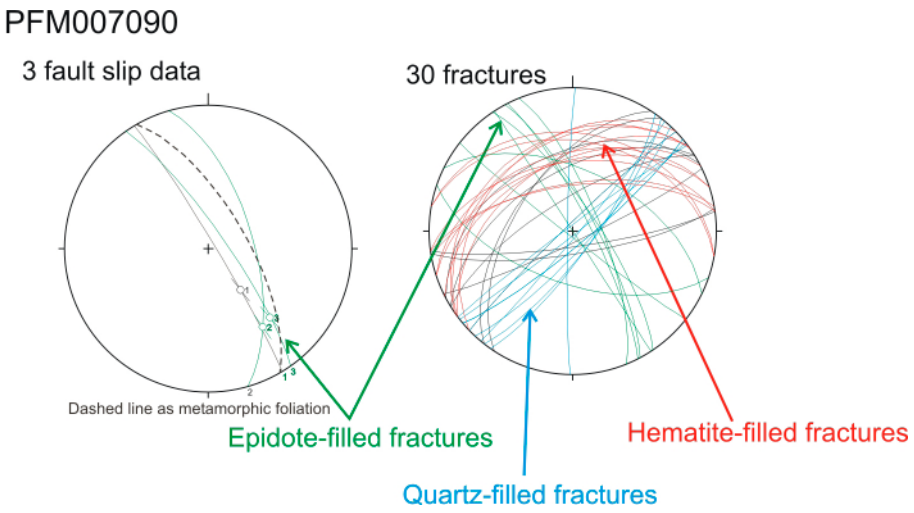

Figure 5-14. *Stereoplots of the brittle structures measured at site PFM007090. NW-SE strike-slip oblique displacements along the NW-SE steep fractures (parallel to foliation and to the EDZ) and the sorting of fractures by plane attitudes and by mineral infill.*

Data from 30 other fractures have been collected and three predominant sets can be identified based firstly, on their attitude and secondly, on their mineral infill. The NW-SE trend mentioned above is characterized by epidote infill (Figure 5-14). A NE-SW set of quartz-filled fractures and NE to ENE-oriented hematite-filled fractures dipping 30–40 degrees to the northwest are the two other consistent sets.

PFM007091

At site PFM007091 there is a several metres wide zone of mylonitic to locally ultramylonitic metagranite, post-dated by foliation-parallel faults and fractures with epidote and some vein quartz. In addition, there is a set of NE-SW fractures that cut the mylonite fabrics and quartz veins in the host rock (Figure 5-15). The fault slip data set show that the main NW-SE ductile fabric along the EDZ trend was reactivated in a brittle regime with striae showing strike-slip and NW-plunging oblique slip with a well defined dextral component. Combined with the NE-SW set of fractures they define a conjugate system of faults that developed under a strike-slip regime with a N-S trend of compression and an E-W trend of extension (Figure 5-15).

At this locality, there is also a carbonate-cemented fault breccia oriented parallel to the ductile fabric. The breccia post-dates the development of a fine-grained cataclasite occurring in a foliated, medium-grained metagranite. Euhedral calcite fills the interstices between the angular fragments of cataclasite (see /Nordgulen and Braathen 2005/). The total width of the breccia zone is ca. 50 cm and includes three zones of carbonate-cemented breccia and a thin quartz vein. Figure 5-16 illustrates a typical example from the breccia.

PFM007092

Several sets of fractures have been identified at this site. One NW-SE trend is parallel to the EDZ (number 12 on Figure 5-17). It is filled with breccia fault rock (Figure 5-18, stereoplot at the left). A set of younger quartz-filled tension gashes has been developed along the same trend (Figure 5-19, stereoplot at the left). The most common fractures are oriented E-W to NE-SW and are steep or dip 50–60 degrees to the south or north (Figure 5-17). Those dipping to the north are pale, green epidote-filled tension gashes (green stereoplot of Figure 5-18). A large fault also follows this trend and displays a normal component of movement as determined by an offset of the metamorphic fabric (Figure 5-19, stereoplot at the right).

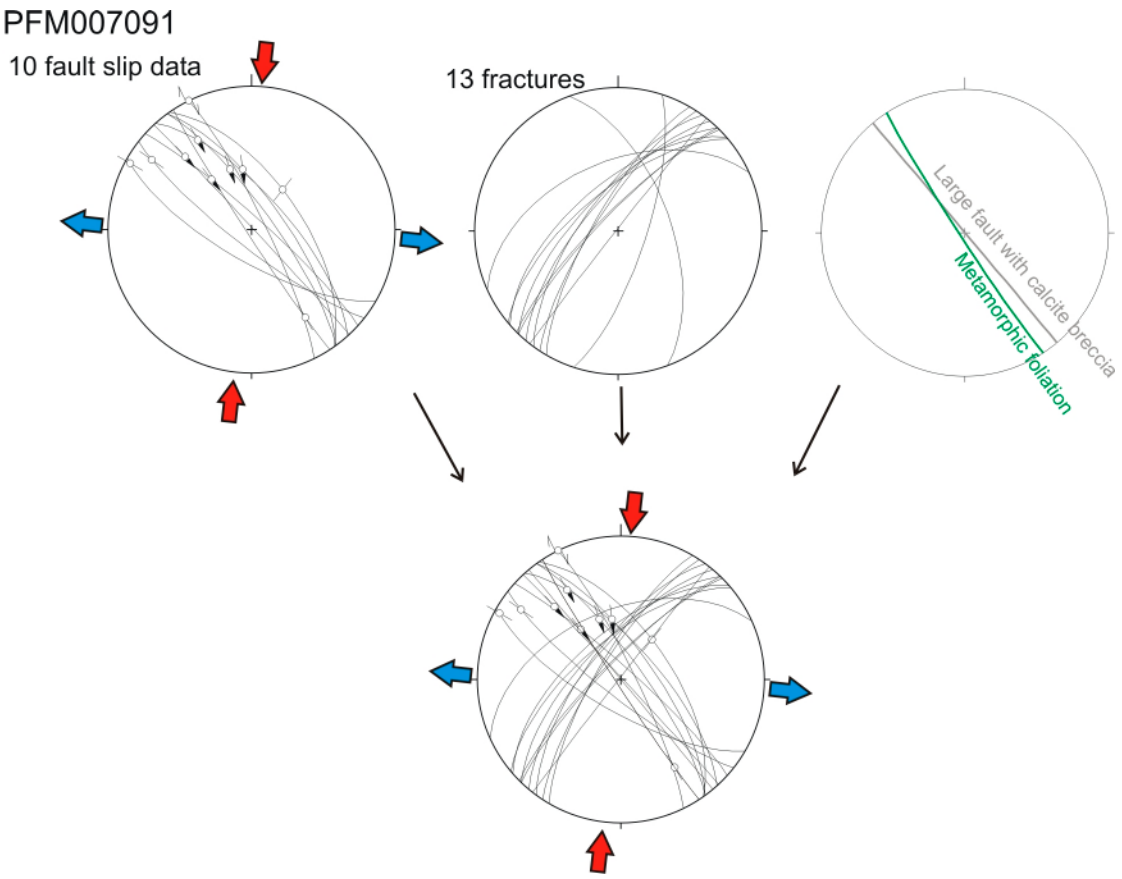

Figure 5-15. *Stereoplots showing all data measured at site PFM007091. The brittle structures are consistent with a strike-slip regime with N-S compression (red arrows) and E-W extension (blue arrows).*

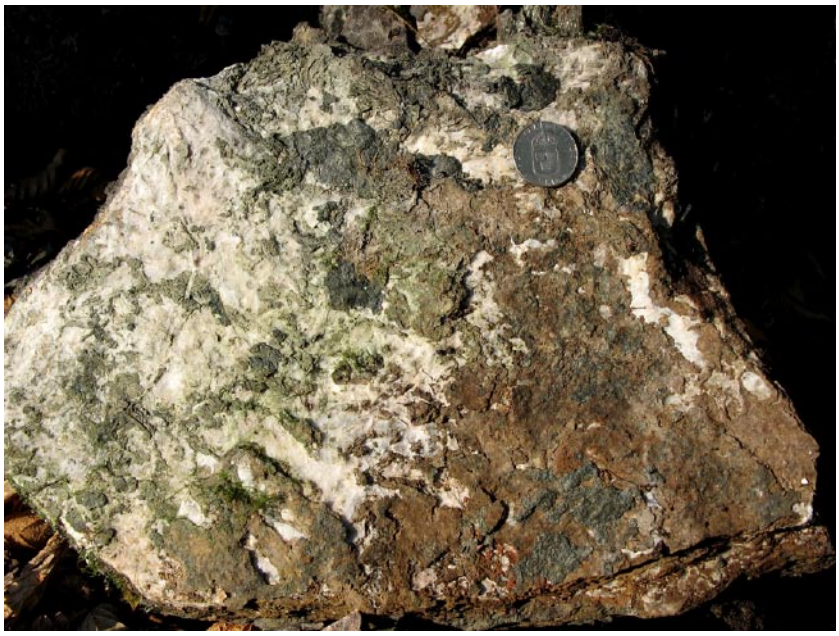

Figure 5-16. *Calcite-cemented fault breccia with angular fragments of fine-grained cataclasite. Photo approximately normal to the planar breccia, coin for scale. PFM007091.*

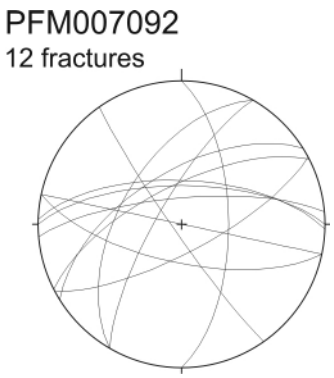

Figure 5-17. *Stereonet of fractures showing the main E-W to NE-SW trending and steep to 50–60 degrees S- or N-dipping fracture set. PFM007092.*

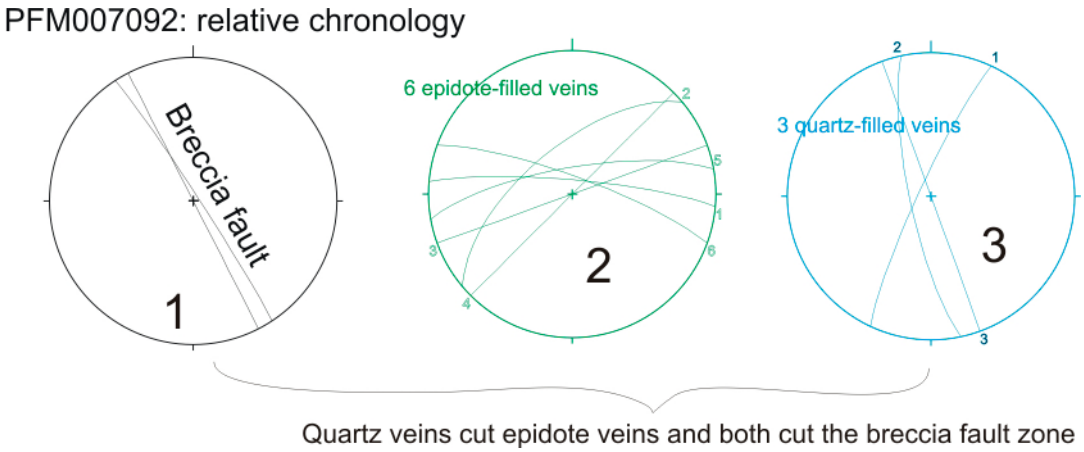

Figure 5-18. *From left to right, and from older to younger structures: 1) trend of the fault breccia parallel to the EDZ; 2) E-W- to NE-SW-trending tension gashes dipping 60 degrees to the north; and 3) approximately N-S-oriented, steep, quartz-filled tension gashes. From left to right: from the older structures to the younger structures. PFM007092.*

Figure 5-18 also shows the relative chronology between three different types of fractures. The chronology has been established using cross-cutting field relationships and is as follows from the oldest to the youngest: 1) NW-SE breccia fault zone parallel to the EDZ (black stereoplot); 2) N-dipping, pale green, epidote-filled tension gashes (green stereoplot); and 3) N-S-oriented steep quartz veins (blue stereoplot).

Relative chronology has been also observed between vertical quartz veins (Figure 5-20, stereoplot to the left): a NE-SW-oriented set is older than an E-W set. Finally, there are NE-SW vertical quartz veins that are cut by pale green epidote-filled veins (Figure 5-20, stereoplot to the right). The strike-slip offset and chronology of the fractures may suggest that they define a conjugate system of NE-SW and E-W faults as shown in Figure 5-20. The inferred orientation of compression and extension in this strike-slip stress regime is similar to that determined at site PFM007086 (see relevant section).

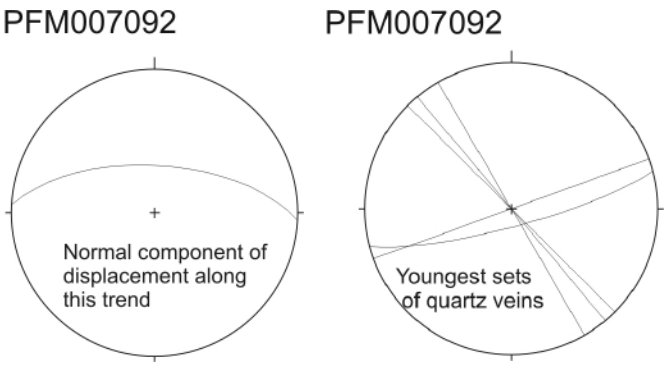

Figure 5-19. *To the left: Sets of vertical quartz veins, one of the trends is parallel to the EDZ. These veins cut many other types of structures. To the right: Normal component of movement along E-W-trending fault. PFM007092.*

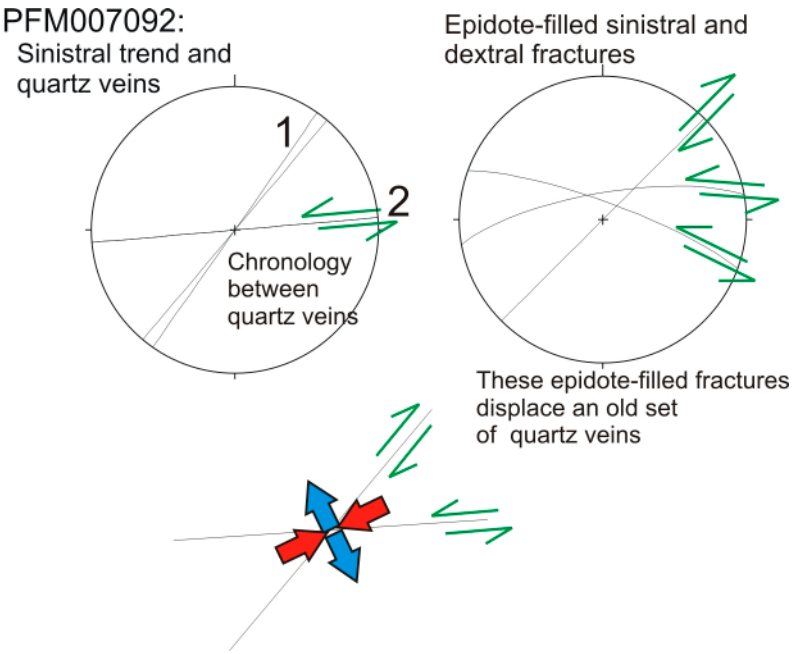

Figure 5-20. *Chronology between different trends of veins and due to significant strike-slip offset of pre-existing structures, determination of a conjugate system of strike-slip faults (with trend of compression as couples of red convergent arrows and trend of extension as couples of blue divergent arrows). PFM007092.*

PFM007093

The rock types at this locality are a fine-grained reddish pink metagranite with some coarse pegmatite. In addition to a quartz-filled breccia with angular fragments of the metagranite /Nordgulen and Braathen 2005/, there are two main sets of fractures. The older N-S trending fractures are steep and filled with pale green epidote (Figure 5-21). These are cut by NW-SE trending mainly steep fractures with quartz. Other non-mineralised fractures trend parallel to the quartz veins (Figure 5-21).

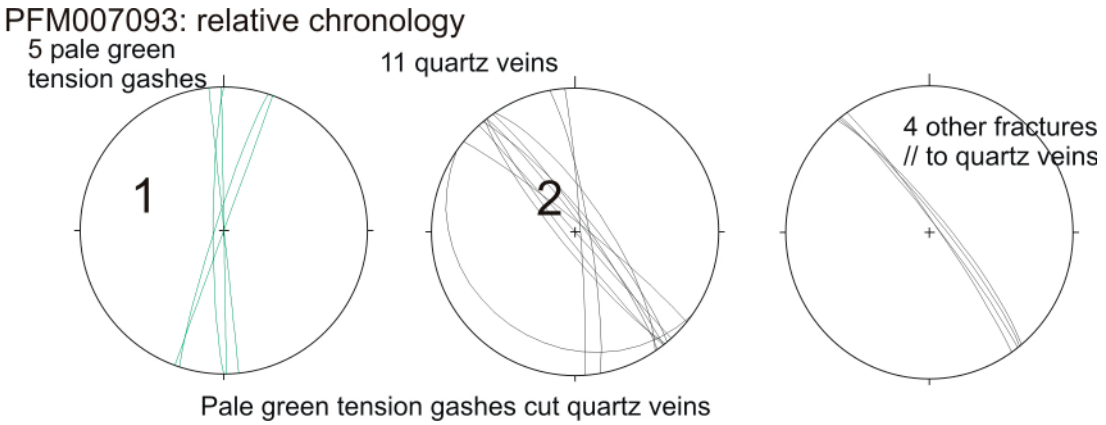

Figure 5-21. *Epidote-filled fractures (1) are cut by quartz-filled veins forming a network of predominantly steep NW-SE-oriented fractures. Non-mineralized fractures (to the right) are parallel to the quartz-filled fractures. PFM007093.*

PFM007094

The outcrop at this site consists mainly of reddish grey fault rocks (cataclasite) developed from foliated to mylonitic metagranite. Abundant fractures are present, some of which show a small amount of offset. Fault slip data were collected on three NW-SE-trending faults that dip 50 degrees to the SW. Oblique slickensides on the fault planes plunge 40 degrees to the SE (Figure 5-22). A well-defined set of NE-SW vertical fractures is also present at this site. Many of these are coated by hematite (red stereoplot of Figure 5-23).

The cross-cutting relationships between structures indicate a complex chronology of fracture evolution. The NE-SW hematite-filled fractures offset a NW-SE quartz vein in a strike-slip manner whereas one of the NW-SE quartz veins cuts across the NE-SW hematite veins (stereoplot at the bottom of Figure 5-23).

PFM007095

This site is a small outcrop consisting of reddish pink proto-cataclasite cut by abundant small micro-faults and by a 2 cm wide NW-SE-oriented (ultra-)cataclasite (Figure 5-24). A thin section of the fault reveals a complex history of brittle deformation with the development of at least three generations of cataclasite prior to quartz+calcite deposition in the matrix of the fault followed by the development of thin quartz veinlets (Figures 5-25 and 5-26).

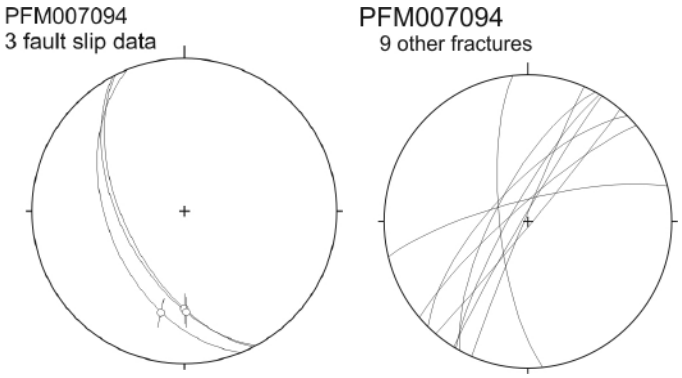

Figure 5-22. *Fault slip data set (left) and steeply dipping, non-mineralized NE-SW-oriented fractures (right). PFM007094.*

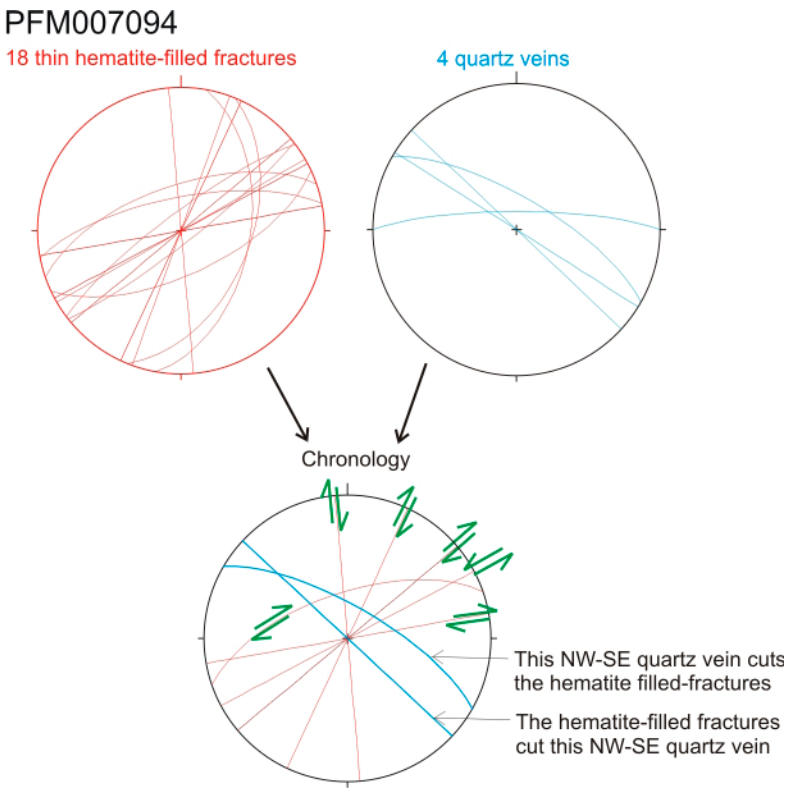

Figure 5-23. *Red stereoplot (upper left) showing the hematite-filled NE-SW vertical fractures; blue stereoplot (upper right) shows the NW-SE vertical quartz veins. The complex cross-cutting relationships between structures at this site indicate a complex fracture evolution (bottom; see text for explanation). PFM007094.*

Figure 5-24. *Reddish pink (oxidized) proto-cataclasite is cut by a number of thin micro-fractures and by a 2 cm wide (ultra-)cataclasite (eroded) oriented ca. 320/88, i.e. sub-parallel to the EDZ. Sub-horizontal outcrop, up is to the southeast. PFM007095.*

Figure 5-25. *Scanned thin section from site PFM007095. Along the margins of the sections there is greenish to reddish cataclasite with variably sized angular fragments of cataclasite in 2nd generation fault rock. Hence, this part of the section is preserving two events of brittle deformation. The central part of the section consists of a fine-grained fault rock with clasts of reddish cataclasite embedded in a matrix of mainly quartz and calcite. See Figure 5-26 for details. The field of view is 35 mm wide.*

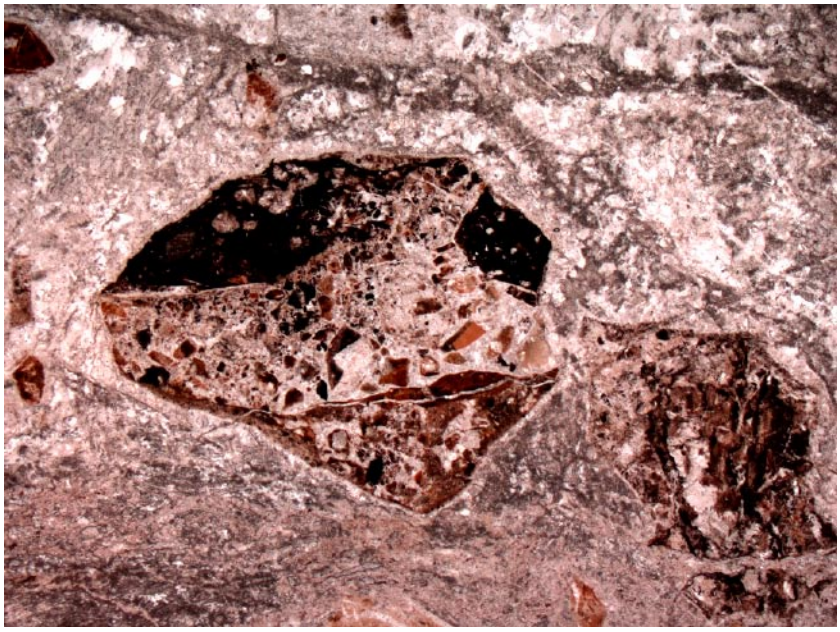

Figure 5-26. *Photomicrograph showing a detail from the central part of thin section of Figure 5-25. Composite, angular clasts that consist of different types of earlier formed cataclasite sit in a fine-grained groundmass and are cut by very thin quartz veins. The field of view is ca. 4.5 mm wide.*

Among the minor faults, an ENE-WSW vertical and brecciated fault zone (stereoplot to the left of Figure 5-27) shows left-lateral kinematics determined using R-Riedel structures, secondary fractures, etc along the trend of the zone. The EDZ has been reactivated with the opening of thin quartz veins along its trend (blue stereoplot of Figure 5-27). This event is clearly the youngest brittle event at this site as the quartz veins cut across all pre-existing fabrics.

PFM007095

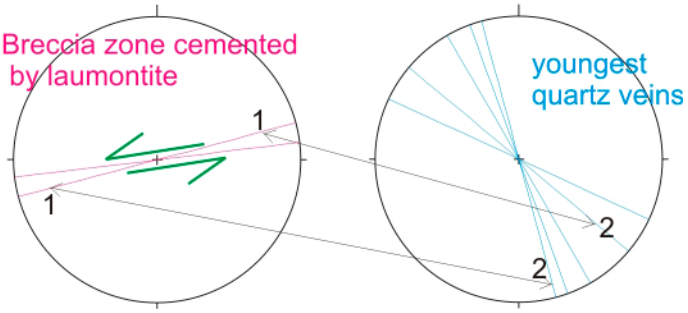

Figure 5-27. *Stereoplot to the left: ENE-WSW vertical and brecciated left-lateral strike-slip fault zone. These structures are post-dated by NW-SE vertical quartz veins developed parallel to the trend of the EDZ (stereoplot to the right). (1, 2 and arrows between them, refer to the cross-cutting relationships, or the relative chronology, between fractures: '1' being cut by, or older than, '2'). PFM007095.*

5.1.2 Other field stations

PFM007085

This is an open pit that was excavated in 2–3 m thick moraine, and is situated close to drill site 7. During the time of fieldwork, the site was being prepared for a thermal conductivity experiment. The main rock type is a medium- to coarse-grained, pale pinkish grey, foliated metagranite intruded by sheets of amphibolite and coarse granite pegmatite.

At this site a ductile dextral shear parallel to metamorphic foliation is observed (Figure 5-28). Faults following the ductile zone carry quartz, chlorite, calcite and sporadic laumontite (see below).

16 fault slip data has been collected at site PFM007085 (Figure 5-29). Based on the attitude of the fault planes and the orientation of slickensides on chlorite-coated surfaces, three consistent sub-sets have been determined. The first set consists of gently N-dipping faults with pink red staining and locally preserved chlorite coating. The chlorite has dip-slip oriented slickensides, but with unknown sense of displacement (Figure 5-29, bottom left). The second NW-SE trending set dips about 60 degrees to the southwest and show dip-slip normal movement (Figure 5-29, second stereoplot from bottom left). This set of normal faults developed along the pre-existing foliation (see Figure 5-28). The third set comprise gently (ca. 30 degrees) dipping NNE-SSW faults with sinistral to reverse slip (Figure 5-29, third stereoplot from bottom left).

Some faults that cannot be assigned to any of the three sets described above are also shown in Figure 5-29 (bottom right). In addition, a steep E-W-oriented calcite vein has been observed cutting across one of the NNE-SSW reverse sinistral fault planes.

PFM007085

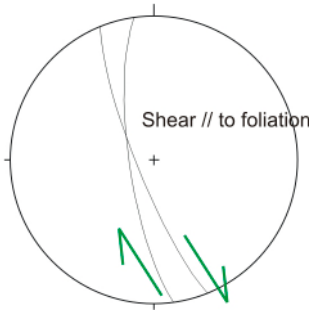

Figure 5-28. *Dextral ductile shear along the metamorphic foliation at site PFM007085.*

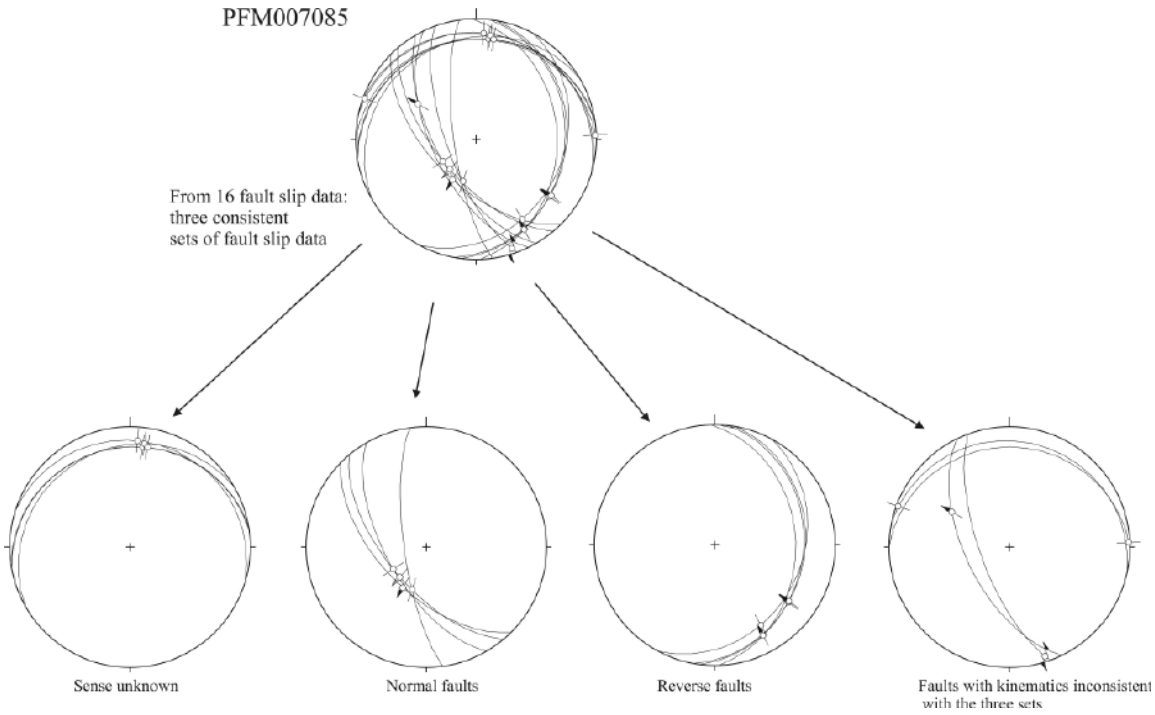

Figure 5-29. *Sorting of the 16 fault slip data into consistent sets based on the kinematics observed on variably oriented faults. See text for details. PFM007085.*

PFM007096

Site PFM007096 is a steeply dipping fault zone trending NW-SE that crops out along Linjevägen/Turbinvägen close to the nuclear power plant (Figure 5-30). Interest in this locality derives from the fact that it is oriented parallel to and some distance to the east of the EDZ. In contrast to most outcrops along the EDZ, the fault itself allows for the study of the damage zone and fault core zones (several tens of centimetres in width) along a continuous, vertical strike section several tens of metres in length. Hence, observations made would be relevant also for the understanding of the EDZ.

Figure 5-30. *The NW-SE large fault plane that crops out at site PFM007096, viewed towards the south.*

The fault cuts medium-grained, strongly foliated metatonalite. The foliation is steep and trends ca.140°; mineral lineations plunge ca. 25° towards the SE. Sheets of fine-grained amphibolite occur parallel to the foliation; these may represent deformed mafic dykes. There are also some younger, cross-cutting dykes of pegmatite and fine-grained greyish pink granite. The main fault rock is a dark greenish, chlorite-rich cataclasite with small clasts of red feldspar. Hematite is common. Locally, a coating of grey clay minerals (?) or carbonate occurs. Carbonate-cemented breccias were also found at the base of the outcrop and probably form the core of the fault.

On the fault plane itself, 41 kinematic indicators determined by striae, steps on the fault surface and Riedel shears were obtained (Figure 5-31). Some E-W and ENE-WSW trending structures that are inferred to be related to the main fault have been observed and measured (Figure 5-31) and are described in more detail below.

The NW-SE fault zone displays two distinct sets of slickensides related to two different episodes of displacement. The most abundant set is linked to a sinistral displacement (Figure 5-32). An E-W fault zone is interpreted as a large R-Riedel shear to the main NW-SE fault (Figures 5-32 and 5-33). A dextral ENE-WSW-oriented fault is a conjugate structure associated with the sinistral NW-SE fault (Figures 5-32 and 5-34). All these structures described above certainly developed under a strike-slip stress regime with a WNW-ESE trend of compression and a NNE-SSW trend of extension (Figure 5-32). The less abundant set of slickensides on the NW-SE fault surface reflects dextral normal displacement (Figure 5-35), which is the record of another state of stress. Unfortunately, no relative chronology could be determined between the two sets of kinematic indicators, and thus between the two stress regimes.

PFM007097

This site exposes grey to pink medium-grained metagranite gneiss along a ca. 20 m long and 3 m wide trench excavated in moraine near drill site 7. The trench is oriented ca. 165°. The horizontal surface exhibits few striated faults. However, a number of joints and mineral-filled fractures and some minor breccias are present. Chlorite is a very common fracture infill. Quartz is also common, and hematite alteration occurs mainly along NNW-oriented fractures (see below).

The trench displays three different types of brittle structures. Firstly, there is a set of thin open fractures with hematite infill that have a general NNW-SSE trend (Figure 5-36a). Secondly, a system of NNE-SSW to NE-SW quartz tension gashes (Figure 5-36b). The latter developed en echelon between ENE-WSW trending fractures (Figure 5-36c) and as such evidenced the sinistral character of the ENE-WSW structures (Figure 5-36d, Figure 5-36). Quartz tension gashes clearly cut across hematite-filled fractures and are thus younger (Figure 5-36d). Figure 5-36f also shows the other joints collected at site PFM007097 with the predominant trends being these of the quartz infill tension gashes and the sinistral minor-faults.

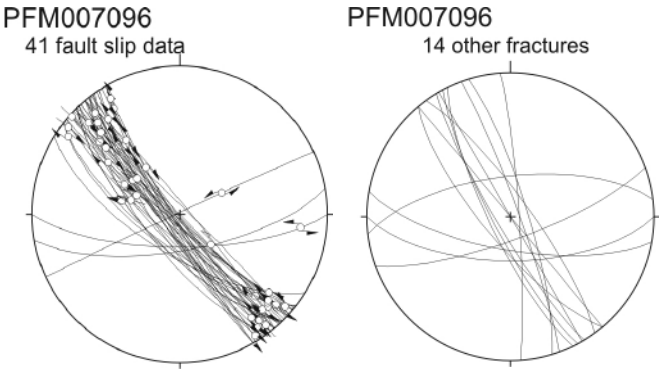

Figure 5-31. *A) The complete set of 41 fault slip data collected at site PFM007096. The kinematic indicators were obtained from the NW-SE-trending fault surfaces representing individual strands in the steep and large main fault zone (see Figure 5-29). B) Other fractures measured at site PFM007096. These do not exhibit kinematic indicators, but their attitude is consistent with those of the striated faults.*

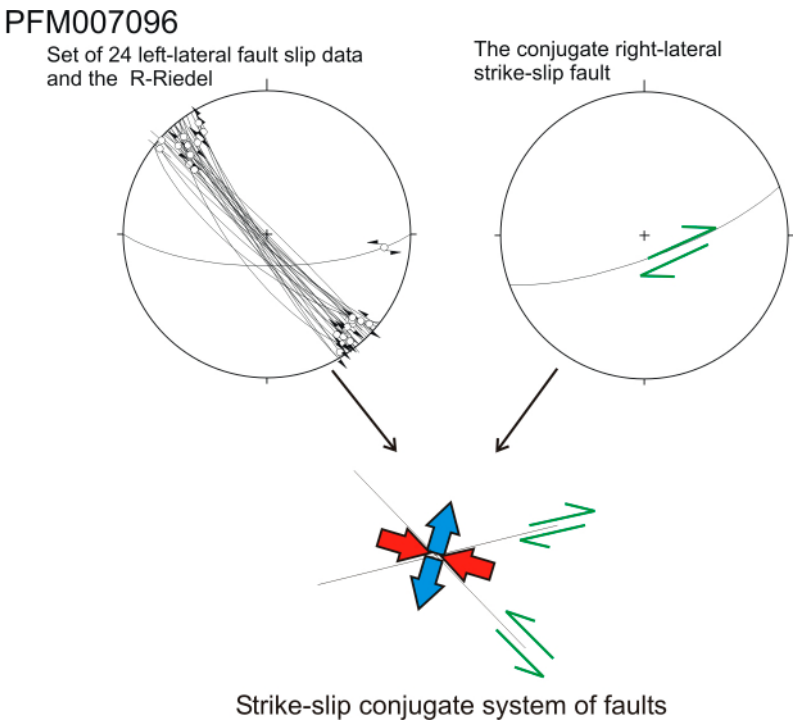

Figure 5-32. *Top left: faults with slickensides showing sinistral slips along the NW-SE large fault zone and one E-W R-Riedel shear (Figure 5-33). Top right: a dextral fault, conjugate to the NW-SE sinistral fault (Figure 5-34). Bottom: the fault geometries suggest that the observed structures form a conjugate system of faults (with an angle of 60 degrees between the planes) that developed under a strike-slip stress regime with a WNW-ESE trend of compression (couple of red arrows) and a NNE-SSW trend of extension (couple of blue arrows).*

Figure 5-33. *Outcrop (left) and line-drawing (right) showing the major NW-SE sinistral fault and its E-W R-Riedel structure.*

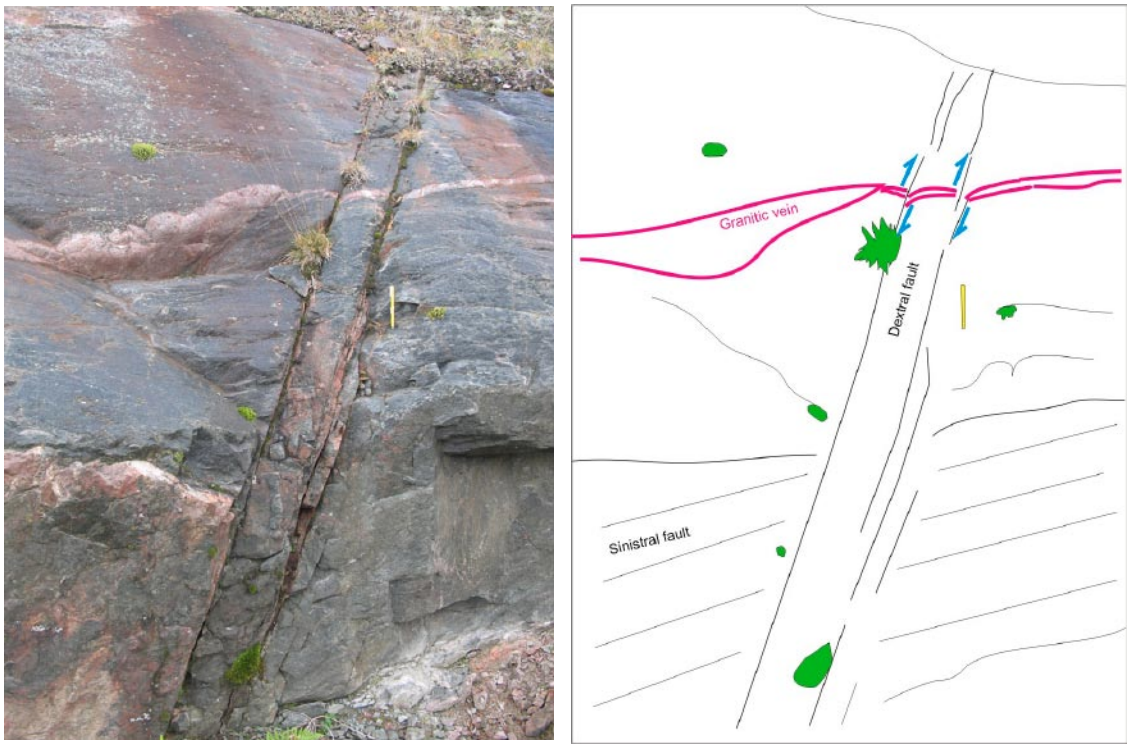

Figure 5-34. *Outcrop (left) and line-drawing (right) showing the NW-SE sinistral fault and its ENE-WSW conjugate dextral fault. Note the dextral offset of the granitic vein.*

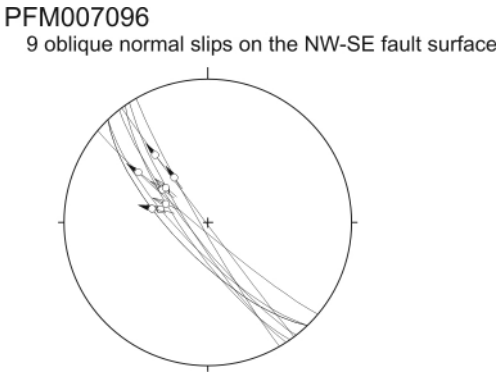

Figure 5-35. *Normal dextral slips along the NW-SE large fault zone.*

The third important set of structures is the dip-slip NNW-SSE-oriented normal faults (Figure 5-38). They trend parallel to the hematite-filled fractures described above.

Local brecciation occurred mainly at the intersection between fractures having different orientations. The best example in the trench is shown in Figure 5-39 (left).

5.1.3 Summary of the results of the field data analysis

Apart from the NW-SE trend of the EDZ, which is well represented in the investigated area, NE-SW to E-W trends are abundant and mainly correspond to steep fractures. The slickensides have been mainly observed along the NW-SE fractures. Both strike-slip and dip-slip slickensides are present. The various fracture trends are decorated or filled with a variety of minerals (e.g. epidote, quartz, chlorite, calcite), suggesting reactivation during repeated episodes of movement along the same structures. However, the quartz tension gashes tend to occur only along NW-SE to NNW-SSE and NE-SW steep trends.

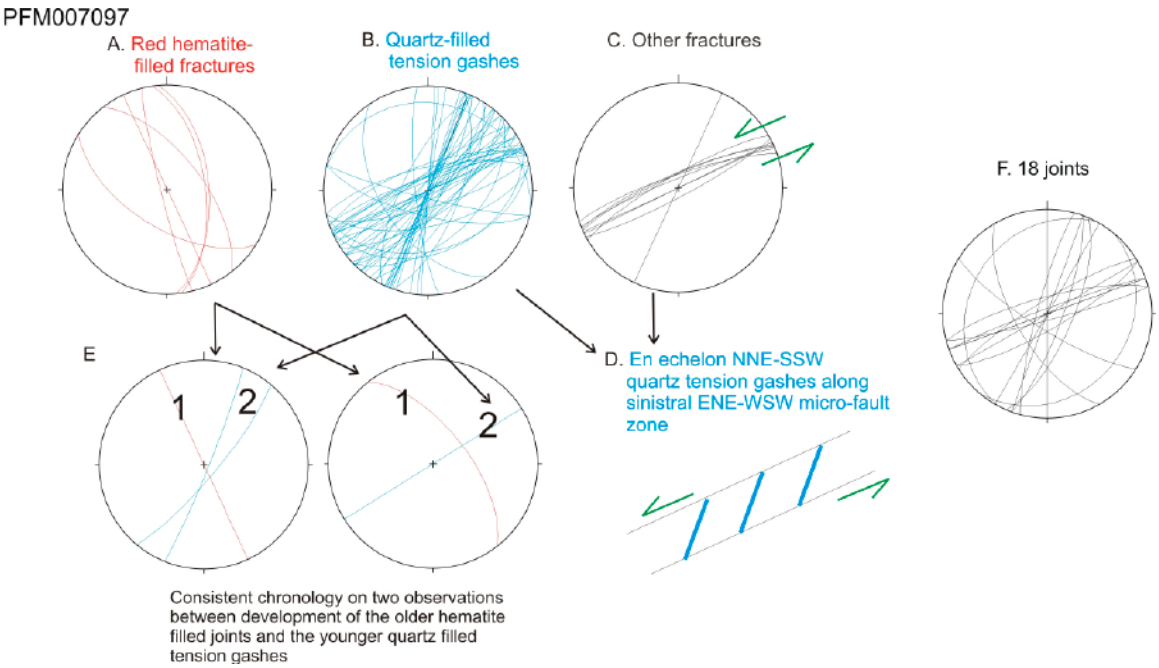

Figure 5-36. *Stereoplots of fracture data collected at site PFM007097. A) Hematite-coated fractures. B) Quartz tension gashes developed en echelon along sinistral faults. C) ENE-WSW sinistral faults. D) Drawing illustrating the strike-slip opening of quartz-filled tension gashes along ENE-WSW sinistral trends. E) Relative chronology between tensional fractures. F) Joints with similar trends.*

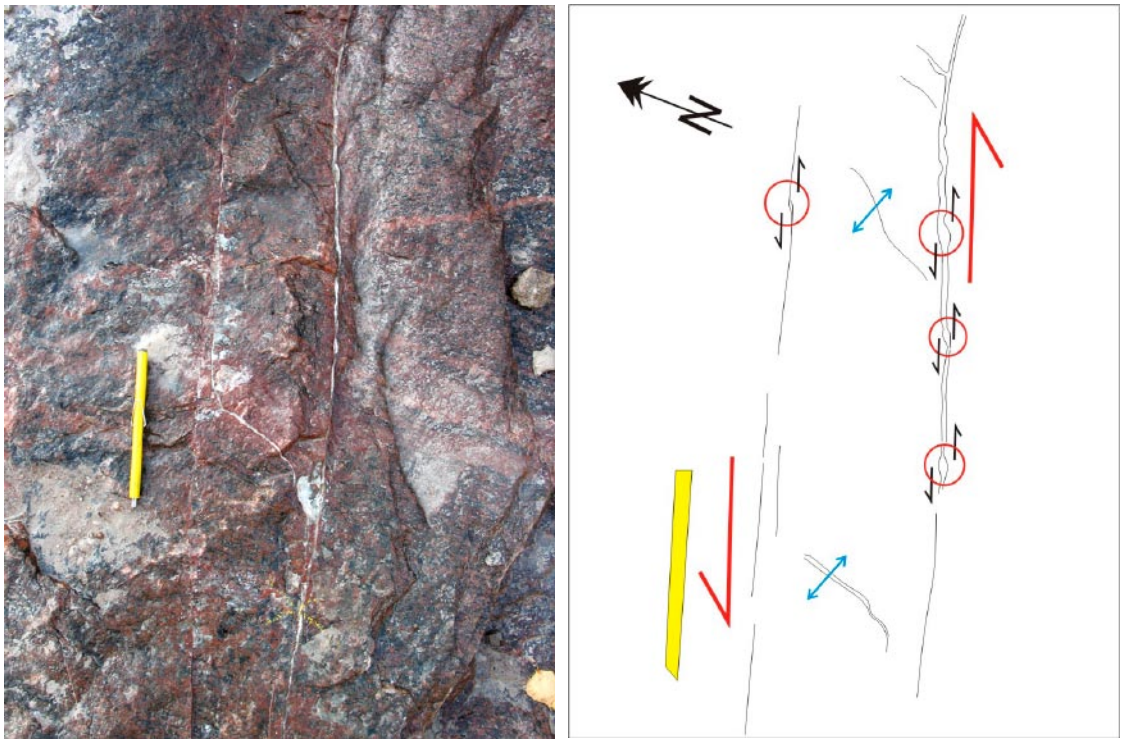

Figure 5-37. *En echelon distribution of NNE-SSW tension gashes along a ENE-WSW sinistral zone. Some sinistral steps of quartz are also observed along the ENE-WSW sinistral faults (into red circles). (Note that the line drawing is enlarged compare to the picture).*

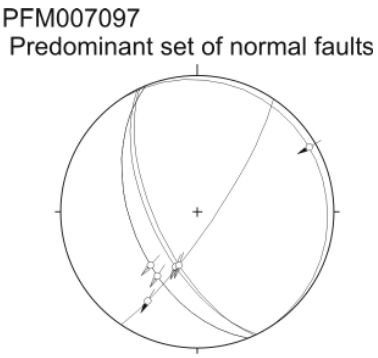

Figure 5-38. *Faults measured at site PFM007097 with a predominant set of normal faults.*

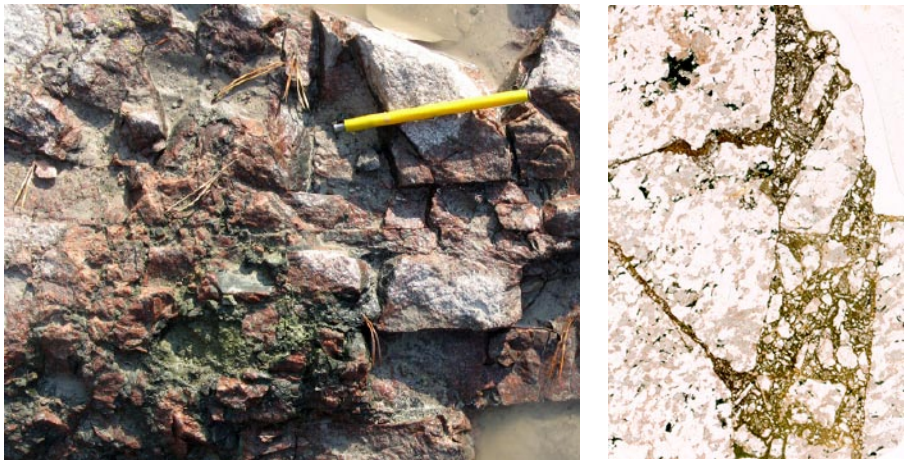

Figure 5-39. *Left: Detail from horizontal outcrop in the trench at site PFM007097. Steep NNW-oriented fractures (vertical on the photograph) intersect with NE- and ENE-fractures. Note green chlorite infill, strong oxidation and local brecciation of the metagranite host rock. Right: Scanned thin section from a sample collected at the outcrop. The metagranite is strongly crushed and brecciated along fractures. Dark, hematite-dusted chlorite-rich material with minor epidote fills the voids between angular clasts in the breccia. Note that the breccia developed preferably, but not exclusively, along NE- and ENE-trends. The field of view is ca. 20 mm wide.*

Some of the field data provided good constraints on the local kinematics (see descriptions of individual sites). The inversion of such data allows for the interpretation of local stress states. Another and more challenging step in the analysis would be to link the local stress states to the kinematics of the major fault zone(s) (such as the EDZ).

Dextral movement could have taken place along the NW-SE regional faults. Evidence for such sense of displacement along NW-SE fractures are recorded at site PFM007091. The trend of extension was E-W, and the N-S trending epidote-filled tension gashes at site PFM007093 could have developed under this stress field.

Sinistral movements have also been identified along the NW-SE regional trend of faults, for example at site PFM007096 where the data suggest strike-slip movement with a nearly E-W compressional axis.

In many sites along the EDZ, the trend of maximum compression appears to have been oriented NW-SE (PFM07088), and thus parallel to the fault zone, or NE-SW, i.e. perpendicular to the fault zone (PFM007086, PFM007092). If these local conditions were representative for the regional stress field, it would imply that no movement would have taken place along the EDZ. However, it is also possible that the strike-slip stress fields described in the two previous paragraphs (one characterised by an E-W extensional axis and the other by a nearly E-W compressional axis) deviated somewhat in proximity to the major fault zone. In this case, the observed local conditions would not necessarily reflect the regional situation.

5.2 Drill core investigations

5.2.1 Investigated drill cores

Selected sections from 12 boreholes were inspected with the aim of investigating the style of deformation in the previously defined deformation zones classified with uncertainty 3 in the respective single-hole interpretations (Table 5-1). The geographic location of the boreholes is shown in Figure 5-40. During this investigation, samples for petrographic analysis were collected from characteristic fault rocks (see sample list in Appendix 1). The boreholes and deformation zones (DZ) that were studied are listed in Table 5-1. Previous studies of the drill cores have been reported in the single-hole interpretations for each borehole. The detailed studies of fracture mineralogy by /Sandström et al. 2004, Sandström and Tullborg 2005/ have also been used.

In the following, the character and structural relationships of each deformation zone is described with emphasis on the occurrence of deformation products such as crush zones, cataclasites, breccias and fracture networks. Observed cross-cutting relationships between fractures and faults with different orientations and mineral fill are pointed out, providing a framework for an improved understanding of the geological history of the investigation area. The kinematic data are described in relation to the mineralogy of the faults and fractures. For most deformation zones, a figure showing the distribution of prominent brittle structures is provided. These figures also include plots showing the variation in fracture frequencies along the zone, i.e. total fractures, sealed fracture networks (not always available), open fractures and sealed fractures, as obtained from SICADA. A short summary of the results from each borehole is provided.

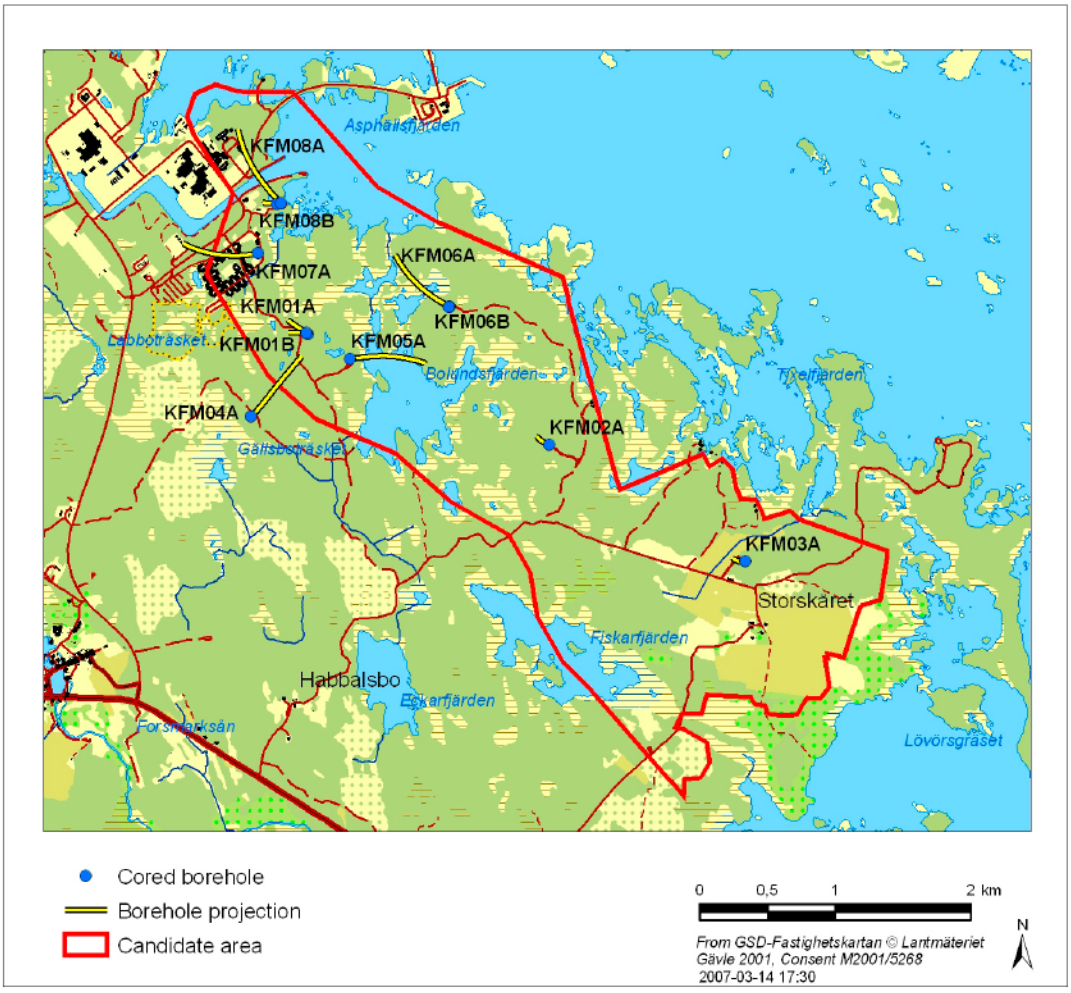

Figure 5-40. *Map of the Forsmark area showing candidate investigation area (red line) and the geographic location of the boreholes.*

Table 5-1. Overview of drill cores inspected in the project.

Drill core	Length, direction	Deformation zone section	Deformation zone identification
KFM01A	1,001 m, 318/85	639–684 m	DZ3 /Carlsten et al. 2004a/
KFM01B	500 m, 268/79	16–53 m	DZ1 /Carlsten et al. 2004a/
		107–135 m	DZ2 /Carlsten et al. 2004a/
		415–454 m	DZ3 /Carlsten et al. 2004a/
KFM02A	1,002 m, 276/85	110–122 m	DZ2 /Carlsten et al. 2004b/
		160–184 m	DZ3 /Carlsten et al. 2004b/
		415–520 m	DZ6 /Carlsten et al. 2004b/
		893–905 m	DZ8 /Carlsten et al. 2004b/
		922–925 m	DZ9 /Carlsten et al. 2004b/
KFM03A	1,001 m, 272/86	356–399 m	DZ1 /Carlsten et al. 2004e/
		448–455 m	DZ2 /Carlsten et al. 2004e/
		638–646 m	DZ3 /Carlsten et al. 2004e/
		803–816 m	DZ4 /Carlsten et al. 2004e/
		942–949 m	DZ5 /Carlsten et al. 2004e/
KFM03B	101.5 m, 264/85	62–67 m	DZ2 /Carlsten et al. 2004e/
KFM04A	1,001 m, 045/60	202–213 m	DZ2 /Carlsten et al. 2004c/
		232–242 m	DZ3 /Carlsten et al. 2004c/
		412–462 m	DZ4 /Carlsten et al. 2004c/
KFM05A	1,003 m, 081/60	102–114 m	DZ1 /Carlsten et al. 2004d/
		416–436 m	DZ2 /Carlsten et al. 2004d/
		606–619 m	DZ3 /Carlsten et al. 2004d/
		712–720 m	DZ3 /Carlsten et al. 2004d/
KFM06A	1,001 m, 301/60	126–148 m	DZ1 /Carlsten et al. 2005a/
		195–245 m	DZ2 /Carlsten et al. 2005a/
		260–278 m	DZ3 /Carlsten et al. 2005a/
		318–358 m	DZ4 /Carlsten et al. 2005a/
		740–775 m	DZ7 /Carlsten et al. 2005a/
		788–810 m	DZ8 /Carlsten et al. 2005/
		882–905 m	DZ9 /Carlsten et al. 2005a/
		925–933 m	DZ10 /Carlsten et al. 2005a/
		950–990 m	DZ11 /Carlsten et al. 2005a/
KFM06B	1,003 m, 297/84	55–93 m	DZ1 /Carlsten et al. 2005a/
KFM07A	1,001.5 m, 260/60	108–183 m	DZ1 /Carlsten et al. 2005b/
		196–205 m	DZ2 /Carlsten et al. 2005b/
		417–422 m	DZ3 /Carlsten et al. 2005b/
		803–899 m	DZ4 /Carlsten et al. 2005b/
KFM08A	1,001 m, 321/61	172–342 m	DZ1 /Carlsten et al. 2005c/
		479–496 m	DZ2 /Carlsten et al. 2005c/
		672–693 m	DZ4 /Carlsten et al. 2005c/
		915–946 m	DZ6 /Carlsten et al. 2005c/
KFM08B	200.5 m, 270/59	167–185 m	DZ2 /Carlsten et al. 2005c/

5.2.2 KFM01A

The drill site is located in the north-western part of the investigation area some distance to the east of the EDZ (Figure 5-40). The borehole has a length of 1,001 m and is oriented 318/85 /Carlsten et al. 2004a/. Within the investigated deformation zone (DZ3), two striated NE-striking faults with laumontite and calcite were observed.

KFM01A: 639–684 m – DZ3

The main rock type is a medium-grained metagranite with finely recrystallised biotite. Minor rock occurrences include pegmatite, fine-grained granite and amphibolite. A section in the central part of the zone (652–674 m) has a markedly increased frequency of laumontite-sealed fractures and local fracture networks (Figure 5-41), whereas the upper and lower parts of the exhibit lower fracture frequencies. The laumontite-sealed fractures locally carry some chlorite and rare calcite. Pink colour of the host rock (oxidation) is observed in the sections with highest frequency of laumontite-sealed fractures; see photo inset in Figure 5-41.

In the central part of the deformation zone, two steep NE-SW faults with striation on laumontite + chlorite are observed with an oblique normal component of displacement to the south on one of these (Figure 5-42). One subordinate component of movement is dextral strike-slip.

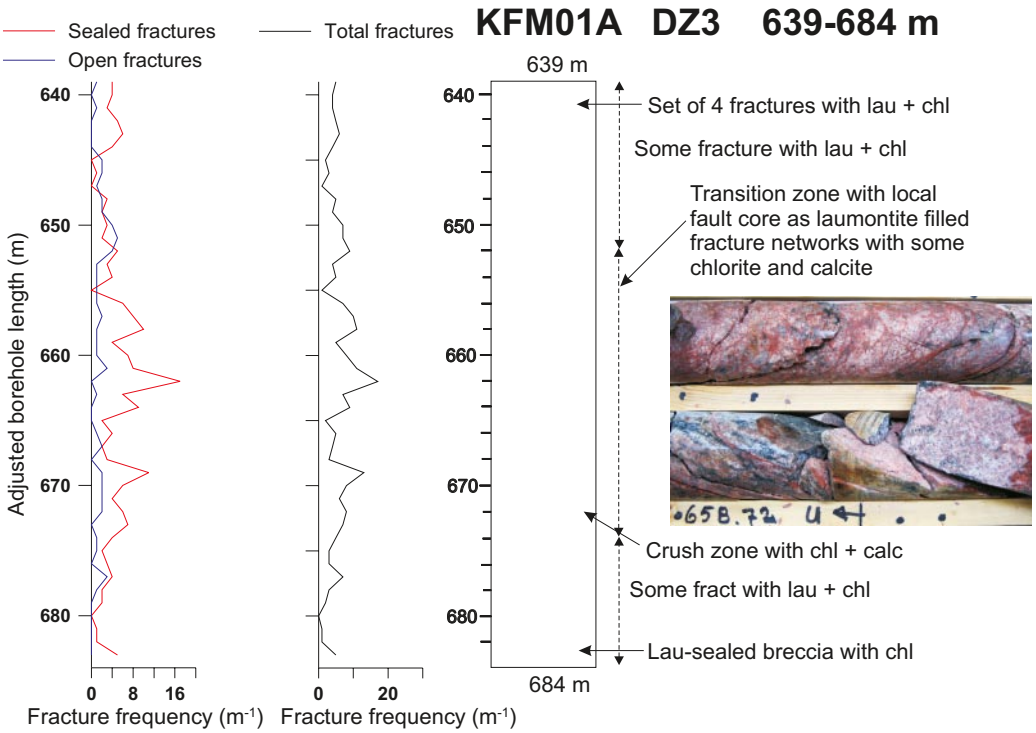

Figure 5-41. *Simplified drawing of DZ1 showing the most prominent brittle structures. The photo (inset) shows sections in the central part of the zone with a relatively high abundance of laumontite-sealed fractures. Abbreviations used throughout the report: Ep=epidote, Chl=chlorite, Qtz=quartz, Lau=laumontite, Corr=corrensite, Py=pyrite, Fract=fracture(s), w/=with.*

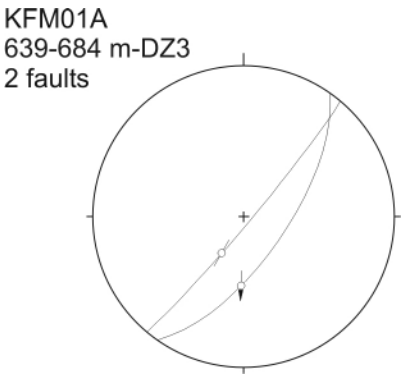

Figure 5-42. *Stereoplot of fault slip data in DZ3 (KFM01A).*

5.2.3 KFM01B

The drill site is located in the north-western part of the investigation area some distance to the east of the EDZ (Figure 5-40). The borehole is oriented 268/79 has a length of 500 m /Carlsten et al. 2004a/. Three deformation zones with a total length of 104 m were investigated (Table 5-1). Six steeply dipping striated faults striking NNW show evidence of strike slip as well as normal and reverse sip slip movement.

KFM01B: 16–53 m – DZ1

Alternating medium- and coarse-grained pinkish grey metagranite-granodiorite with finely recrystallised biotite. Minor occurrences of pegmatite, fine-grained pink granite and amphibolite are also present. Several intervals display strongly increased frequency of open, commonly gently dipping fractures. Fractures are filled and/or coated mainly by chlorite, epidote, calcite, clay minerals, quartz, iron oxides/hydroxides, and minor calcite and asphaltite. Steep fractures with local brecciation (fracture networks) are sealed with epidote (Figure 5-43). These structures commonly pre-date sets of dense, sub-horizontal open fractures with chlorite and clay mineral coatings (< 20 fractures/m).

At approximately 23 m there is a marked fault with epidote-cemented fault breccia of uncertain orientation that contains small, angular fragments of pink, altered meta-metagranite and quartz. This is post-dated by white vein quartz (Figure 5-44).

Two nearly N-S-oriented strike-slip faults with striation on chlorite ± hematite have been measured in the zone (Figure 5-45). The sense of strike-slip displacement could not be determined with certainty.

KFM01B: 107–135 m – DZ2

Medium-grained grey to grayish pink metagranite. Locally, an increase in sealed fractures with epidote ± quartz and less commonly laumontite is observed. Epidote-sealed fractures generally have intermediate dips. Gently-dipping fractures are commonly younger and have little or minor mineral fill that may include chlorite, calcite and oxides. Pyrite and prehnite are also present.

Most of the zone is defined as a transition zone /Munier et al. 2003/ with a local fault core defined by raised fracture frequency and sporadic sealed fracture network (Figure 5-46). No fault slip data have been identified in the zone.

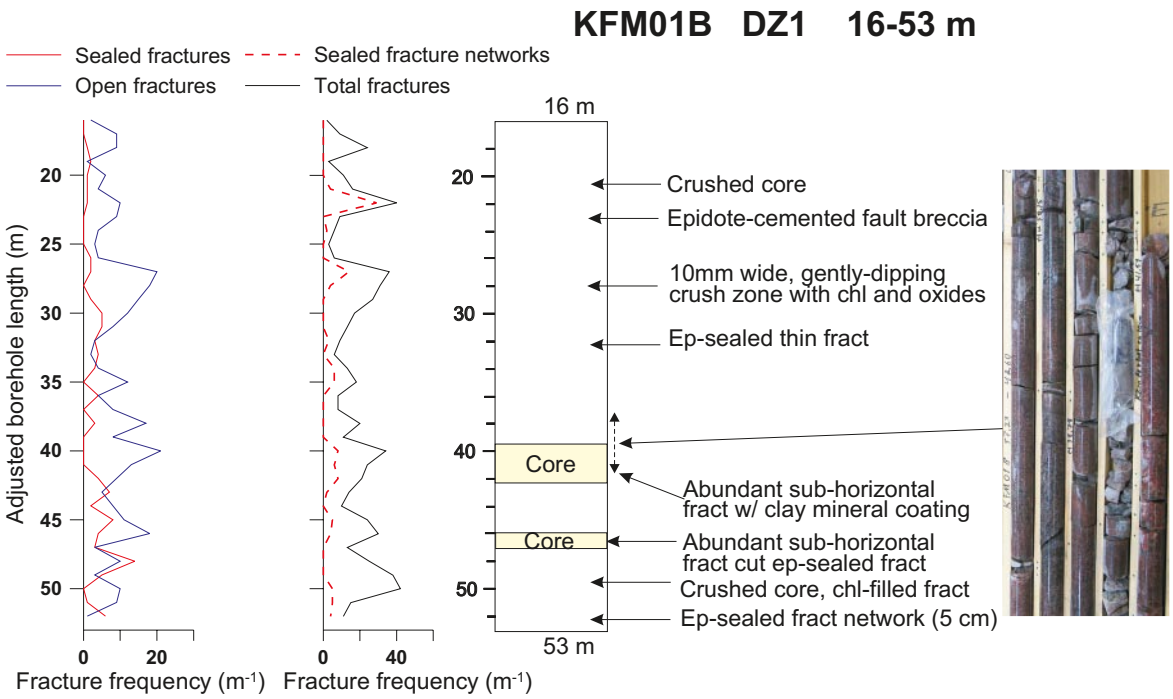

Figure 5-43. *Simplified drawing of DZ1 showing the most prominent brittle structures. At approximately 28 m the zone exhibits high fracture frequency and a ca. 10 mm wide crushed fault rock with chlorite and iron oxides (?). The photo (inset) shows the section between 37.2 and 41.6 m. Relatively strong deformation with abundant open, sub-horizontal fractures commonly with clay mineral coating continues down to ca. 42.5 m. The interval between ca. 46 – 48 m has abundant sub-horizontal fractures that cut steeper epidote-sealed fractures. Abbreviations used throughout the report: Ep=epidote, Chl=chlorite, Qtz=quartz, Lau=laumontite, Corr=corrensite, Py=pyrite, Fract=fracture(s), w/=with.*

Figure 5-44. *Overview showing the upper part of DZ1. At approximately 23 m there is a marked fault with epidote-cemented fault breccia that contains small, angular fragments of pink, altered metagranite and quartz. This is post-dated by white vein quartz.*

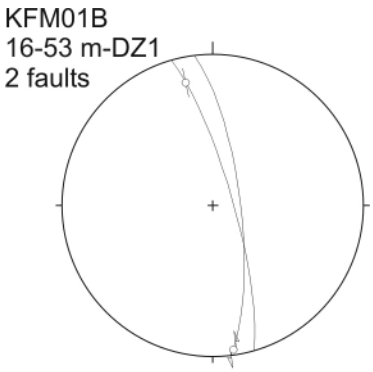

Figure 5-45. *Stereoplot of fault slip data in DZ1 (KFM01B).*

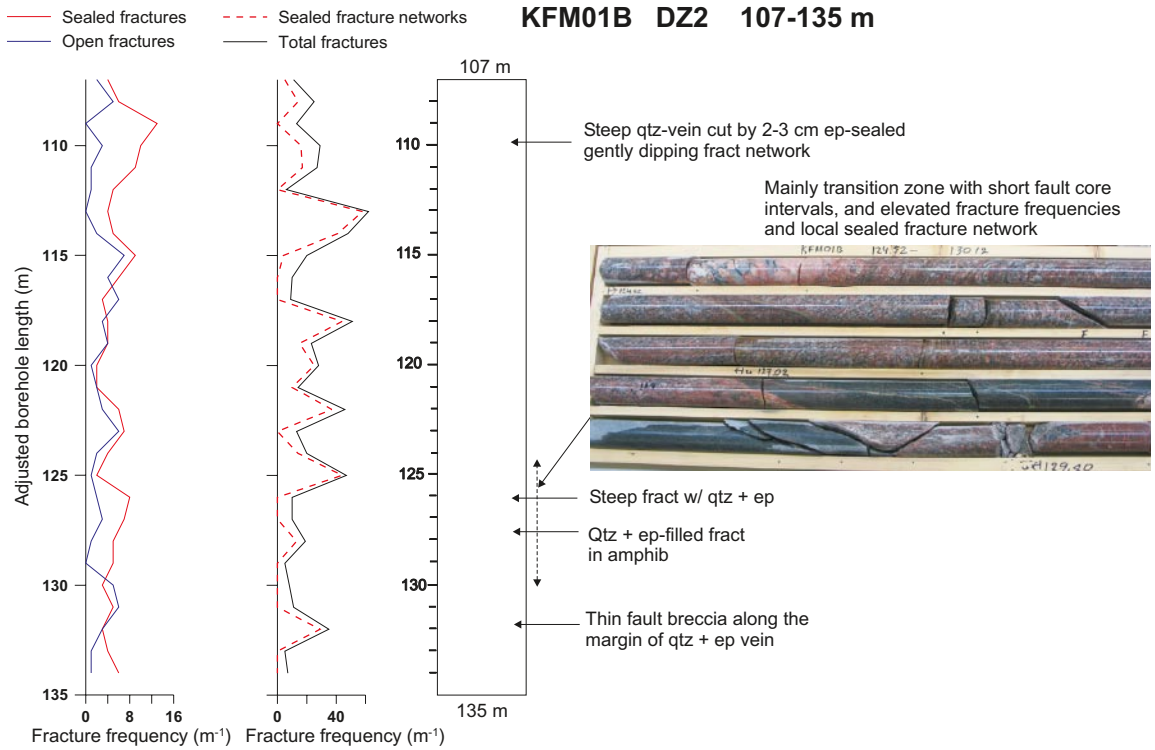

Figure 5-46. *Simplified drawing of DZ2 showing brittle structures. The photo (inset) shows the section between 124.5 and 129.8 m.*

KFM01B: 415–454 m – DZ3

Medium- to coarse-grained, pinkish grey metagranite with subordinate pegmatite, fine-grained granite and amphibolite. The fracture frequency is variable from a low background level to high in, and adjacent to, marked intervals with strong crushing of the core (Figure 5-47). Most fractures are thin and sealed with minerals including epidote, quartz, chlorite, laumontite, calcite and hematite.

At 418.5 m there is calcite-cemented breccia containing angular fragments of dark reddish, fine-grained cataclasite containing epidote + quartz + opaques (?) (Figure 5-47). The calcite occurs as blade-shaped euhedral crystals that appear to have grown normal to fractures in the cataclasite. Laumontite-sealed fracture networks with local cataclasite are also common in this deformation zone.

Four NNW-SSE trending steep faults are observed with different types of displacements: two faults with dip-slip normal striae (chlorite ± calcite), one with dip-slip reverse striae, and one with left-lateral strike-slip striae (chlorite ± epidote) (Figure 5-48).

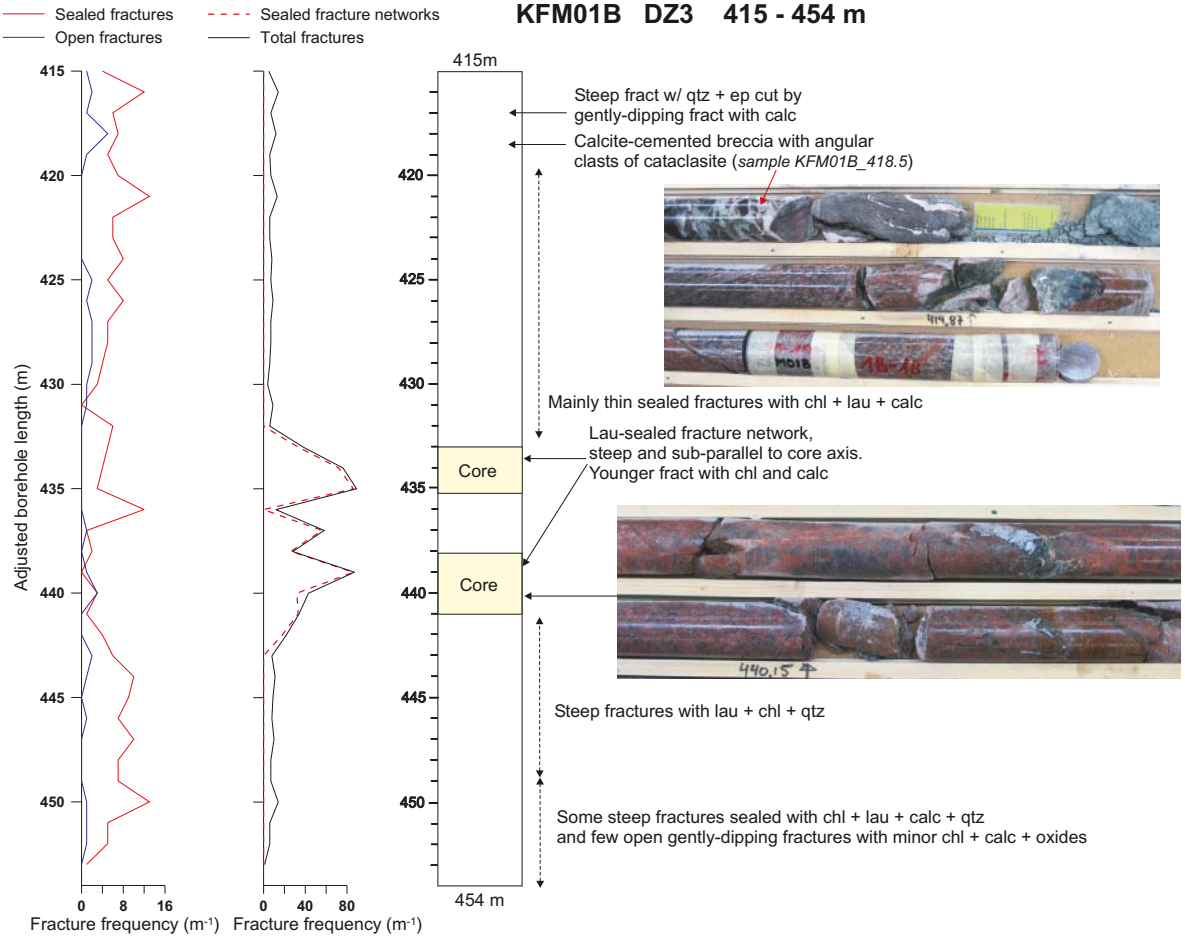

Figure 5-47. *Simplified drawing of DZ3 with photo insets showing the most prominent brittle structures. Fragments of reddish, fine-grained cataclasite in calcite-cemented breccia occurs at 418.5 m (see upper photo). Note strong crushing of the core below the calcite-cemented breccia. Abundant laumontite-sealed fractures and fracture networks (433–434 m) are similar to those present in KFM01A (Figure 5-40). Some fractures contain chlorite and/or calcite. From about 438 m there are abundant fractures sealed with laumontite. In several places, there are thin zones with cemented breccias containing small fragments of quartz and host rock. Younger fractures contain chlorite and calcite. Note reddish staining in the host rock.*

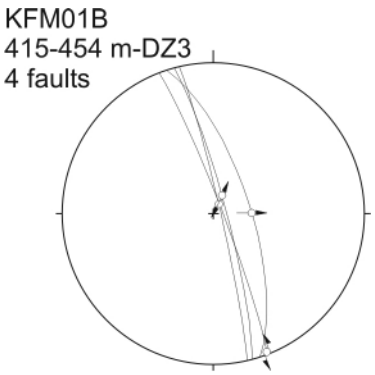

Figure 5-48. *Stereoplot of fault slip data in DZ3 (KFM01B).*

5.2.4 KFM02A

This borehole is located in the central southeast part of the investigation area (Figure 5-40). The borehole is oriented 276/85 has a length of 1,002 m /Carlsten et al. 2004b/. Five deformation zones were investigated. One of these (DZ6) has a length of 105 m, whereas the remaining zones have a total length of 61 m (Table 5-1). Along the investigated part of the core, 49 fault slip data have been obtained. The stereoplot with all the data for the measured fault planes (Figure 5-49) shows a significant spatial dispersion of the strikes. However, faults striking NE-SW are predominant. The faults dip mainly at 30, 40 and 50 degrees to the SE with mostly dip-slip reverse slickensides being predominant. The faults dip mainly at 30, 40 and 50 degrees to the SE with mostly dip-slip reverse slickensides (Figure 5-49).

In the studied area, notable seismic reflectors that are reported to be dipping gently southeast were interpreted as thrusts by /Juhlin and Stephens 2006/. Gently SE-dipping faults that exhibit reverse sense of movement are common in the deformation zones of KFM02A (see below). Thus, the analysis of kinematic data from KFM02A is consistent with the conclusion of /Juhlin and Stephens 2006/.

KFM02A: 110–122 m – DZ2

Medium-grained metagranite with subordinate amphibolite/foliated metadiorite and pegmatitic granite. The borehole was studied from ca. 101 m and the core is missing between ca. 112 and 116.5 m. Fractures have mainly gentle to intermediate dips and are sealed and/or coated by chlorite, calcite, hematite, adularia and clay minerals. Minor prehnite and pyrite are also present. Reddish alteration of the wall rock is common. Elevated fracture frequency occurs at ca. 110 to 111 m and locally abundant fractures with chlorite are present at 117.3 m. Minor fractures filled with calcite occurs in somewhat altered metagranite with clay minerals (118–119 m). The deformation zone is considered a transition zone with short intervals of fault core development (Figure 5-50).

Six faults with chlorite slickensides were observed inside and immediately above the inferred zone DZ2 (Figure 5-51). One of the predominant fault sets as identified in Figure 5-49, is well represented in this zone and clearly reflects reverse faults that strike NE-SW and dip 40 degrees to the southeast.

KFM02A: 160–184 m – DZ3

The rock types in this zone are interlayered medium-grained metagranite to metagranodiorite and finer-grained metagranitoid with subordinate heterogeneous mafic rocks and amphibolite. Minor pegmatite veins are present.

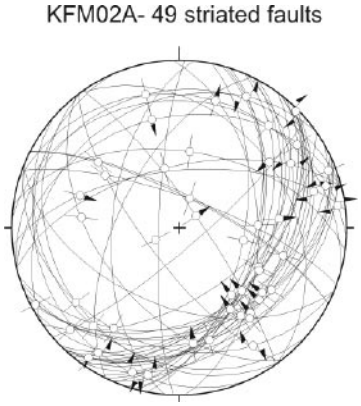

Figure 5-49. *Stereoplot showing all the fault slip data collected along all the studied DZ of drill core KFM02A.*

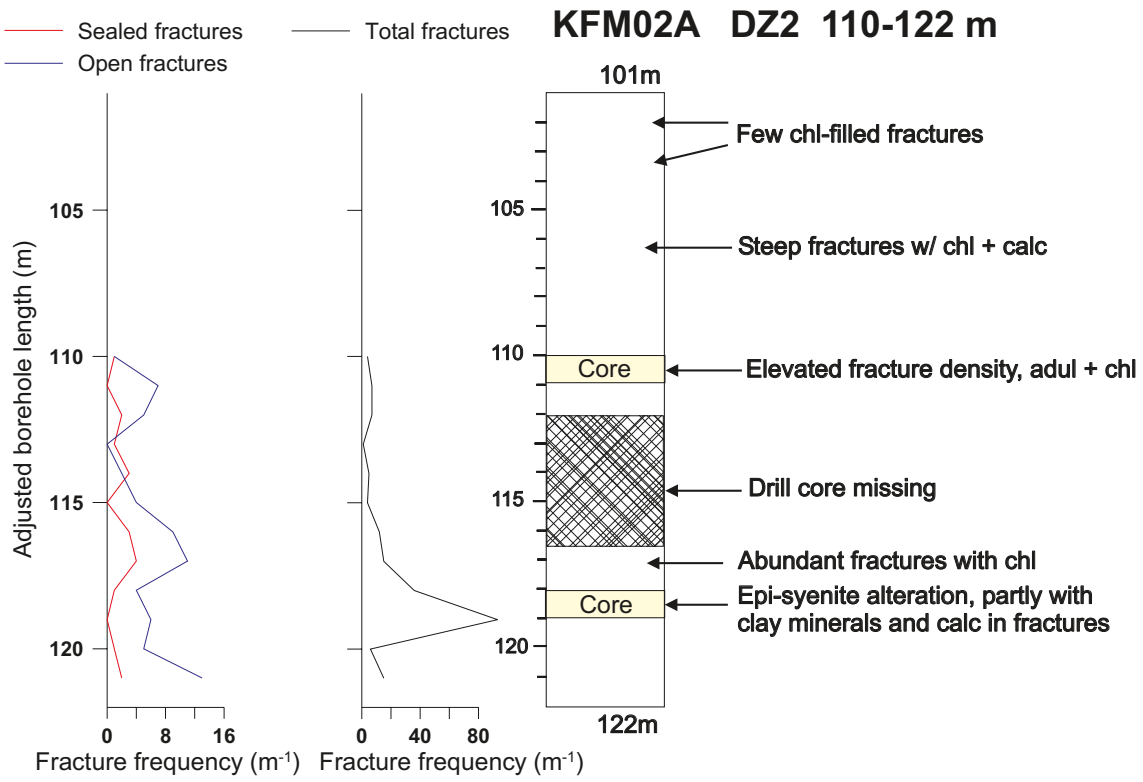

Figure 5-50. *Simplified drawing of DZ2 showing the most prominent occurrences of brittle structures. Note that the core is missing over several metres from 112 metres. Elevated fracture frequency occurs at ca. 110 to 111 m and locally abundant fractures with chlorite are present at 117.3 m. Fractures filled with calcite occurs in somewhat altered metagranite with clay minerals (118–119 m).*

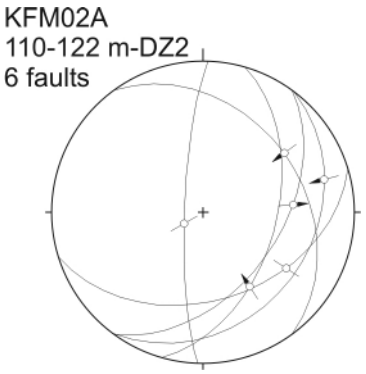

Figure 5-51. *Stereoplot of fault slip data in DZ2 (KFM02A).*

The frequency of sealed and open fractures is moderate /Carlsten et al. 2004b/, and the zone in general is a transition zone /Munier et al. 2003/. Fractures are predominantly gently-dipping and are sealed or coated by chlorite and/or calcite and less commonly by quartz, corrensite and oxides. The rocks are somewhat red-stained, and there are three intervals (171.3–172; 174.1–175.2; 179.2–180) showing strong alteration yielding a vuggy metagranite (epi-syenitization) (Figure 5-52).

Sixteen striated faults were observed within the zone. The NE-SW gently dipping set of faults are similar to those in the overlying zone DZ2. Most of these have chlorite striation, in cases with corrensite, calcite or minor hematite. In general, they may constitute a conjugate system of dip-slip reverse faults (Figure 5-53). Other oblique to strike-slip slickensides are present on the same fault trends.

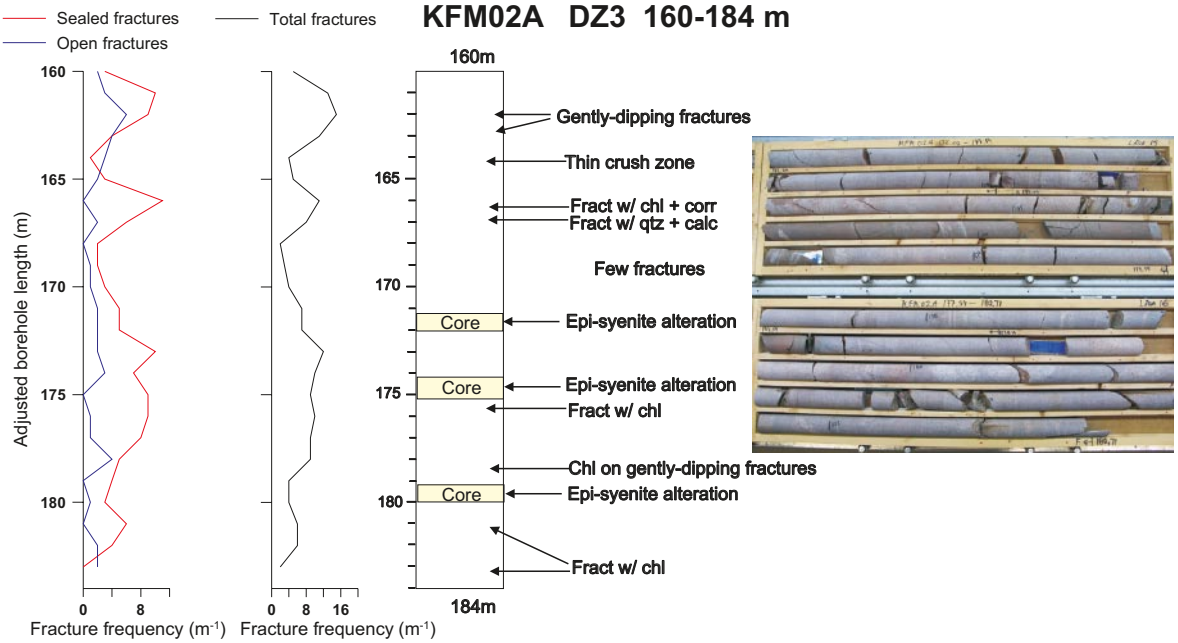

Figure 5-52. *Simplified drawing of DZ3 showing the most prominent brittle structures. The photo shows the lower section of the zone. Note the generally moderate fracture frequency and variable reddish staining of the core.*

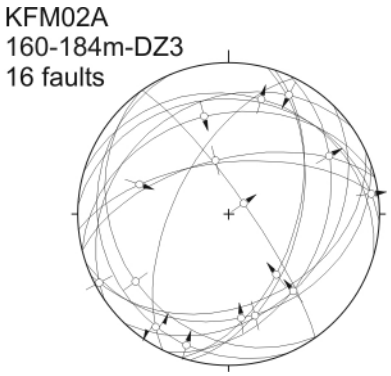

Figure 5-53. *Stereoplot of fault slip data in DZ3 (KFM02A).*

KFM02A: 415–520 m – DZ6

Medium- to coarse-grained, grey to weakly pink metagranite. Subordinate pegmatite and finer-grained metagranite and sporadic occurrences of fine-grained metadiorite and amphibolite (468–470.5 m and ca. 477 m). Early structures carry quartz and epidote. Other fracture minerals include chlorite and calcite, and less commonly prehnite, hematite and laumontite. The fracture frequency in this very wide deformation zone is generally low (< 5/m) to moderate (6–10/m). Over a long section (ca. 430–480 m) there are few fractures, and the status of this interval as part of a deformation zone is questionable. Higher fracture frequencies are more common in the upper and lower parts of the deformation zone, but even in these parts there are sections where several meters of core may have only a few fractures (Figure 5-54).

At ca. 439 m: minor fractures/faults with slickensides occur at the boundaries of amphibolite and fine-grained metadiorite.

At 462.5, 463.9 and 466 m: steeply dipping minor faults with chlorite and calcite showing oblique slip slickensides.

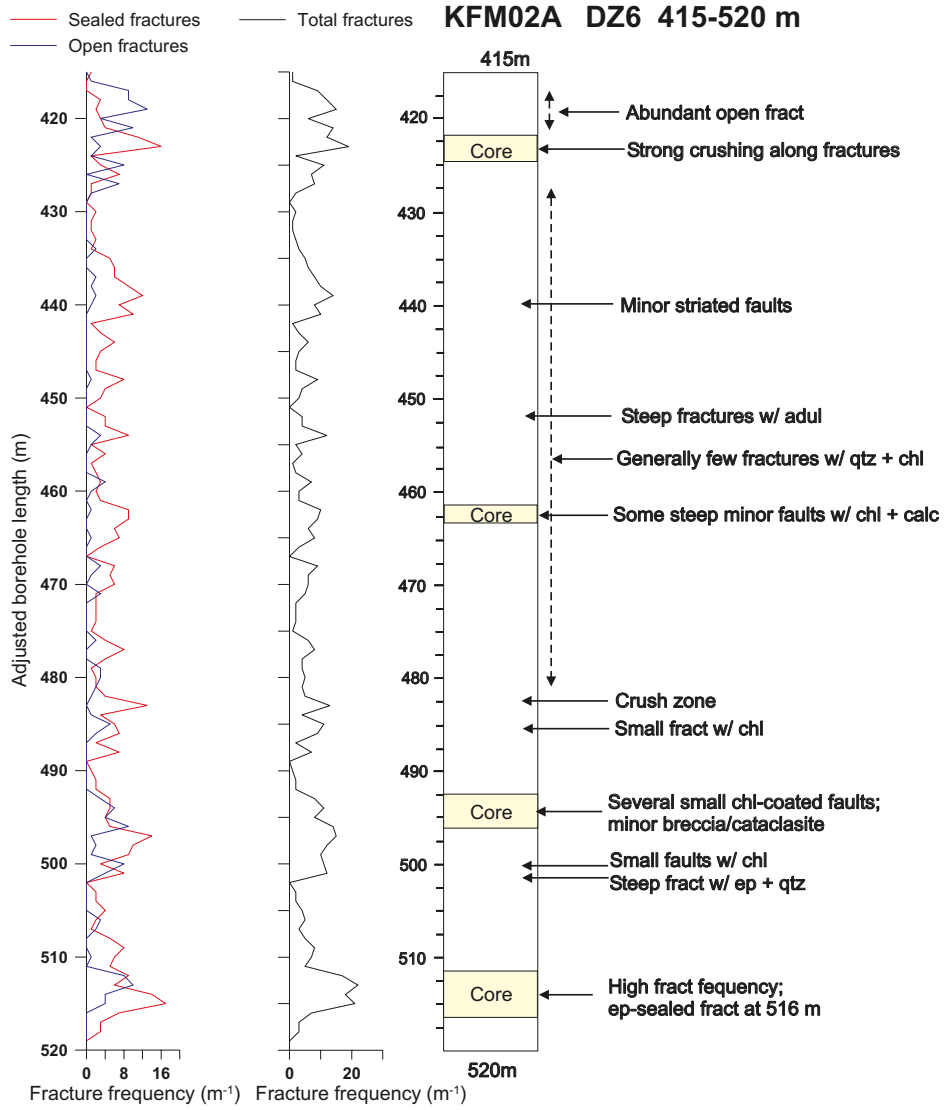

Figure 5-54. *Simplified drawing of DZ6. Note that the interval between 430 and 480 m has low fracture frequency; higher fracture frequencies occur towards the upper and lower end of the deformation zone.*

Interval 492–498 m: several minor chlorite-coated faults, partly with stepped surfaces, and with slickensides showing approximately strike slip as well as dip slip movement. Minor breccia/cataclasite.

Interval 512.5–517 m: high fracture frequency. At 516.0 m there is a dense array of epidote-sealed fractures that cut metadiorite and altered metagranitoid host (Figure 5-55).

The NE-SW gently dipping reverse faults are still present as in the other overlying zones (Figure 5-56). However, the chlorite slickensides along the faults mostly indicate strike-slip displacement. Most of the data were obtained in the deeper part of the deformation zone (Figure 5-56).

KFM02A: 893–905 m – DZ8

This is a narrow deformation zone in medium- to coarse-grained metagranite with minor pegmatite and amphibolite. Open fractures tend to have gentle dips. There is a marked increase in the frequency of sealed fractures in the lowermost part of the zone. Otherwise fracture frequencies are low to moderate with mainly chlorite-coated fractures and minor faults. Some fault surfaces are distinctly polished. However, the sense of displacement could be determined on only one of the faults. Note also the presence of variably oriented faults in the interval.

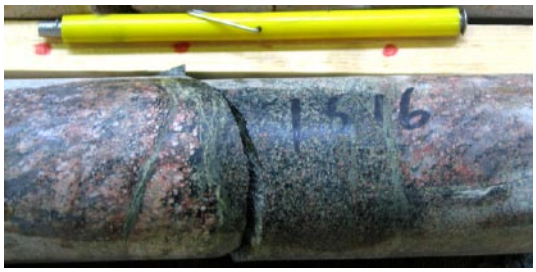

Figure 5-55. *Dense array of epidote-sealed fractures cut mesocratic diorite and altered metagranite. DZ6 (KFM02A, 516 m).*

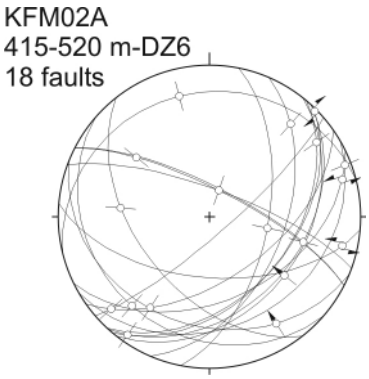

Figure 5-56. *Stereoplot of fault slip data for different sections of DZ6 (KFM02A).*

Five fault slip data defined by striations on polished, chlorite-coated fault surfaces have been measured. As in the previously described DZ along the drill core KFM02A, the main trend is gently southeast-dipping NE-SW faults with dip-slip striae (Figure 5-57). One of these faults is clearly reverse.

KFM02A: 922–925 m – DZ9

Another narrow deformation zone in grey, fine- to medium-grained metagranitoid with some pegmatite and amphibolite. Both open and the more abundant sealed fractures tend to have gentle to intermediate dips. Fracture minerals are mainly chlorite, and some quartz, laumontite and hematite. Fault surfaces with slickensides defined by calcite and laumontite are oriented N-S to NE-SW. Note dip-slip sense of displacement, in one case with reverse movement (Figure 5-58).

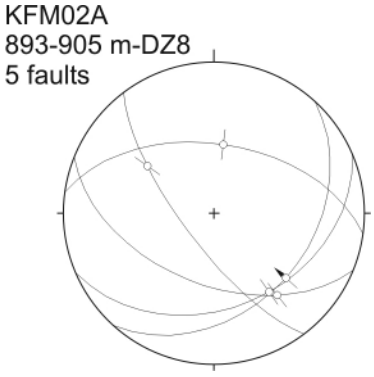

Figure 5-57. *Stereoplot of fault slip data in DZ8 (KFM02A)*

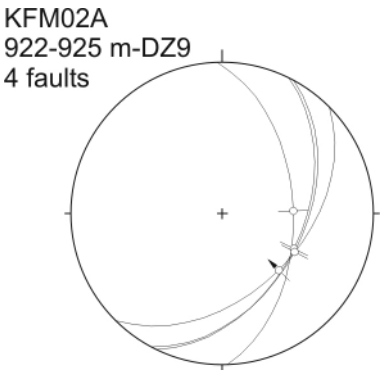

Figure 5-58. *Stereoplot of fault slip data in DZ9 (KFM02A).*

5.2.5 KFM03A

This steep borehole (272/86) has a length of 1,001 m and is located in the southeast part of the investigated area (Figure 5-40). Five previously defined deformation zones /Carlsten et al. 2004e/ with a total length of 78 m were investigated. They are mainly transition zones with short intervals of fault core /Munier et al. 2003/. In general, fractures with quartz and epidote are post-dated by calcite- and laumontite-sealed fractures. The borehole as a whole has predominantly gently-dipping brittle structures that are clearly identified using geophysical methods /Juhlin and Stephens 2006/. However, very few faults provided kinematic data.

KFM03A: 356–399 m – DZ1

In the upper part of the zone, there is grayish pink pegmatitic granite with minor occurrences of fine- to medium-grained metatonalite and quartz-bearing metadiorite. Below 377–378 m the core is dominated by medium-grained metatonalite to quartz-bearing metadiorite with hornblende and biotite, and minor amphibolite and pegmatite. The zone in general has few and mainly gently-dipping open and sealed fractures, with a total number of ca. 180 fractures over the entire interval /Carlsten et al. 2004e/. However, an increase in fracture frequency over short intervals has, in combination with geophysical and radar reflector data, established this interval as a deformation zone (see /Juhlin and Stephens 2006/ for en extensive treatment).

Fractures may carry chlorite, calcite and rarely laumontite, but the majority of the fractures are barren. A few narrow intervals (< 10 cm) show stronger crushing and reddish alteration, e.g. at the base of the zone at ca. 398 m (Figure 5-59).

The only two fault slip data are a steep N-S striking plane with a weak strike-slip striation, and a gently south-dipping plane with dip-slip chlorite striae associated with strong crushing and oxidation of the host rock (Figure 5-60). The sense of movement along the faults could not be determined.

KFM03A: 448–455 m – DZ2

The rock type in this zone is a foliated, medium-grained greyish pink metagranite to metagranodiorite with some amphibolite and minor pegmatite. In the zone as a whole, there are 48 fractures that strike E-W with steep to intermediate dips. In addition there are gently-dipping fractures. Most fractures are sealed; minerals include early quartz and epidote, chlorite and corrensite, and late calcite. At 450.6 m, a fine fracture network sealed with quartz + epidote is cut by open fracture coated with chlorite + corrensite. Apart from this narrow interval that defines as a fault core, the deformation zone is regarded a transition zone /Munier et al. 2003/.

Striation was observed on one steep NE-SW strike-slip fault with chlorite + calcite fill. The only measurement in this zone is shown in Figure 5-61.

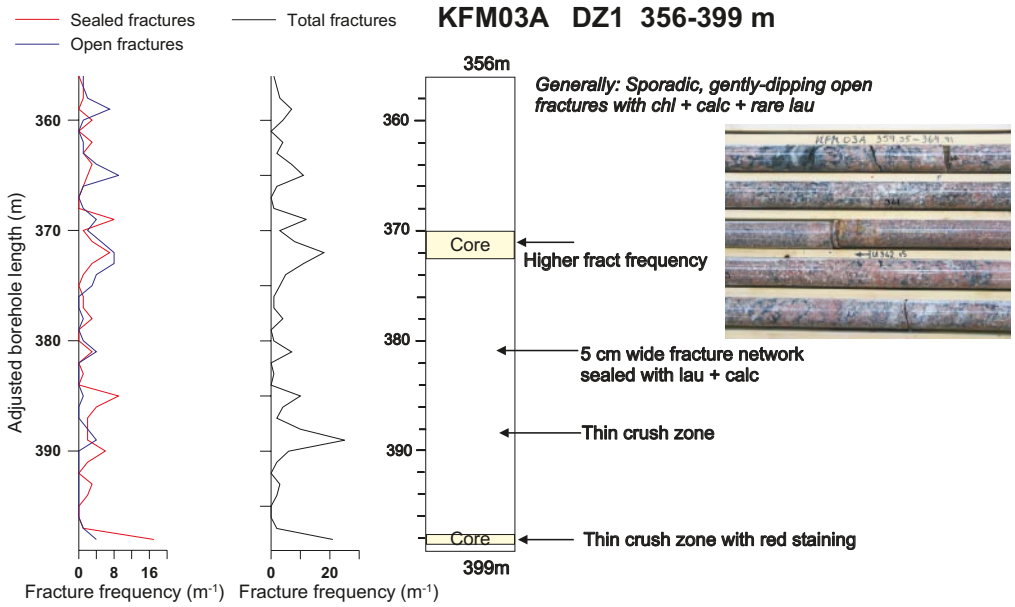

Figure 5-59. *Simplified drawing of DZ1. The photo inset illustrates the pegmatitic granite in the upper part of the deformation zone. Note that this interval has a low fracture frequency. Higher frequencies of gently dipping fractures occur in narrow zones that are clearly identified using geophysical methods.*

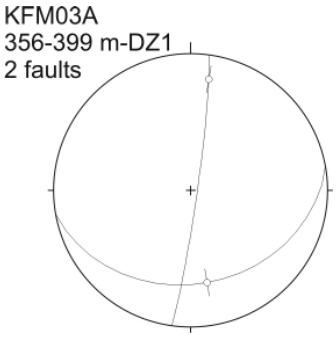

Figure 5-60. *Stereoplot of fault slip data in DZ1 (KFM03A).*

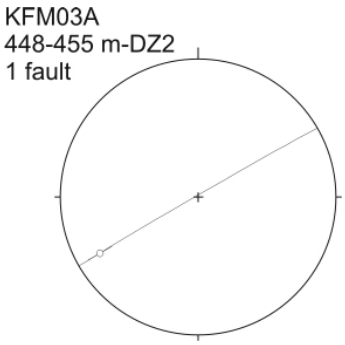

Figure 5-61. *Stereoplot of fault slip data in DZ2 (KFM03A).*

KFM03A: 638–646 m – DZ3

Narrow deformation zone with rock types similar to DZ2 (see above). The zone has a total of 50 fractures /Carlsten et al. 2004e/, most of which are gently dipping and sealed/coated with quartz, epidote, chlorite and late calcite and laumontite. Following the definition of /Munier et al. 2003/ this zone is regarded a transition zone. Pink alteration and whitening of feldspar in the metagranitoid over a 3 m interval below amphibolite at 641–642 m. No fault slip data were obtained, and there is no evidence of shear deformation along the fractures in this zone.

KFM03A: 803–816 m – DZ4

Narrow deformation zone with rock types similar to DZ2 (see above). The zone contains less than 50 fractures. Most of these are gently dipping and filled/coated mainly with quartz, epidote, chlorite, calcite and corrensite; rare hematite and pyrite also observed. Increase in fracture frequency occurs in the upper (ca. 804 m) and lower parts of the zone, where there is pink alteration and abundant, partly open, fractures with quartz + epidote + calcite at 813.9–815 m. This interval is regarded a fault core /Munier et al. 2003/. Otherwise the deformation zone is regarded as a transition zone. No fault slip data were obtained, and there is no evidence of shear deformation along the fractures in this zone.

KFM03A: 942–949 m – DZ5

Narrow deformation zone with rock types similar to DZ2 (see above). The zone has less than 40 and generally gently-dipping, mostly sealed fractures with chlorite, hematite, calcite and coating of clay minerals. However, there is a slight increase in fractures at the base of an amphibolite. Pink alteration and a few fractures with chlorite + corrensite at ca. 946.5 m. This narrow interval is considered a fault core, however, in general the zone is a transition zone (/Munier et al. 2003/). No fault slip data were obtained, and there is no evidence of shear deformation along the fractures in this zone.

5.2.6 KFM03B

This is a short borehole (264/85) with a length of 101.5 m (Figure 5-40). One 5 m wide deformation zone was investigated.

KFM03B: 62–67 m – DZ2

This deformation zone is defined as 5 m wide occurring in medium- to coarse-grained, grey-pink metagranite with minor pegmatite and fine-grained mafic amphibolite. There are 17 fractures in the zone /Carlsten et al. 2004e/, some of which are sealed with quartz + epidote (also above the DZ), and some coated with chlorite and calcite. Between 65 and 66 m the core is highly fractured and broken into variably sized pieces forming a fault core. The rock is oxidised with quartz and epidote on broken fragments (Figure 5-60). Apart from this crush zone, which may be highly conductive, there is very little deformation of the drill core. No fault slip data were obtained, and there is no evidence of shear deformation along the fractures in this zone.

Figure 5-62. *The drill core is highly fractured and broken into variably sized pieces. The rock is oxidised with quartz and epidote on broken fragments DZ2, ca. 65 m (KFM03B).*

5.2.7 KFM04A

This borehole is 1,001 m long and begins to the southwest of the investigation area and is oriented 045/60, i.e. directed towards the investigation area to the northeast (Figure 5-40). Three deformation zones defined by /Carlsten et al. 2004c/ with a combined length of 71 m were investigated.

A total of 29 fault slip data were obtained from the investigated deformation zones. A predominant set of vertical fault planes are oriented approximately NW-SE with slickensides that show both dip slip and strike slip displacement. Another set with less abundant faults that strike ENE-WSW is predominantly strike slip (Figure 5-63). However, with one exception the relative sense of movement along the faults could not be determined.

KFM04A: 202–213 m – DZ2

The host lithology is a strongly foliated, medium-grained metagranite with minor pegmatitic granite, amphibolite and finer-grained metagranitoid. Steeply dipping, sealed fractures occur in addition to important gently-dipping, open fractures. Fracture minerals include calcite, hematite and chlorite and less commonly laumontite and epidote. Fracture frequencies of open and sealed fractures are generally 10–20/m /Carlsten et al. 2004c/. At 212 m a cataclasite cuts the metagranite. The fault rock consists of variably sized angular to sub-rounded, rotated fragments of the host metagranite set in a fine-grained cataclasite groundmass (Figure 5-64). The cataclasite is cut by 1) thin veins filled with euhedral calcite, and 2) a vein of hematite-decorated laumontite (see Figure 5-65).

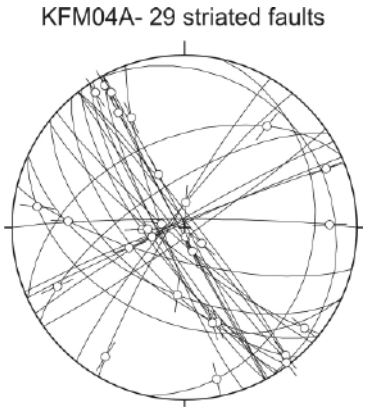

Figure 5-63. *Stereoplot showing all the fault slip data collected along all the studied DZ of drill core KFM04A.*

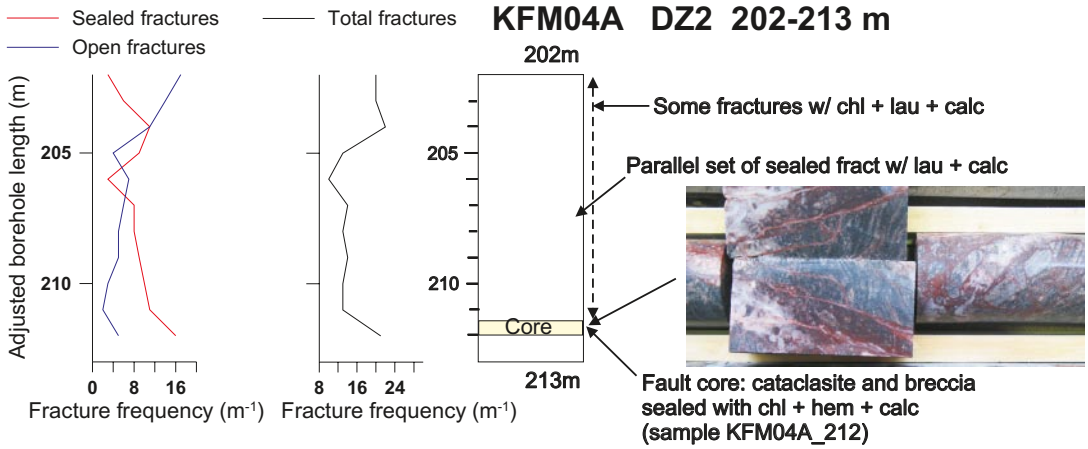

Figure 5-64. *Simplified drawing of DZ2. The photo (inset) illustrates the fault rock at ca. 212 m. It consists of variably sized angular to sub-rounded, rotated fragments of the host metagranite set in a fine-grained cataclasite groundmass (for details, see below).*

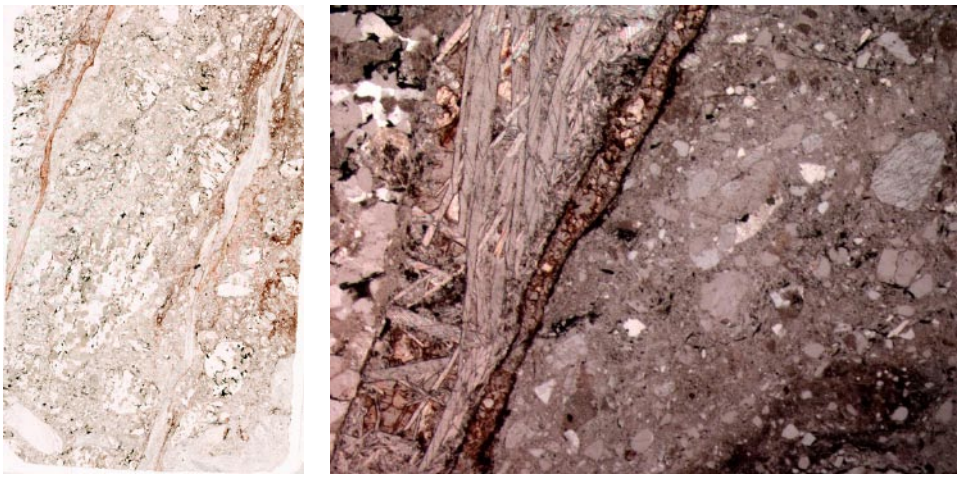

Figure 5-65. *Scanned thin section (left) from sample KFM04A_212 showing angular to sub-rounded fragments of the host metagranite randomly oriented in a fine-grained cataclasite. The field of view is ca. 20 mm wide. A photomicrograph (right) reveals details from the upper left part of the thin section. The fragmented nature of the cataclasite is clearly seen. Platy, euhedral calcite is post-dated by a marked vein of hematite-decorated laumontite that crosses the photograph. The field of view is ca. 5 mm wide. DZ2 (KFM04A).*

Two steep faults with chlorite, hematite and minor calcite that belong to the more abundant sets trending NW-SE and ENE-WSW are characterised by high angle striae, i.e. predominantly dip-slip displacement (Figure 5-66). A gently east-dipping N-S fault with chlorite, hematite and calcite is also present with strike-slip striae. The sense of shear could not be determined on any of the faults.

KFM04A: 232–242 m – DZ3

Structural observations were obtained from the interval 229–244 m, i.e. about 5 m outside the extent of the defined zone. Lithology: medium-grained, strongly foliated, mostly grey-pink to pink metagranite to metagranodiorite with finely recrystallised biotite; subordinate amphibolite (1 m). In general, the zone has variably oriented steep to gently dipping sealed fractures and a set of flat to gently dipping open fractures. Predominant fracture minerals are chlorite, calcite, laumontite, hematite, chlorite and epidote (Figure 5-67). Epidote appears as an early fracture fill postdated by laumontite, hematite and calcite. The upper part of the investigated interval (229–237 m) is considered a transition zone with local fault core /Munier et al. 2003/. The lower part (237–244 m) is considered to be a fault core with relatively abundant sealed fractures and small faults (Figure 5-68). In places there are abundant laumontite-sealed fractures and breccias with local cataclasite (Figures 5-69 and 5-70).

Striations on chlorite+hematite-coated NE-SW-trending fault surfaces were observed in four cases. Three of the faults show strike-slip to oblique slip relative motion, while the fourth shows mainly dip-slip displacement. However, the sense of motion could not be determined (Figure 5-71).

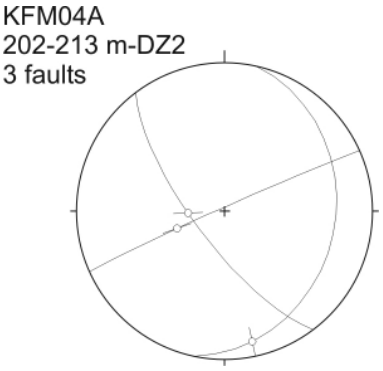

Figure 5-66. *Stereoplot of fault slip data in DZ2 (KFM04A).*

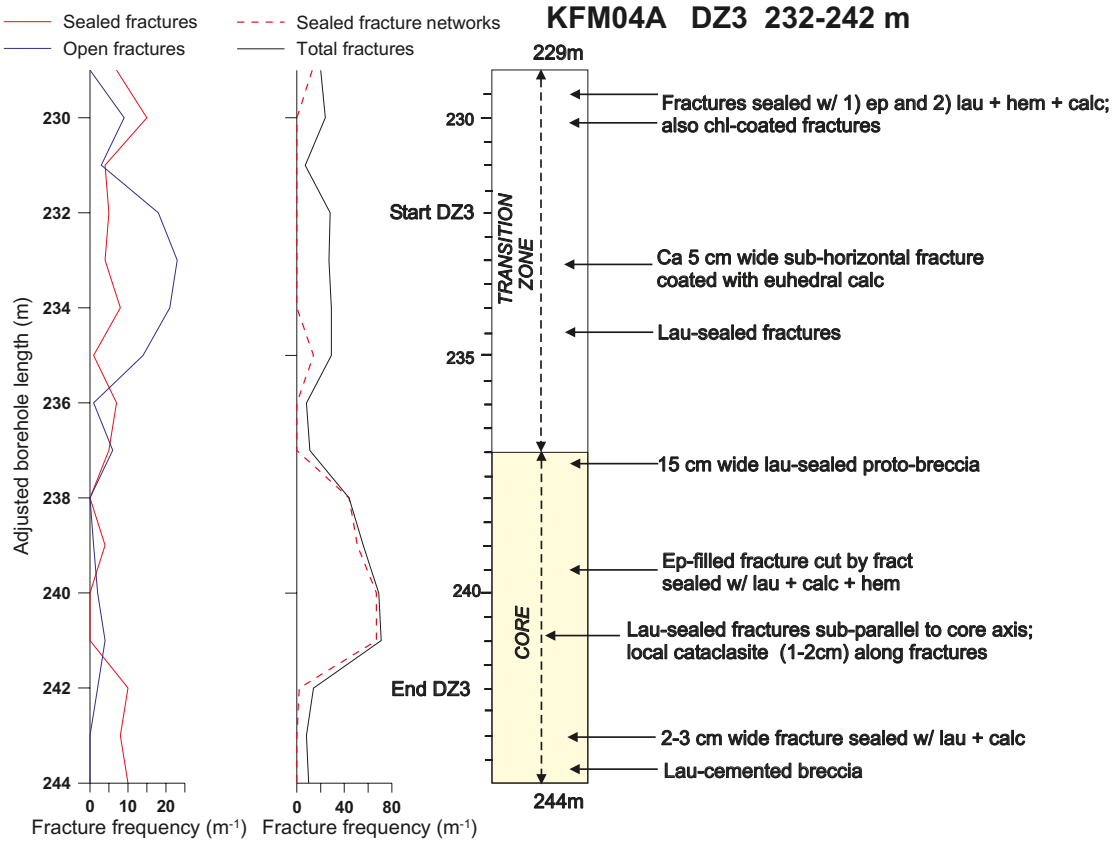

Figure 5-67. *Simplified drawing of DZ3. The upper part of the investigated interval (229–237 m) is considered a transition zone with local fault core /Munier et al. 2003/. The lower part (237–244 m) is a fault core with relatively abundant sealed fractures and small faults. Specific features include: At 229.4 m: Fractures sealed with 1) epidote; 2) laumontite+hematite+calcite. Also chlorite-covered fractures with calcite and prehnite (?). At 237.3 m: Laumontite-cemented proto-breccia (ca. 15 cm wide); little rotation of the clasts. From 237 m and below (see Figure 5-68): Faults and network of sealed fractures sub-parallel to the core axis. Very fine-grained zones of cataclasite (laumontite+hematite+calcite), 1–2 cm wide, are developed along the faults. Note that strong fracturing continues below the defined base of the zone at 242 m.*

Figure 5-68. *Overview showing the lower part of DZ3. Note the abundant fractures and faults that are sub-parallel to the core and filled with laumontite and calcite.*

Figure 5-69. *Section of core showing laumontite-cemented breccia and cataclasite. KFM04A, DZ3; 244.10 m.*

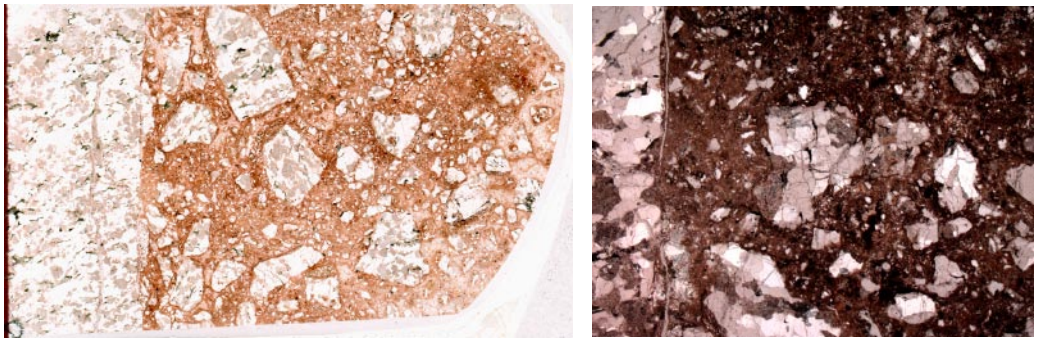

Figure 5-70. *A) Scanned thin section KFM04A_244.1 showing sharp contact between foliated metagranite to metagranodiorite (left part) and fine-grained cataclasite with angular, rotated fragments of the host rock. Field of view is 35 mm wide. B) Photomicrograph showing details from the thin section shown in A). The matrix is an extremely fine-grained cataclasite decorated by hematite. Field of view is ca. 5 mm wide.*

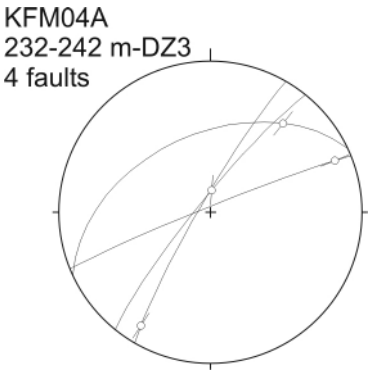

Figure 5-71. *Stereoplot of fault slip data in DZ3 (KFM04A).*

KFM04A: 412–462 m – DZ4

The rock types present in this zone are a variety of interlayered, grey to pink, fine- and medium-grained metagranites with strong foliation. In parts, there are strongly foliated biotite-rich metagranites with muscovite, fine to medium-grained metadioritic to amphibolitic rocks, and minor pegmatite. In the zone, there are fractures and networks of fractures mainly sealed by laumontite, calcite, chlorite, and hematite and less commonly quartz and epidote. Some epidotization, reddish alteration (hematite oxidation) and minor clay alteration occurs in parts of the zone /Carlsten et al. 2004c/.

Several sections of the deformation zone are characterized by abundant, steeply dipping laumontite-sealed fractures and fracture networks that are oriented sub-parallel to the core axis. Local brecciation of the host rock has occurred along these faults. Good examples of this are at e.g. 413–419 m, 439–443 m, and 450–452 m. Later growth of platy calcite characterizes several of these fractures. Fractures and fracture networks with epidote and quartz are less common. Examples are present e.g. at 430–431 m (see Figure 5-72), and 434–435 m. These fractures generally predate the laumontite-sealed fractures. The entire deformation zone is a transition zone with some intervals having higher fracture frequencies defined as fault core according to /Munier 2003/.

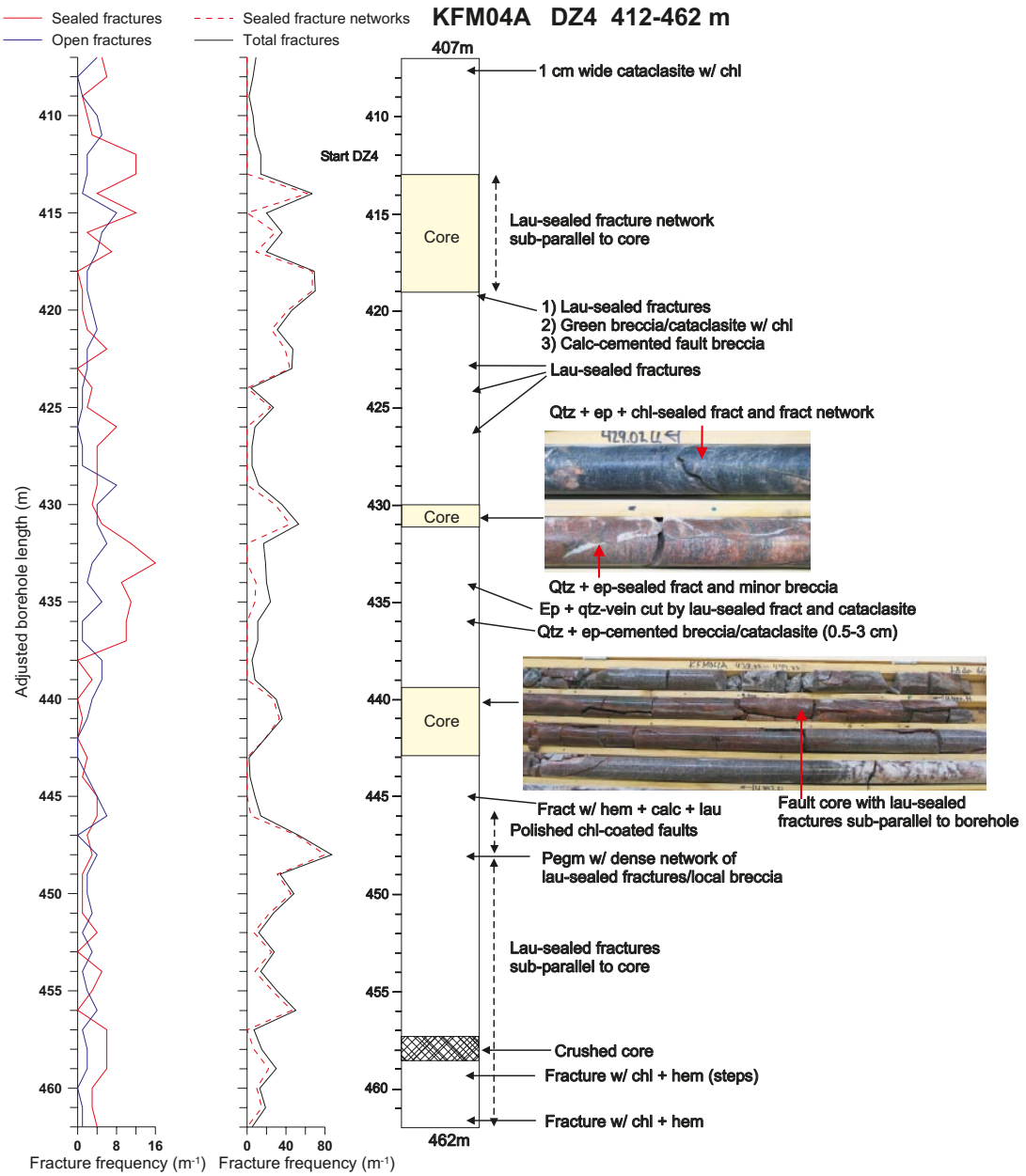

Figure 5-72. *Simplified drawing of DZ4. A number of sections along this interval are characterized by abundant laumontite-sealed fractures and fracture networks. The photo of the core at ca. 431 m shows a reddish, oxidized host rock cut by a sharply defined fault and fracture network sealed mainly with epidote and quartz. The amphibolite (ca. 430 m, upper part) is cut by a quartz+epidote+chlorite-sealed minor fault and fractures. These fractures predate the laumontite-sealed fractures. Calcite-cemented fractures and fault breccias are younger than the laumontite-sealed fractures.*

Inspection of the core began at 407 m. At 407.4 m, a 1 cm wide greenish, chlorite-rich semi-ductile shear zone predates thin cataclasites (Figure 5-73). The zone is also cut by a polished fault surface with chlorite striation.

At 419.2 m, a fault rock was collected for thin section analysis. This sample shows a sequence of events involving deformation and growth of minerals beginning with alteration (chlorite, epidote) associated with cataclasis/brecciation of the host rock. This stage was followed by reactivation and growth of laumontite and feldspar (?), and finally growth of euhedral quartz followed by calcite on the walls of open voids and fractures (see Figures 5-74 and 5-75).

The zone contains several fault surfaces with good striations defined by chlorite, laumontite, calcite and hematite (see Figure 5-6 in /Nordgulen and Braathen 2005/). Several faults have good chlorite striations. In some cases, the lineation is defined by uneven grooves coated with chlorite. However, the relative motion on the faults could generally not be confidently determined. One of the faults has a stepped surface suggesting sinistral sense of movement (Figure 5-76). The majority of the striated faults are oriented NW-SE to WNW-ESE and show both strike-slip and dip slip movement defined mainly by chlorite, and in a few cases also with hematite and laumontite (Figure 5-77). A subordinate set of striated NE-SW faults are sealed with laumontite, however, the age of these faults with respect to NW-SE faults was not clarified.

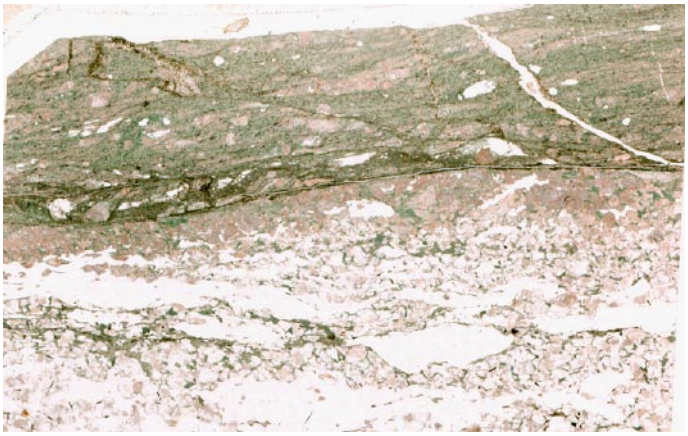

Figure 5-73. *Scanned thin section from DZ4 of KFM04A_407.4. A ca. 1 cm wide greenish, chlorite-rich semi-ductile shear zone (upper half) predates a thin cataclasite occurring along a planar zone along the shear zone. The vein-like feature in the upper left has no mineral fill. Field of view is 35 mm wide.*

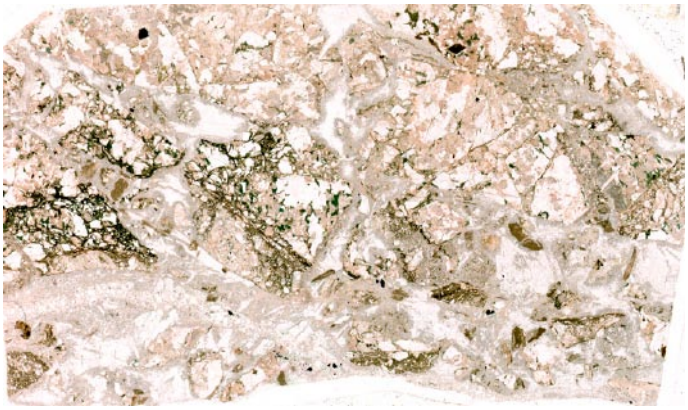

Figure 5-74. *Scanned thin section from DZ4 of KFM04A_419.2. The sample shows 1) early alteration (chlorite, epidote) associated with cataclasis/brecciation of the host rock, 2) reactivation and growth of laumontite and feldspar(?), 3) growth of euhedral quartz followed by calcite on the walls of open voids and fractures (see Figure 5-75 below). The field of view is 35 mm wide.*

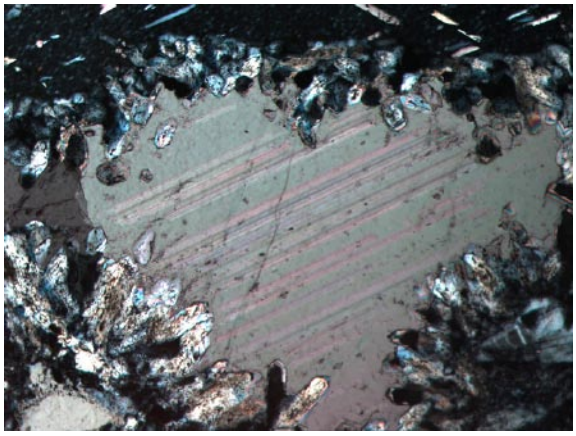

Figure 5-75. *Details from thin section KFM04A_419.2 shown in Figure 5-74. Growth of euhedral quartz followed by calcite has taken place on the walls of open voids and fractures in the fault rock. The field of view is ca. 1.3 mm wide.*

Figure 5-76. *Planar fractures with chlorite, hematite and laumontite. Note steps on the surface. Later laumontite-filled fractures intersect the fault surface. KFM04A, 459.3 m.*

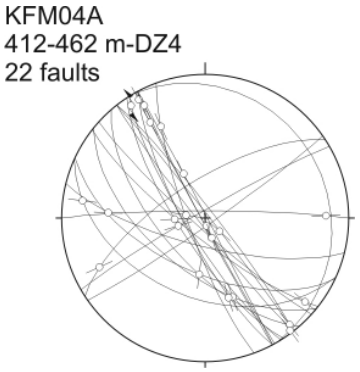

Figure 5-77. *Stereoplot of fault slip data in DZ4 (KFM04A).*

5.2.8 KFM05A

The borehole 1,003 m long is oriented 089/56. Three deformation zones /Carlsten et al. 2004d/, with a total length of 47 m were investigated. Very few kinematic data were retrieved from the inspected deformation zones.

KFM05A: 102–114 m – DZ1

In this zone, there is casing down to 110 m. The rock type is homogeneous, fine- to medium-grained, grey-pink metagranite with a strong planar fabric. Generally there is a low frequency of variably oriented sealed fractures and more abundant gently dipping open fractures. Open fractures with calcite and asphaltite and a couple of narrow zones with strong crushing of the core were observed near the base of the zone. There are a total of 102 fractures, and the deformation zone is classified as a transition zone with narrow crush zones that are considered to be local development of fault core. No fault slip data have been identified in the zone.

KFM05A: 416–436 m – DZ2

Medium- to coarse-grained metagranite, with minor occurrences of pegmatite and fine-grained metadiorite. The zone is characterized by an increase in the frequency of mostly sealed, NW- to NE-fractures with steep to intermediate dips. The total number of recorded fractures is ca. 140, and fracture minerals include quartz, epidote, chlorite, calcite, laumontite and rare prehnite. Moderate oxidation causes reddish colour in parts of the zone (see Figure 5-78). Thin zones (< 3 cm wide) of breccia and cataclasite occur in a few places (Figures 5-78, 5-79 and 5-80). The cataclasite are postdated by laumontite-sealed fractures. Two faults with striations were observed in this deformation zone (Figure 5-81).

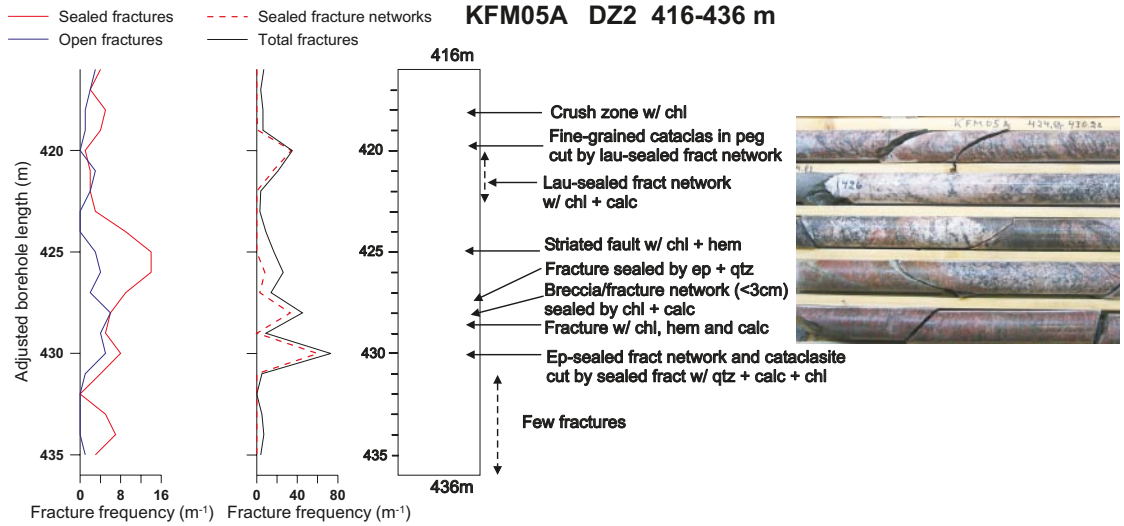

Figure 5-78. *Simplified drawing of KFM05A, DZ2. A number of different deformation products are present throughout the zone, however, relatively few fractures are present in the upper and lower part of the investigated section. A crush zone with chlorite is present near the top of the zone. The photo of the core shows the interval between ca. 425 and 430 m. Note moderate fracture frequency and weak reddish to pink alteration of the metagranite. Fractures are filled/coated with quartz + epidote, and chlorite + calcite ± laumontite ± hematite. Laumontite and calcite generally postdate quartz and epidote as fracture fill.*

Figure 5-79. *KFM05A, DZ2, ca. 419.8 m, up is to the left. Fine-grained cataclasite with fragments of the host metagranite. Note thin fractures in the hanging wall that relate to the cataclasite and a younger, reddish fracture filled with laumontite(?) close to the footwall of the cataclasite.*

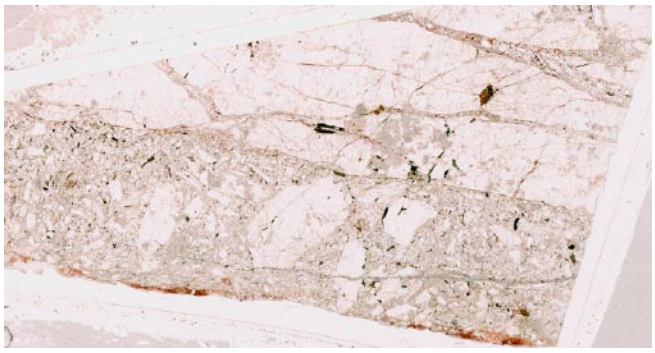

Figure 5-80. *Scanned thin section of sample KFM05A, DZ2, ca. 419.8 m. Note angular fragments of variable size in the cataclasite occupying the lower half of the section. Strong crushing has also occurred along variably oriented, discrete fractures in the hanging wall of the main cataclasite. The field of view is ca. 35 mm wide.*

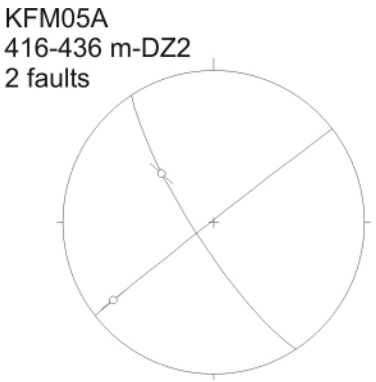

Figure 5-81. *Stereoplot of fault slip data in DZ2 (KFM05A).*

The two identified striated faults are steep and strike NW-SE and NE-SW, respectively. On the former plane, the oblique striae are defined by chlorite + hematite and plunge to the NW. The second plane exhibits strike-slip striae defined by chlorite + hematite and some calcite. In both cases, the sense of shear is not known (Figure 5-81).

KFM05A: 609–616 m – part of DZ3 (590–796 m)

This is a short interval of the core close to the upper limit of DZ3 (Figure 5-82). The rock type is a medium- to coarse-grained metagranite with minor amphibolite. Fractures occur mainly in the interval 610–614 m. At ca. 610 m, the rock is strongly fractured and sealed with laumontite, minor epidote, and calcite. A 2 cm wide cemented fault breccia occurs in this interval. Similar strong fracturing with local brecciation is present around 612 m and 613 m.

Chlorite striation showing strike-slip movement was observed on one N-S-oriented fault plane (Figure 5-83).

KFM05A: 712–720 m – part of DZ3 (590–796 m)

Short interval in the lower part of DZ3. The rock type in the upper part of the interval is a medium- to coarse-grained metagranite with minor amphibolite. Finer-grained pale to grey metagranite occurs in the lower part. From ca. 713.5 down to 720.5 m, the rocks are cut by dense arrays of mainly laumontite-filled fractures with local fault breccias containing small clasts in a laumontite-sealed matrix (Figure 5-84). In addition, there are minor fractures containing quartz, calcite, and hematite, and minor faults with chlorite and corrensite coating. This part of DZ3 is a fault core /Munier et al. 2003/. One steeply dipping NE-SW- oriented fault with chlorite striae shows oblique slip movement with a strong strike-slip component (Figure 5-85).

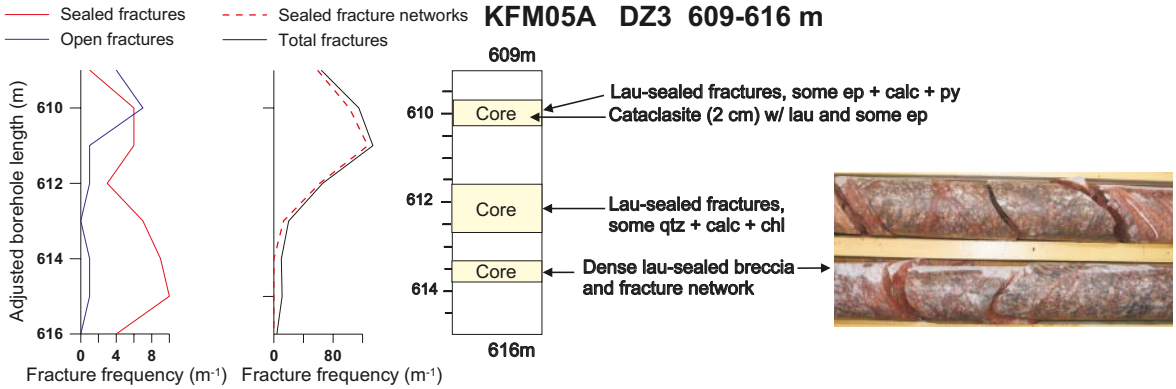

Figure 5-82. *Simplified drawing of the upper part of KFM05A, DZ3. In some intervals, the rocks are cut by dense arrays of mainly laumontite-sealed fractures. A thin cataclasite is also present at ca. 610 m. The photo shows an interval from the fault core with abundant fractures sealed with laumontite and some calcite.*

Figure 5-83. *Stereoplot of fault slip data in the upper part of DZ3 (KFM05A).*

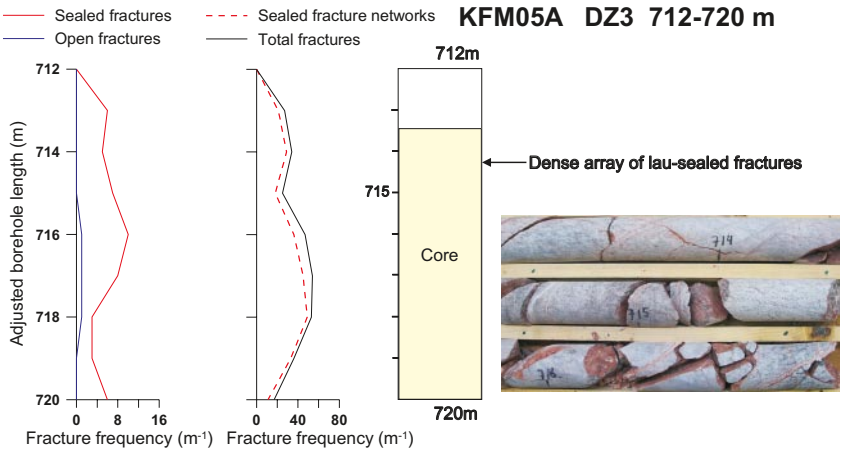

Figure 5-84. *Simplified drawing of the lower part of KFM05A, DZ3. From ca. 713.5 down to 720.5 m, the rocks are cut by dense arrays of mainly laumontite-sealed fractures with local fault breccias containing small clasts in a laumontite-sealed matrix. The photo shows an interval from the fault core with abundant laumontite-filled fractures.*

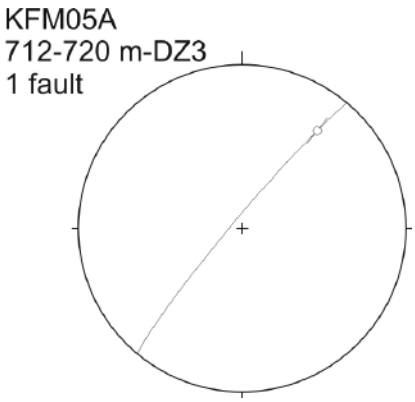

Figure 5-85. *Stereoplot of fault slip data in the lower part of DZ3 (KFM05A).*

5.2.9 KFM06A

This borehole is located in the central northeast part of the investigation area (Figure 5-40). The borehole is oriented 301/60 and has a length of 1,001 m /Carlsten et al. 2005a/. Nine deformation zones were investigated with a combined length of 270 m (Table 5-1).

A total of 41 fault slip data were obtained from the investigated deformation zones along the core. Fault planes are largely oriented ENE-WSW and are steeply dipping. Slickensides are mostly strike-slip and plunge 20 degrees to the WSW (Figure 5-86). Note that most of the kinematic data were obtained from DZ7–11, i.e. from the deeper levels of the borehole.

KFM06A: 126–148 m – DZ1

This interval transects 22 m of medium- to coarse-grained, equigranular metagranite with minor pegmatite. In general, the zone has few fractures with several intervals having only 1–3 fractures/m (Figure 5-87). Fracture minerals are calcite, chlorite and some clay mineral coatings commonly occurring as fill or as coating on minor fault surfaces. Some pink alteration of the host rock is also present.

Only one NNE-SSW steep fault showing a south-plunging oblique chlorite slickenside has been measured (Figure 5-88).

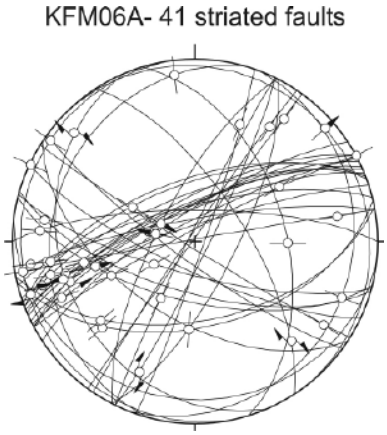

Figure 5-86. *Stereoplot showing all the fault slip data collected along all the studied DZ of drill core KFM06A.*

Figure 5-87. *Photo of drill core from the interval between 128.5 and 133.4 m in DZ1 (KFM06A).*

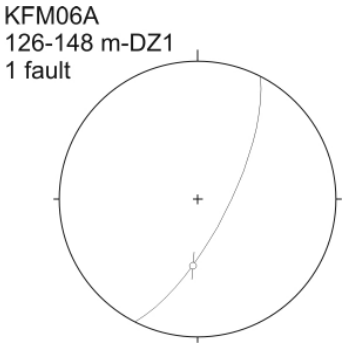

Figure 5-88. *Stereoplot of fault slip data in DZ1 (KFM06A).*

KFM06A: 195–245 m – DZ2

The zone has been defined along a 50 m long borehole interval and consists of medium- to coarse-grained, equigranular metagranite and some finer-grained metagranite. Minor occurrences of pegmatite and fine-grained metadioritic rock are also present. The zone as a whole contains mainly sealed NE-SW striking fractures that are filled with quartz, chlorite, laumontite, calcite and feldspar. Some pink alteration of the host rock has occurred. On average, there are 6–7 fractures/m in the zone /Carlsten et al. 2005a/. Apart from short intervals of fault core with abundant laumontite-sealed fractures (Figure 5-89), DZ2 is a transition zone according to the definition of /Munier et al. 2003/. Based on cross-cutting relationships, the earliest fracture generation with quartz and chlorite is cut by laumontite+calcite-sealed fractures. Late growth of quartz has also been recorded in laumontite-rich fault rocks (Figures 5-90, 5-91 and 5-92).

At 234.8 m, a discrete, narrow crush zone with dark mineral fill cuts the host rock. A thin section reveals the angular nature of the fragments of quartz and feldspar in the crush zone with fine-grained chlorite constituting the main infill between the fragments (Figures 5-93 and 5-94).

Three fractures with striations showing different sense of movement were found in the zone (Figure 5-95). The three faults show a moderate to steep dip and strike WNW-ESE and ENE-WSW. The 63 degrees south dipping WNW-ESE plane is characterised by oblique reverse chlorite + calcite striae plunging to the west (fault marked as number 2 on Figure 5-95). The two other faults (number 1 with chlorite + calcite, number 3 with chlorite) show pure strike-slip displacement, however, the sense of movement could not be determined.

KFM06A: 260–278 m – DZ3

This is a narrow zone penetrating mainly medium- to coarse-grained, grey-pink, metagranite with some layers of finer-grained metagranitoid and amphibolite. The zone contains mainly sealed NE-SW striking fractures that are filled with chlorite, calcite and minor epidote, clinozoisite and laumontite. Some reddish alteration of the metagranite is present.

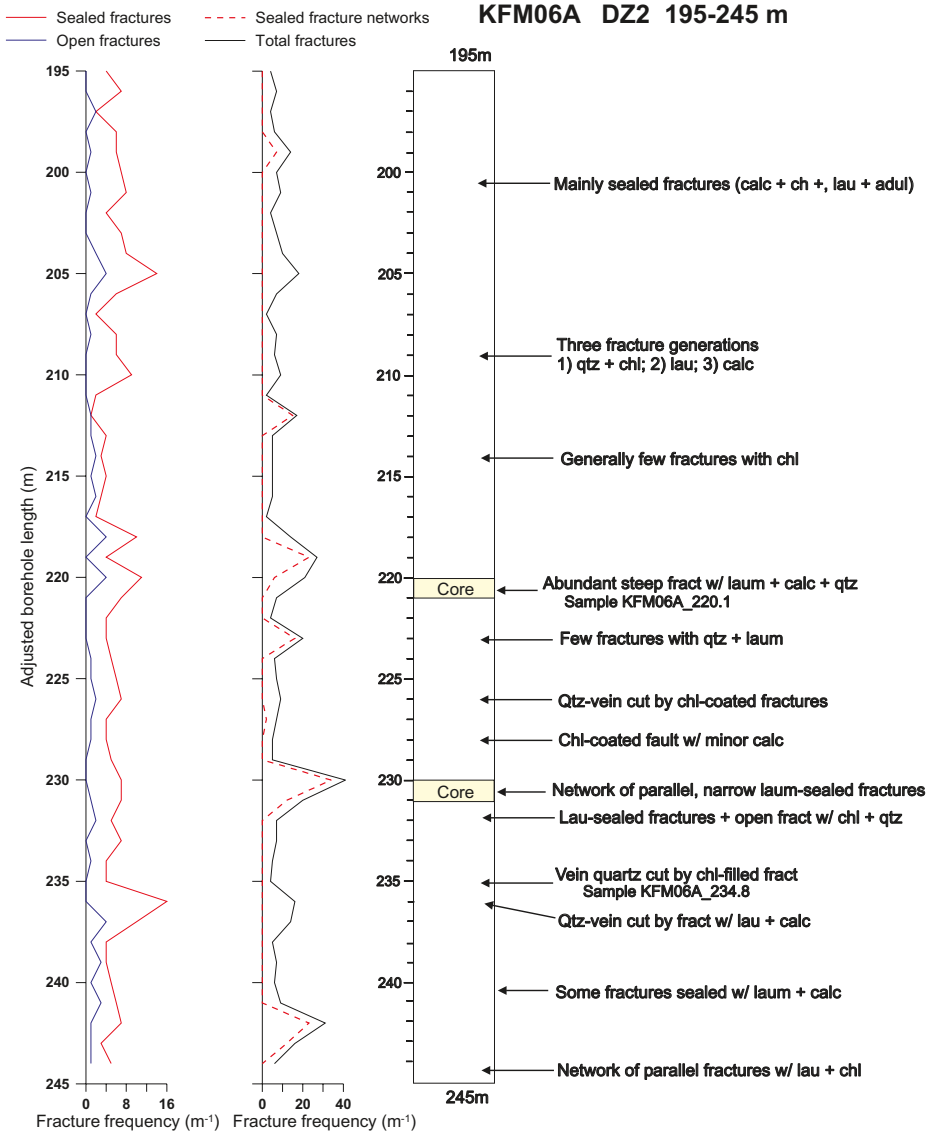

Figure 5-89. *Simplified drawing of KFM06A, DZ2, showing the occurrences of the most significant brittle deformation features. At ca. 220–221 m, there are abundant steep fractures filled with laumontite, quartz and some calcite (Figure 5-89, 5-90 and 5-91). Networks consisting of narrow laumontite-sealed fractures occur at 230–231 m. These intervals are defined as fault core; otherwise DZ2 is a transition zone /Munier et al.2003/.*

Figure 5-90. *KFM06A, DZ2, ca. 220.1 m, up is to the left. Medium-grained metagranite with pink staining is cut by a sealed fault with laumontite and quartz, and minor fractures with laumontite, calcite and quartz (for textural details, see Figure 5-91, below).*

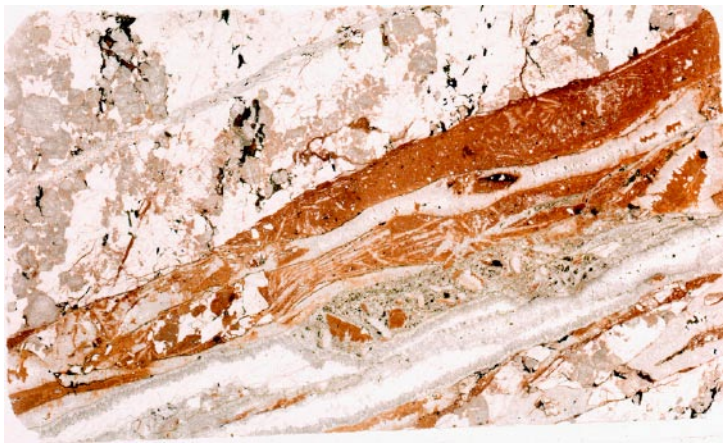

Figure 5-91. *Scanned thin section of sample KFM06A_220.1, DZ2. The metagranite (up to the left) is traversed by a fracture zone containing quartz and calcite. The lower part of the section exhibits a brownish laumontite fracture fill followed by quartz that has grown as euhedral crystals perpendicular to the walls of the fractures. The textures suggest that the quartz has grown in dilational open voids rather than during incremental opening of fractures in the laumontite (see detail from thin section in Figure 5-92, below). This reflects a change in the fluid composition through time. The field of view is 35 mm wide.*

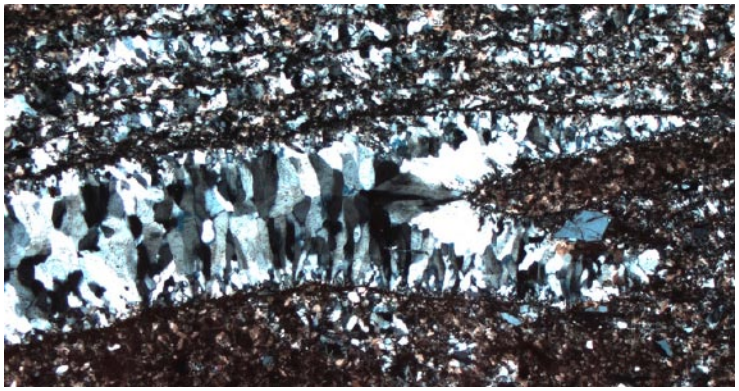

Figure 5-92. *Photomicrograph from thin section of sample KFM06A_220.1, DZ2, showing quartz that has grown as euhedral crystals perpendicular to the walls of open voids. The field of view is ca. 3 mm wide.*

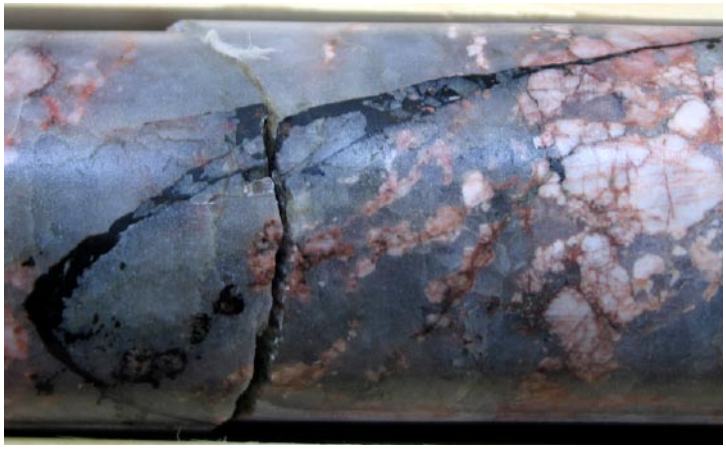

Figure 5-93. *Core from KFM06A_234.8, DZ2, up is to the left. A narrow, black crush zone that contains small angular fragments of the host rock cuts coarse-grained vein quartz (dark grey) and feldspar. The dark material in the crush zone consists of fine-grained chlorite (see thin section in Figure 5-94).*

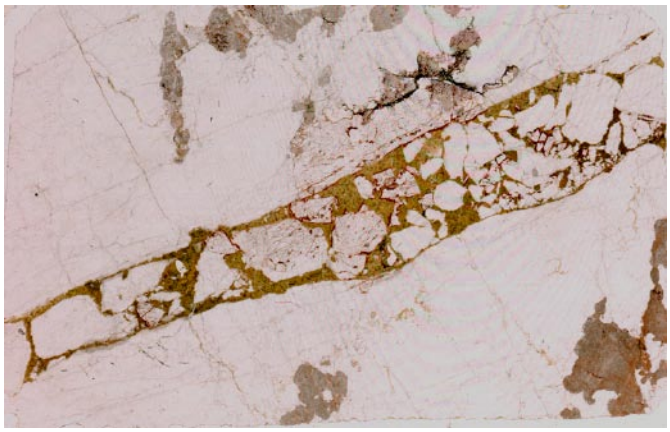

Figure 5-94. *Scanned thin section of sample KFM06A_234.8, DZ2. Crush zone with angular fragments of quartz and feldspar. Fine-grained greenish chlorite fills the space between the fragments. The field of view is ca. 35 mm wide.*

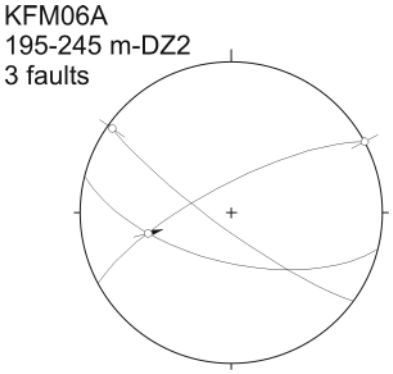

Figure 5-95. *Stereoplot of fault slip data in DZ2 (KFM06A).*

Chlorite-sealed fracture networks with local crushing of the host rock are present at ca. 260.5 m, at 268.2–269.2 m, and at 274.5 m (Figure 5-96 and 5-97). These are occurrences of fault core. Otherwise, DZ3 has a moderate fracture frequency /Carlsten et al. 2005a/ and is a transition zone according to the definition of /Munier et al. 2003/.

Two fractures showing different sense of movement were found in the zone (Figure 5-98). The first one is sub-horizontal trending NNW-SSE and has normal dip-slip movement defined by chlorite striae and calcite steps. The second one is steep and oriented NNE-SSW with calcite steps that indicate dip-slip reverse movement.

KFM06A: 318–358 m – DZ4

This zone extends along a 40 m borehole interval in rock types similar to DZ3 (see above). Locally, the rocks are strongly oxidized, with associated chloritization of mafic minerals and variable development of vuggy texture (‘episyenite’) in the interval ca. 330–337 m (Figure 5-99).

In the upper part, the zone displays localized, dense fracture networks with laumontite, calcite and chlorite. These tend to have a small angle with the core axis. Minor epidote-sealed fractures forming very localized networks are also present (Figure 5-99). In addition, there are isolated, variably oriented single fractures filled and/or coated with quartz, calcite, laumontite and chlorite, and less commonly hematite, epidote and pyrite. These are present throughout the entire deformation zone. The average fracture frequency for the entire zone is 9–10/m /Carlsten et al. 2005a/. However, with the exception of local occurrences of fractures networks, fracture frequencies are fairly low (ca. 2–8/m) in the interval from 330 m to about 342 m, and somewhat

higher in the upper and lower parts of the deformation zone (Figure 5-99). The fractures generally strike N, NE and E and have steep to intermediate dips. Gently-dipping fractures are also present. Generally, epidote, quartz and chlorite predate laumontite and calcite. However, in some cases, chlorite-coated fractures post-date laumontite, and late quartz growth has also been recorded followed by calcite (see below).

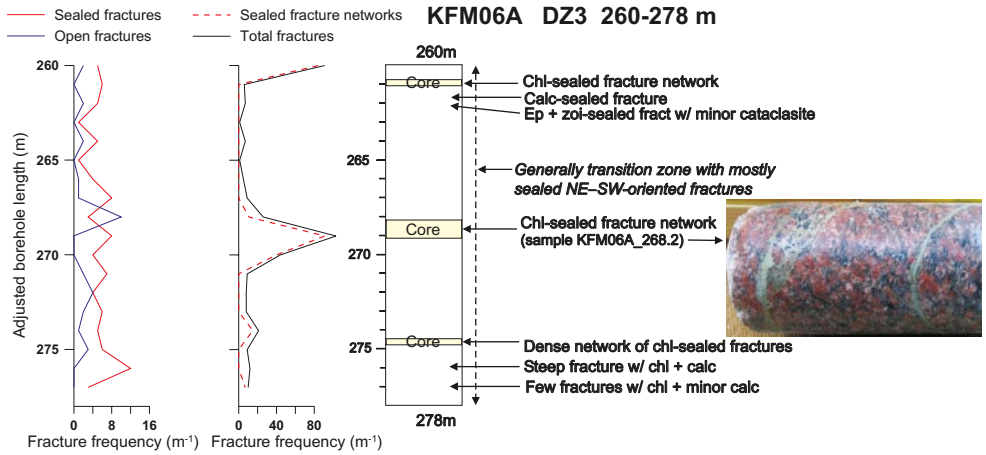

Figure 5-96. *Simplified drawing of KFM06A, DZ3, showing the occurrences of significant brittle deformation features. Chlorite-sealed fracture networks with local crushing of the host rock are present at ca 260.5 m, at 268.2–269.2 m, and at 274.5 m. The photo shows the core section that was sampled at 268.2 m, up is to the left. Medium-grained, pink and partly chloritised metagranite is cut by epidote+zoisite-filled thin veins containing small fragments of the host rock (see Figure 5-97 for textural details).*

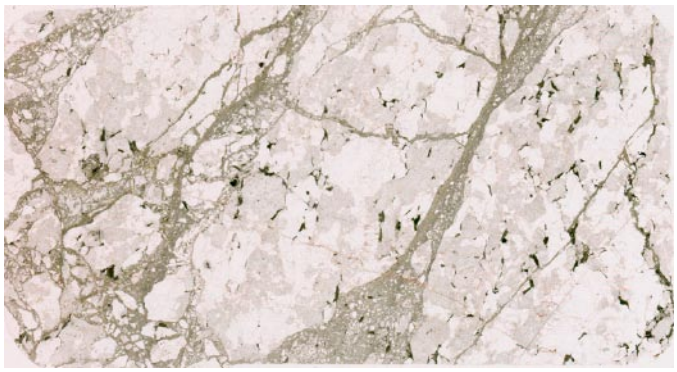

Figure 5-97. *Scanned thin section of sample KFM06A_268.2, DZ3. Variably oriented fractures with crushed and finely crushed metagranite host rock. Chlorite, epidote and clinozoisite fill the space between the angular fragments. The field of view is ca. 35 mm wide.*

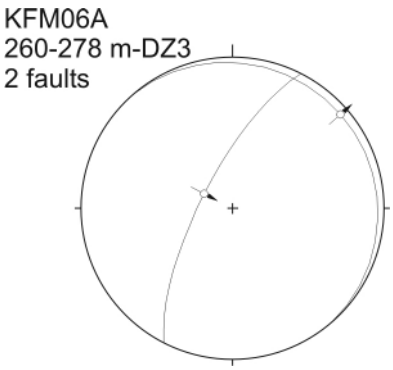

Figure 5-98. *Stereoplot of fault slip data in DZ3 (KFM06A).*

Thin zones with strong grain size reduction and cataclastic textures are present. An example of this is at 330.9 m where laumontite-impregnated fault rocks exhibit a complex sequence of textural and mineralogical development (see Figures 5-99, 5-100 and 5-101). The laumontite-rich cataclasite is post-dated by veins filled with quartz and calcite. The textures of the vein suggest that euhedral quartz has grown normal to the walls of dilational open voids in the cataclasite, later followed by calcite closing the voids.

Only three fractures provided reliable striations on small faults coated with chlorite and some calcite. Two faults are steep and NE-SW striking with oblique striae plunging NE (Figure 5-102). The third fault (number 2) is very flat with a dip-slip slickenside. The sense of shear could not be determined on any of the faults.

KFM06A: 740–775 m – DZ7

The rock types in this zone are heterogeneous and include medium-grained pink-grey metagranite, amphibolite, and fine-grained metadiorite that, in places, is interlayered with leucocratic granite and pegmatite, and leucocratic granite with biotite 'flecks'. DZ7 has an average fracture frequency of ca. 9/m /Carlsten et al. 2005a/ and is a transition zone with two intervals of fault core according to the definition of /Munier et al. 2003/ (Figure 5-103). Stronger fracturing has occurred in the upper part of the zone, and near its base at 768–772 m. Thus, about 30% of the zone appears to have fracture frequencies significantly above the general background level.

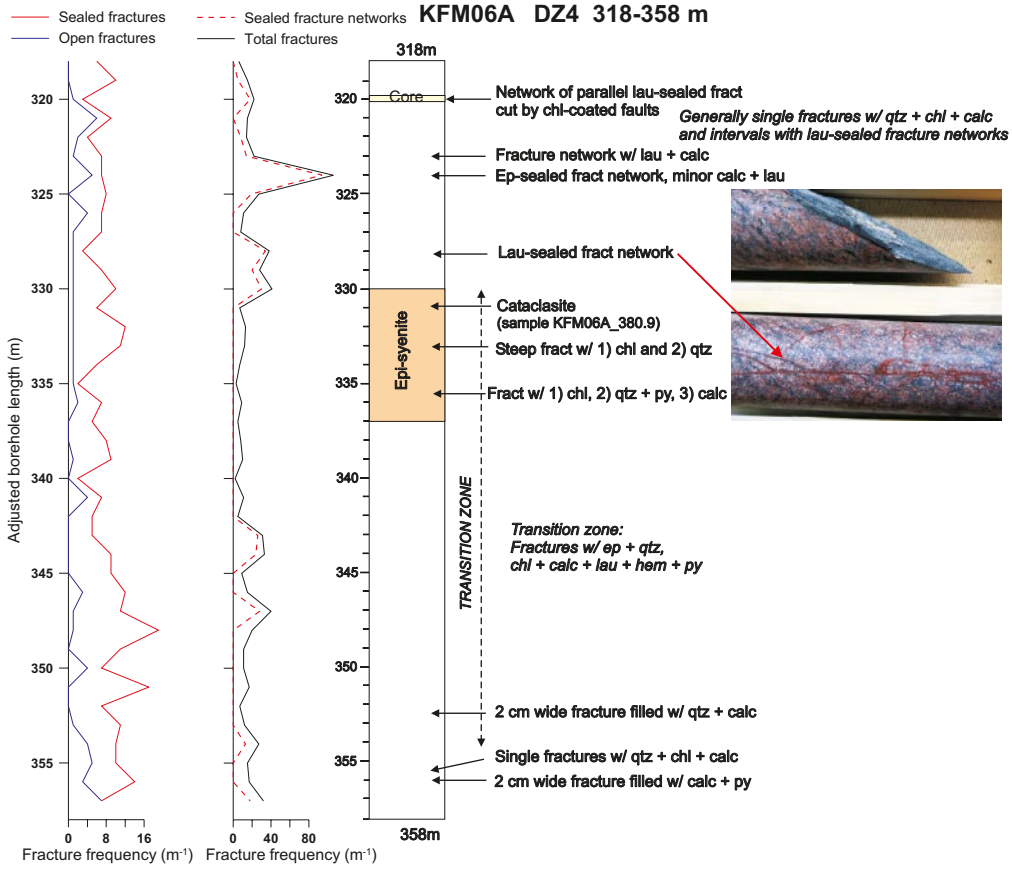

Figure 5-99. *Simplified drawing of KFM06A, DZ4, showing the occurrences of significant brittle deformation features. The interval from 330 to 342 m is considered a transition zone /Munier et al. 2003/. The upper and lowermost parts of DZ4 have sporadic intervals of fault core defined by sealed fracture networks; apart from these intervals this part of DZ4 is a transition zone. The photo shows laumontite-sealed fractures in metagranite from ca. 328 m (lower part) and a chlorite-sealed broken fracture (upper part). Generally, epidote, quartz and chlorite predate laumontite and calcite. However, chlorite-coated fractures post-date laumontite, and late quartz growth has also been recorded followed by calcite (Figure 5-101).*

Figure 5-100. *Scanned thin section of sample KFM06A_330.9, DZ3. Cataclasite and ultracataclasite showing a sequence of increasing degradation of the host metagranite. The colour of the fine-grained fault rocks is due to fine dusting of laumontite. Note that quartz and calcite fill what appear to have been open voids in the cataclasite. The field of view is ca. 35 mm wide. See Figure 5-101 below for details.*

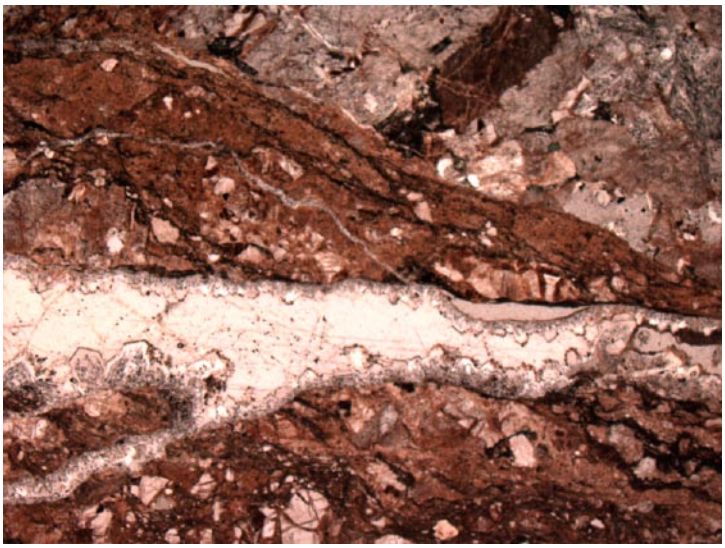

Figure 5-101. *Photomicrograph showing details from the thin section of sample KFM06A_330.9, DZ4 (see Figure 5-100 above). A finely layered or laminated, brownish, fine-grained cataclasite containing small angular fragments transects earlier brittle structures (upper right) also showing cataclastic textures. The brown cataclasite is in turn post-dated by a pale vein with quartz and calcite. The textures of the vein suggest that euhedral quartz has grown normal to the walls of dilational open voids in the cataclasite, later followed by calcite closing the voids. The field of view is ca. 5 mm wide.*

Both steep and gently dipping N to NE-striking fractures are present, and the fractures are filled or coated with chlorite, calcite, laumontite, and less commonly epidote, quartz and occasional pyrite.

At ca. 743.5 m, a ca. 5 cm wide calcite-cemented fault occurs (Figure 5-102). The textures observed here are reminiscent of those in narrow fault cores locally preserved along the Eckardfjärden fault.

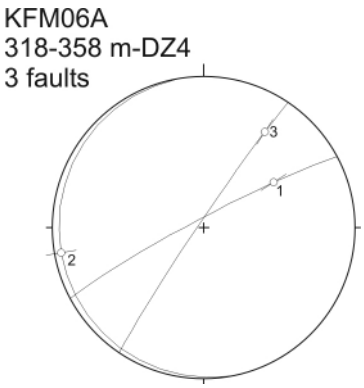

Figure 5-102. *Stereoplot of fault slip data in DZ4 (KFM06A).*

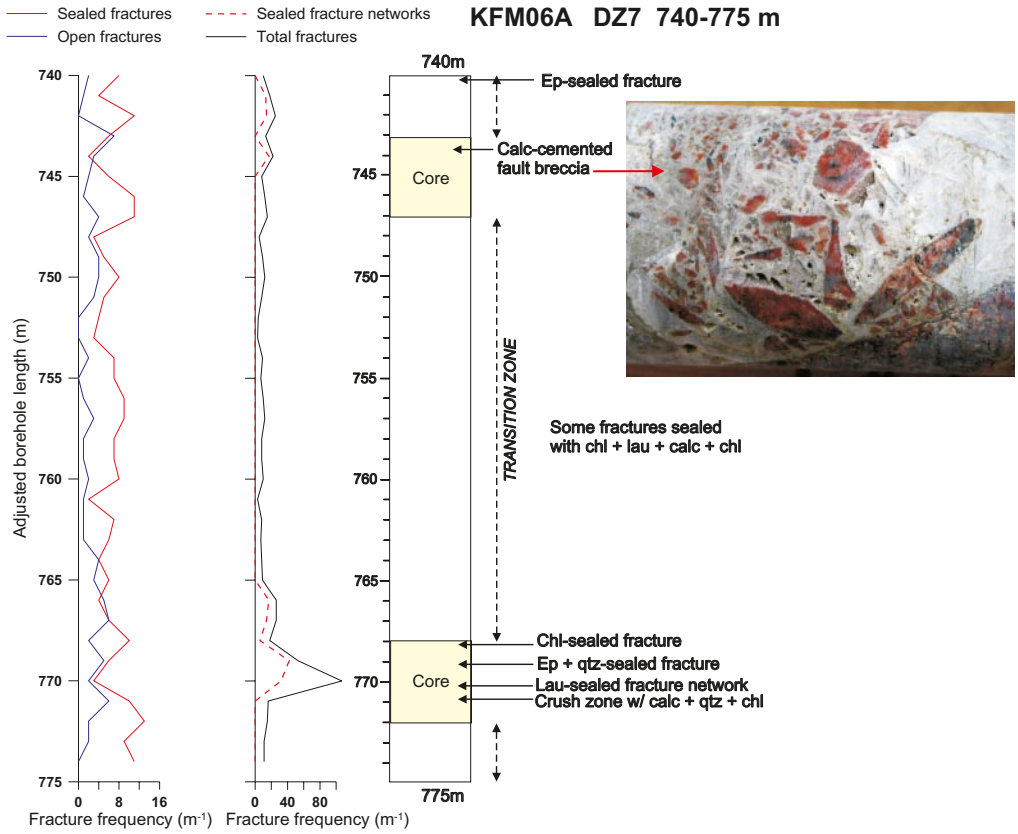

Figure 5-103. *Simplified drawing of KFM06A, DZ7, showing the occurrences of significant brittle deformation features. Two intervals are considered to be fault core, whereas the remaining part of the DZ7 is considered a transition zone /Munier et al. 2003/. The photo shows a section of core from 743.5 m; up is to the left. A ca. 5 cm wide fault consists of angular, rotated fragments of the host metagranite embedded in euhedral calcite that has cemented the fault. Note the sharply defined wall of the fault at lower right. The central damage zone of this small fault may have formed by hydraulic fracturing creating the angular rock fragments.*

Other faults exhibit chlorite-coated walls with mini-grooves defining linear structures. Faults decorated with chlorite striae are present within the intervals with the strongest brittle deformation towards the upper and lower parts of the deformation zone. A total of 10 faults having diverse orientations gave reliable kinematic data (Figure 5-104). The majority of these are oriented ENE-WSW to ESE-WNW and dip to the south. Most of the faults have chlorite striae that are oblique with a variable strike slip component and plunge to the west. The sense

of shear was determined in three cases (Figure 5-104): 1) Dextral oblique-slip striae (chlorite + calcite) plunging 30 degrees south on a NW-SE fault dipping 70 degrees to the east (number 6). 2) Sinistral oblique slip (stepped surface with calcite) plunging 30 degrees west on an ENE-WSW fault dipping 75 degrees NW (number 4). 3) Dextral striae (chlorite + laumontite) with a minor component of dip slip plunging 25 degrees south on a NNE-SSW steep fault (number 5).

KFM06A: 788–810 m – DZ8

The rock types include pale grey to pink, medium- to fine-grained, texturally variable leucocratic metagranite. Minor pegmatite veins are present. The zone has an increased frequency of predominantly NE-striking steeply dipping fractures filled or coated with chlorite, calcite and laumontite /Carlsten et al. 2005a/. Laumontite-sealed network of sub-parallel fractures are seen to post-date chlorite-filled fractures (e.g. at ca. 803.5 m). Epidote, quartz and clay minerals occur less commonly. An example of epidote-sealed breccia is present at ca 794.4 m, whereas a ca. 3 cm wide laumontite-sealed breccia/cataclasite occurs at ca. 795.2 m (Figure 5-105). Laumontite-sealed fractures and minor breccia zones post-date fractures coated or filled with epidote + quartz. DZ8 is best characterized as a transition zone with a short section that may classify as a fault core based on the presence of a variety of breccias and fracture types (Figure 5-105).

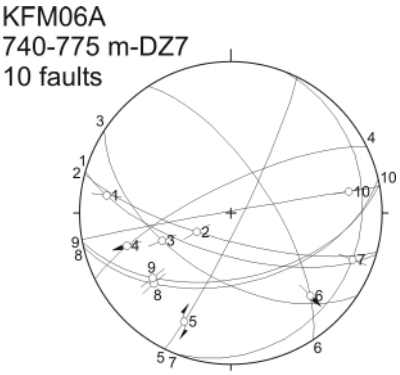

Figure 5-104. *Stereoplot of fault slip data in DZ7 (KFM06A).*

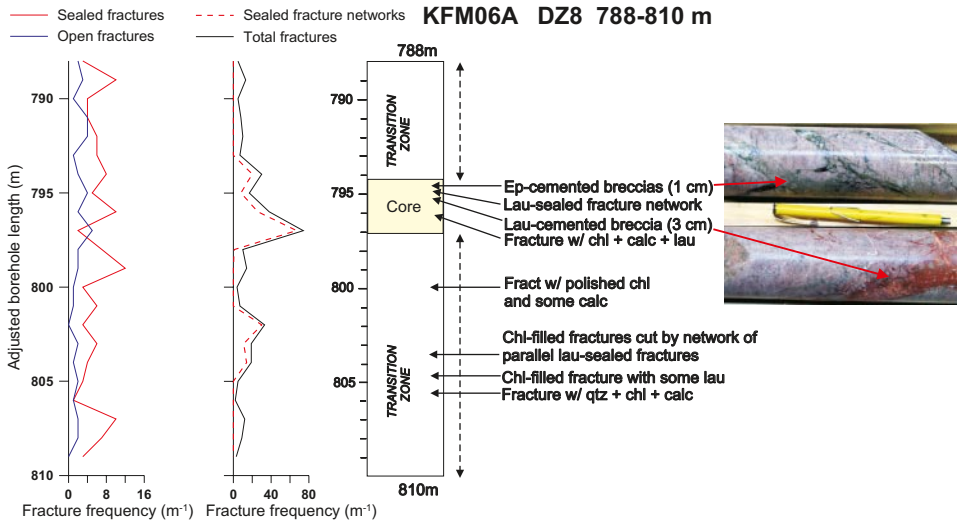

Figure 5-105. *Simplified drawing of KFM06A, DZ8, showing the occurrences of selected brittle deformation features. One interval is considered to be fault core, whereas the remaining part of the DZ7 is considered a transition zone /Munier et al. 2003/. The photo shows two sections of core from KFM06A. The upper part illustrates networks of epidote-cemented breccias and fractures at ca. 794.4 m. The lower part shows a ca. 3 cm wide laumontite-sealed breccia/cataclasite that occurs at ca. 795.2 m.*

Faults with chlorite striation were observed in six cases (Figure 5-106), one of which is located 2.5 m below the defined deformation zone. The pattern is similar to that of DZ7 immediately above. Five of the striated faults are steep with strike-slip slickensides defined by chlorite and less commonly calcite. However, the strikes are different: two are WNW-ESE, two are ENE-WSW and one is NE-SW. A dip-slip N-S fault dipping 60 degrees to the east is also observed. No sense of shear has been determined.

KFM06A: 882–905 m – DZ9

The rock type in this zone is a texturally heterogeneous, leucocratic, medium-grained metagranite with a variable content of unevenly dispersed flakes or small specks of biotite. The rock is partly pegmatitic. The zone has an increase in the frequency of steeply dipping, mostly sealed ENE- and NNE-striking fractures with laumontite, calcite and some chlorite as the main infilling minerals. Laumontite-sealed fractures tend to occur in parallel 'swarms' with a low angle with the core axis, e.g. at 883–884 m, 887 m, and 892–895 m (Figure 5-107, Figure 5-108). These are defined as fault core, whereas the rest of the interval is a transition zone /Munier et al. 2003/.

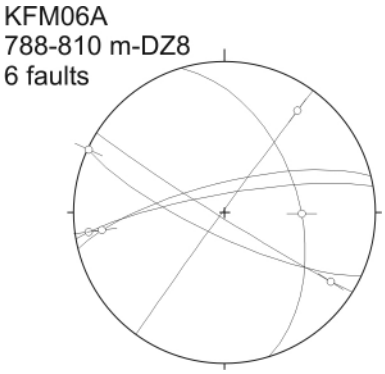

Figure 5-106. *Stereoplot of fault slip data in DZ8 (KFM06A).*

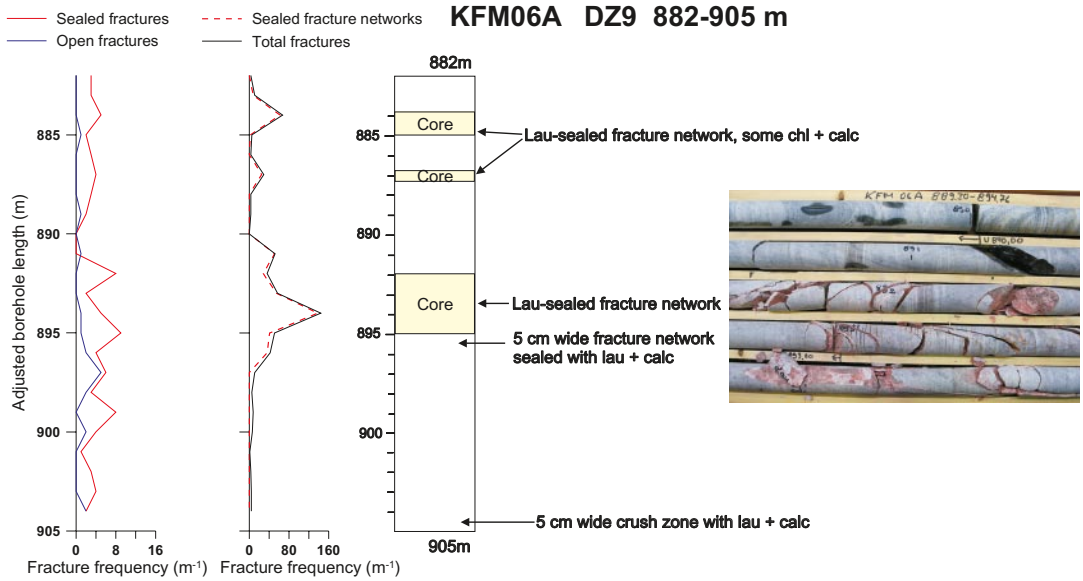

Figure 5-107. *Simplified drawing of KFM06A, DZ9, showing the occurrences of selected brittle deformation features. Three intervals with a high frequency of laumontite-sealed fractures are defined as fault cores. The remaining part of DZ9 is considered a transition zone /Munier et al. 2003/. The photo shows a core section from 890–895 m (core box no. 150). Note few chlorite-coated fractures in the upper part down to 892 m, in contrast to the fairly dense set of laumontite-sealed fractures in the lower part. Some of the laumontite-sealed fractures were probably opened during drilling.*

Nine striated faults with laumontite, calcite and chlorite are mainly oriented ENE-WSW and have predominantly oblique to strike-slip movement (Figure 5-109). Most of these faults exhibit strike-slip slickensides plunging 20 degrees to the west, however, the sense of movement is not clear.

KFM06A: 925–933 m – DZ10

This is a narrow deformation zone in leucocratic metagranite with unevenly distributed small flakes of biotite. The nature of the brittle structures is similar to that described in DZ9 (see above). Laumontite-sealed fractures and fracture networks with some calcite+chlorite appear at 927–928 m, 929 m and 932.4 m. A sample of laumontite-sealed fault rock was collected at 927.3 m. The thin section shows cataclastic textures with variably sized, angular fragments of the host metagranite in a laumontite-rich, fine-grained matrix.

As in the zone above, the two faults strike ENE-WSW, dip steeply to the NNW and contain strike-slip slickensides defined by chlorite that plunge 20 degrees to the west (Figure 5-110). No sense of movement has been determined.

Figure 5-108. *KFM06A_895.4 m. Close-up of fault sealed with laumontite + calcite + minor chlorite. Striation documenting oblique relative movement occurs on a steeply NNW-dipping fault. Absolute movement cannot be determined from this observation.*

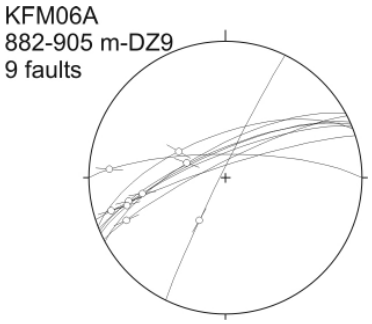

Figure 5-109. *Stereoplot of fault slip data in DZ9 (KFM06A).*

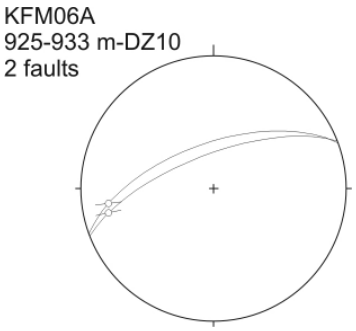

Figure 5-110. *Stereoplot of fault slip data in DZ10 (KFM06A).*

KFM06A: 950–990 m – DZ11

The predominant rock type in this zone is similar to that of DZ10 (see above). In addition, there is some fine- to medium-grained metatonalite containing titanite and minor sulphides. Brittle deformation is expressed mainly as steeply dipping, NE-striking sealed fractures and some few narrow fracture networks. Gently dipping fractures are also present (Figure 5-111). The average fracture frequency is 5–6/m /Carlsten et al. 2005a/. However, the intervals 967–973 m and 980–985 m generally contains fewer fractures that in part is similar to the background level. Higher fracture frequencies occur in the upper and lower parts of DZ11, and some short sections may classify as fault core within a transition zone /Munier et al. 2003/. The fracture infill includes chlorite, laumontite, hematite, calcite, and less commonly epidote, quartz and astrophyllite.

Three sub-horizontal southwest-dipping faults striking from E-W to N-S were observed in the upper part of the zone (Figure 5-112). They have slickensides plunging to the W (laumontite + hematite), NW (chlorite) and to the N (laumontite + hematite) (numbered 1, 2 and 3, respectively on Figure 5-112). A NNE-striking fault have oblique N-plunging striae defined by chlorite and laumontite (number 5 on Figure 5-112), and a SW-striking fault (number 4) has normal dip-slip movement defined by small steps of brick-red hematite.

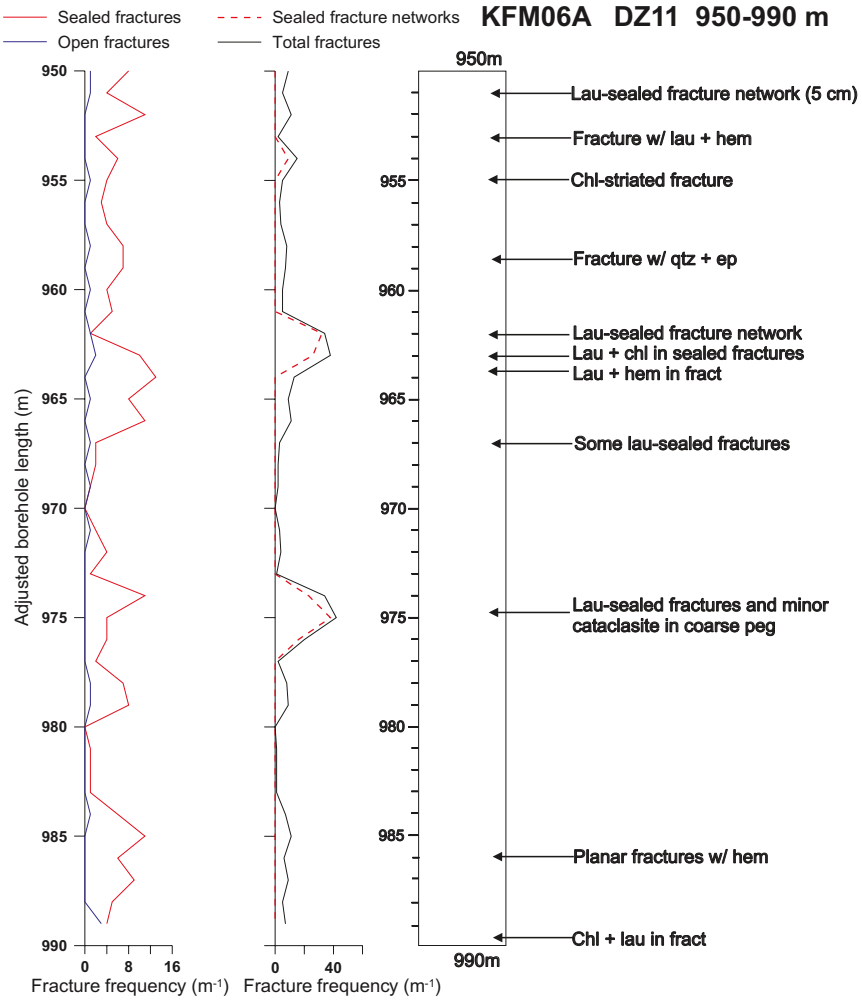

Figure 5-111. *Simplified drawing of KFM06A, DZ11, showing the occurrences of brittle deformation features. The interval 967–973 m and 980–985 m generally contain fewer fractures that in parts is similar to the background level. The highest fracture frequencies occur in the upper and lower parts of DZ11, and some short sections may classify as fault core within a transition zone /Munier et al. 2003/.*

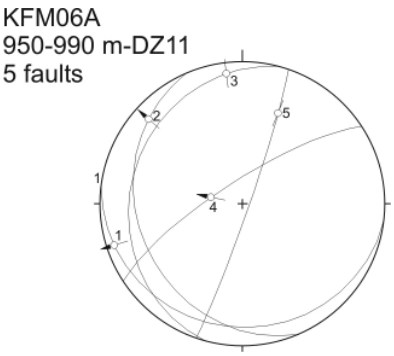

Figure 5-112. *Stereoplot of fault slip data in DZ11 (KFM06A).*

5.2.10 KFM06B

This borehole is located in the central northeast part of the investigation area (Figure 5-40). The borehole is oriented 297/84 and has a length of 1,003 m /Carlsten et al. 2005a/. Only one deformation zone was investigated (Table 5-1).

KFM06B: 55–93 m – DZ1

The zone consists of medium- and fine-grained metagranite with minor occurrences of amphibolite and pegmatite. In parts of the zone, the rocks are strongly oxidised with reddish alteration, and in some cases a somewhat porous texture (e.g. near the top of the zone and at 67–70 m). Fracture minerals comprise chlorite, calcite, clay minerals, quartz, hematite, asphaltite and pyrite. Several gently-dipping open fractures occur in this zone (Figure 5-113). Some of the open fractures are secondary in nature and due to dissolution of previous fracture fill (see Figure 5-114). The overall fracture frequency is moderate (Figure 5-113). Open and sealed, gently dipping fractures dominate in the upper part of DZ1, whereas steep SE-dipping and mainly sealed fractures occur in the lower part /Carlsten et al. 2005a/.

The two measured fault planes with chlorite striation strike N-S and NNW-SSE and dip 40 to 70 degrees to the west, respectively (number 1 and 2 Figure 5-115). The first plane is a reverse fault with oblique N-plunging striae. The second one is a strike-slip fault of unknown sense.

5.2.11 KFM07A

This inclined borehole is oriented 260/60 starting from a location in the northwestern part of the investigation area (Figure 5-40). The borehole has a length of 1,001.5 m /Carlsten et al. 2005b/. Four deformation zones with total length of 253 m were investigated, including the major part of DZ4 in the lower part of the borehole (Table 5-1).

A total of 72 fault slip data were obtained from the investigated deformation zones, the great majority of which derives from the lower the parts of the drill core (Figure 5-116). Predominantly steep fault planes trending NNW-SSE are the most common with slickensides that are strike-slip in character and plunge mainly to the SSE. Both sinistral and dextral sense of movement was recorded. A set of E- to NE-striking faults with variable dip direction also occurs. Chlorite, laumontite and calcite are the predominant fracture minerals.

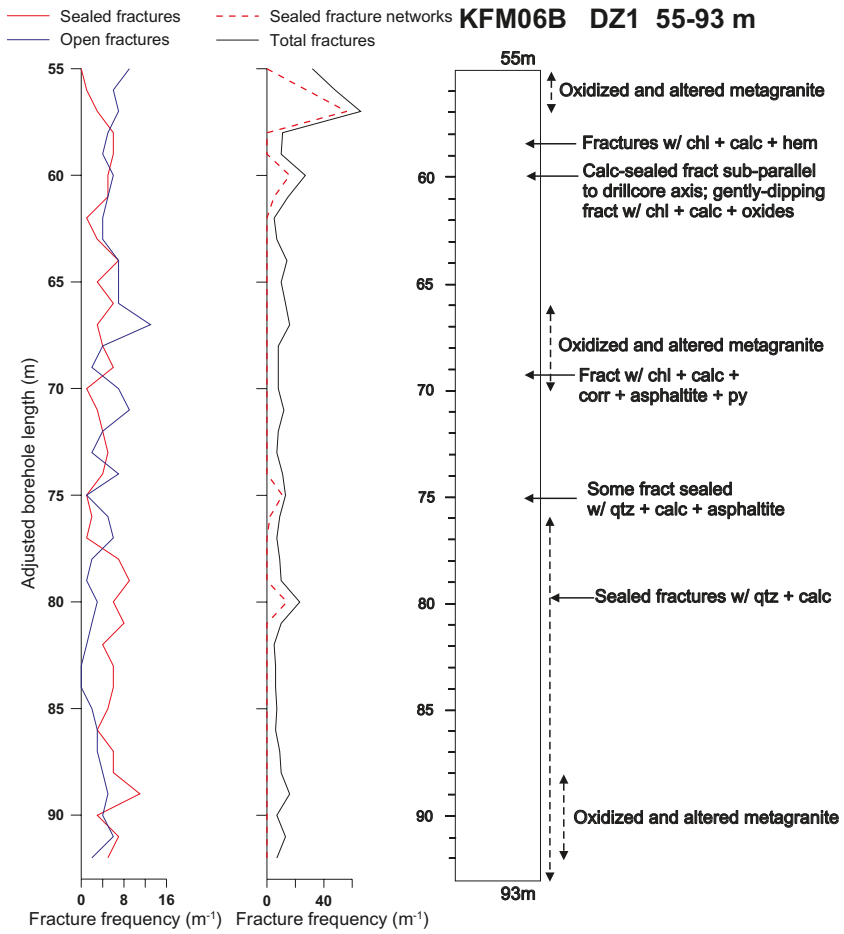

Figure 5-113. *Simplified drawing of KFM06B, DZ1, showing the occurrences of brittle deformation features and alteration of the metagranite. Based on the recorded brittle deformation features, the observed fracture frequencies /Carlsten et al. 2005a/ and the definitions of /Munier et al. 2003/, the interval straddles the boundary between a fault core and a transition zone.*

Figure 5-114. *KFM06B_75 m. Strong reddish alteration and abundant small fractures filled with quartz and calcite that has been partly dissolved.*

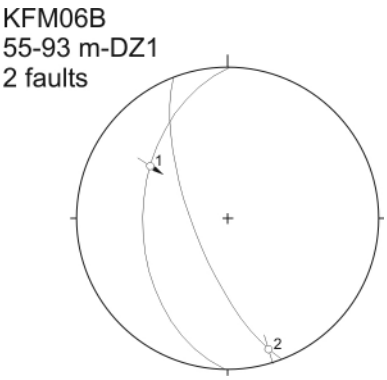

Figure 5-115. *Stereoplot of fault slip data in DZ1 (KFM06B).*

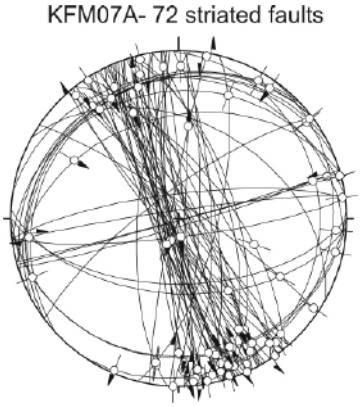

Figure 5-116. *Stereoplot showing all the fault slip data collected along all the studied DZ of drillcore KFM07A.*

KFM07A: 108–183 m – DZ1

The zone penetrates mainly medium-grained metagranite with a few m-wide sections of pegmatite and minor fine-grained amphibolite. The zone consists of a concentration of gently dipping open fractures and a few local crush zones, e.g. at ca. 112 m (Figures 5-117 and 5-118) and probably at 116–117 m (core loss), with a thin coating of epidote + chlorite on broken surfaces. There are also steeply dipping faults and fracture networks that are sealed with laumontite and calcite. Along some of these, there are up to 2 cm wide zones of laumontite-sealed cataclasite containing angular, fine fragments of the host rock (Figure 5-118). Other fracture-related minerals include corrensite and hematite. Good examples of laumontite + calcite sealed faults with local cataclasite are present in the interval 154–159.5 m, and at 147–148 and 164–166 m (Figure 5-119). Strong oxidation is common in sections with abundant laumontite. Several fault surfaces with good striation, defined mainly by chlorite and calcite, occur at ca. 142–145 m.

In parts of the zone, fracture frequencies are quite low, e.g. at ca. 130–142 m, at 148–154 m, at 160–164 m, and below 170 m. Thus, the zone as whole is composed of intervals of variable length with elevated fracture frequencies defined as fault core separated by longer intervals where fractures are much less prevalent (Figure 5-117).

Most of the faults dip gently to the NNW with mainly strike-slip striae defined mainly by chlorite + calcite (Figure 5-120), and one striae is sinistral reverse (number 4). However, two striae are also dip-slip reverse on these planes (numbers 3 and 5). Two steep ENE-WSW faults are strike-slip, but show opposite sense of shear (numbers 7 and 8). One fault plane dipping 15 degrees to the south shows strike-slip striae (number 2 on Figure 5-120). A steeply ENE-dipping fault has weak chlorite (?) slickensides defining a dextral oblique sense of shear.

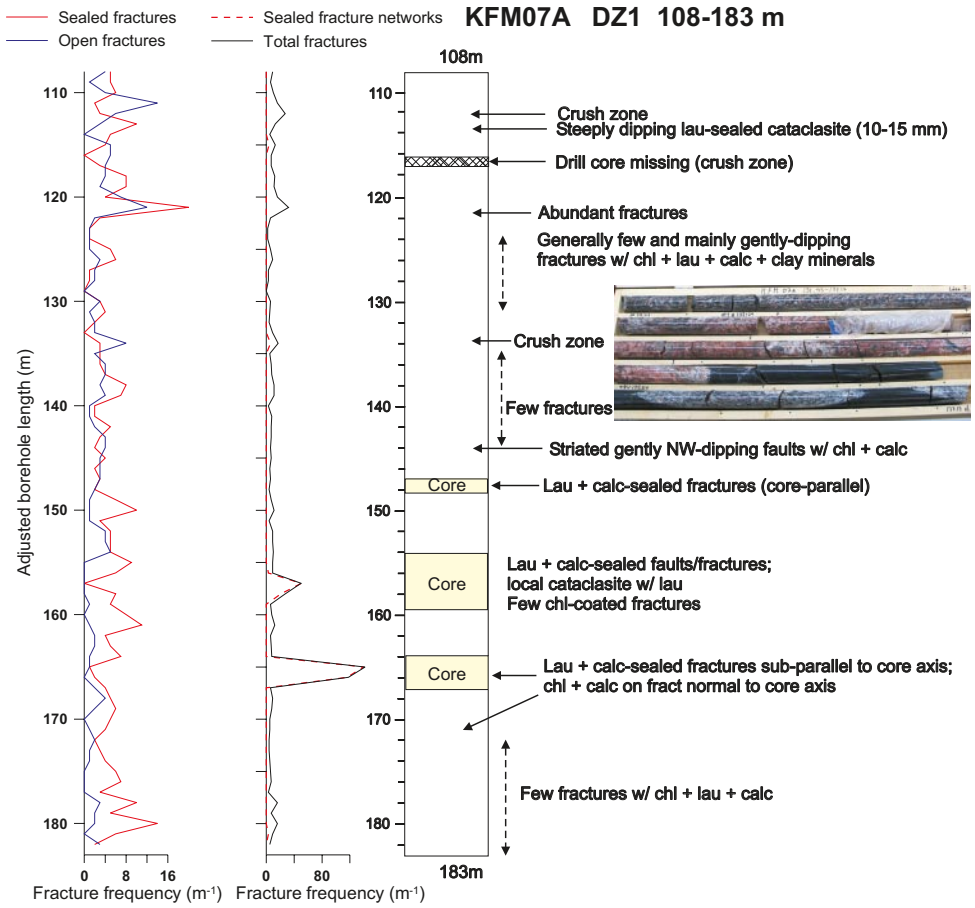

Figure 5-117. *Simplified drawing of KFM07B, DZ1, showing the occurrences of important brittle deformation features. The deformation zone is for the most part a transition zone /Munier et al. 2003/, with some sections that are classified as fault core due to the presence of crush zones or core-parallel sealed fault sets.*

Figure 5-118. *KFM07A_112–114 m. A crush zone is shown in the upper part of the figure. In the centre, there is a good example of laumontite-sealed cataclasite. Note small clasts of the host metagranite in the cataclasite. The lower part shows pristine metagranite.*

Figure 5-119. *KFM07A_155 m. Faults sealed with laumontite and euhedral calcite.*

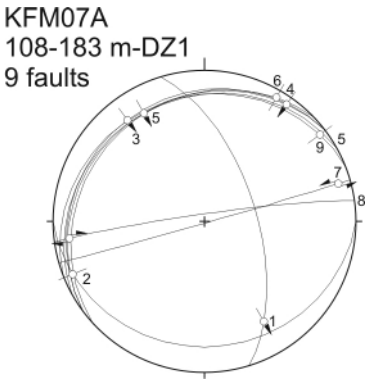

Figure 5-120. *Stereoplot of fault slip data in DZ1 (KFM07A).*

KFM07A: 196–205 m – DZ2

This is a narrow deformation zone transecting metagranite similar to that in DZ1. The nature of brittle deformation is also comparable to DZ1. Abundant sealed fractures and fracture networks that are sub-parallel to the core axis are filled with chlorite, laumontite and calcite (Figure 5-121). These sections constitute fault core /Munier et al. 2003/ and are present for about 2 m from ca. 197.5 m and from ca. 200.5 m. Some gently-dipping fractures also occur.

One steeply dipping ENE-WSW strike-slip fault with laumontite + chlorite is the only measurement on this zone (Figure 5-122).

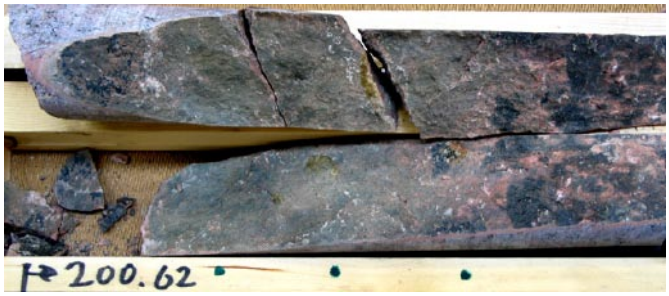

Figure 5-121. *Photograph of core section at ca. 200.5 m. The fracture is sub-parallel to the core axis and sealed with laumontite + some calcite and chlorite. Note oxidation.*

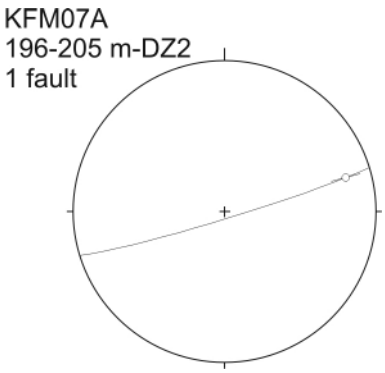

Figure 5-122. *Stereoplot of fault slip data in DZ2 (KFM07A).*

KFM07A: 417–422 m – DZ3

This deformation zone is defined along a 5 m borehole interval in grey, foliated, medium-grained metagranite with subordinate amphibolite and pegmatite. The zone is characterized by steep, N-striking fractures sealed with chlorite and calcite. Open fractures are also present and are coated with chlorite, calcite and some hematite. On average, there are ca.12 fractures/m in the zone. Striation defined by chlorite and hematite is well developed on two faults (Figure 5-123). The two measurements show strike-slip steep NNW-SSE trending faults (Figure 5-124).

KFM07A: 803–999 m – DZ4 (excluding intervals 843–857 m and 900–920 m)

This is an extensive zone with a total borehole length of 164 m that contains several sections with brittle structures with fault slip data (see below). The host rocks are predominantly foliated to strongly foliated grey to weakly pink metagranite to metagranodiorite with fine-grained recrystallised biotite. Several 5–10 m long sections are composed of white to grey pegmatite. Amphibolites occur sporadically in 10–30 cm wide sections, one occurrence of a 1 m wide section occurs at ca. 923 m. The brittle structures do not appear to be dependent on lithology. Reddish alteration of the core occurs in some intervals.

The most common brittle structures are steeply dipping sealed fractures that strike NNW to ESE. Open or partly open fractures are significantly less abundant and strike NNW to NE with steep dips. Gently dipping structures are also present but are less common than steep ones. The predominant fracture-filling minerals are chlorite, laumontite and calcite. Laumontite-sealed fracture networks with local cataclasites are present in several places. Less commonly observed fracture minerals are oxides (hematite), feldspar (adularia) and clay mineral coating.

Figure 5-123. *KFM07A DZ3, 419.5 m. Striated fault surface with chlorite and dark red hematite.*

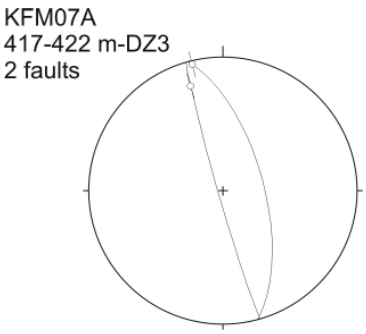

Figure 5-124. *Stereoplot of fault slip data in DZ3 (KFM07A).*

Based on fracture frequency data /Carlsten et al. 2005b/, DZ4 is generally a transition zone with subordinate development of fault core associated with short sections of higher fracture frequency.

In the following, representative features of the deformation zone are described and illustrated (Figures 5-125, 5-126 and 5-127).

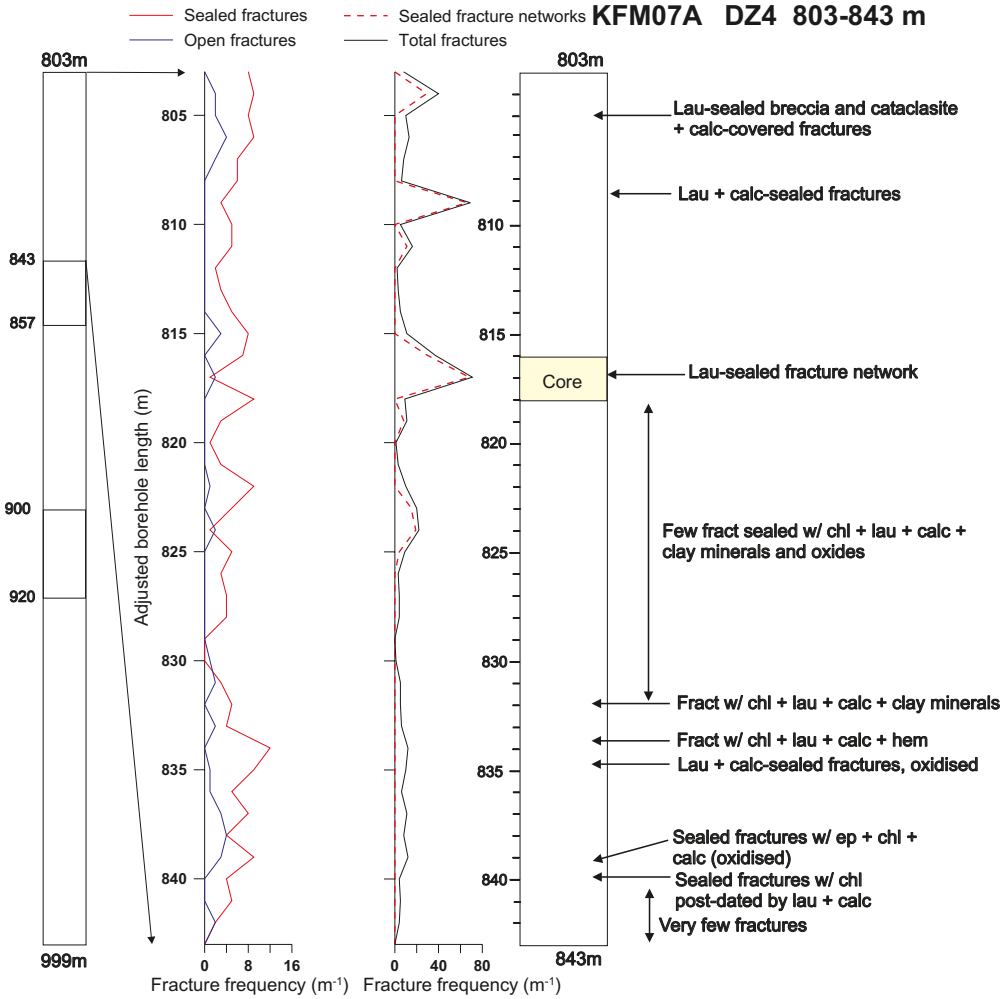

Figure 5-125. *Simplified drawing of KFM07A, DZ4, showing the occurrences of brittle deformation features in the upper part of the zone (803–843 m). At 816–818 m, there are sub-parallel arrays of fractures and dense fracture networks that form up to ca. 10 mm wide zones cutting the foliation in the metagranite to metagranodiorite at a high angle (Figure 5-128). There is marked grain size reduction due to local crushing along the fractures (Figure 5-129).*

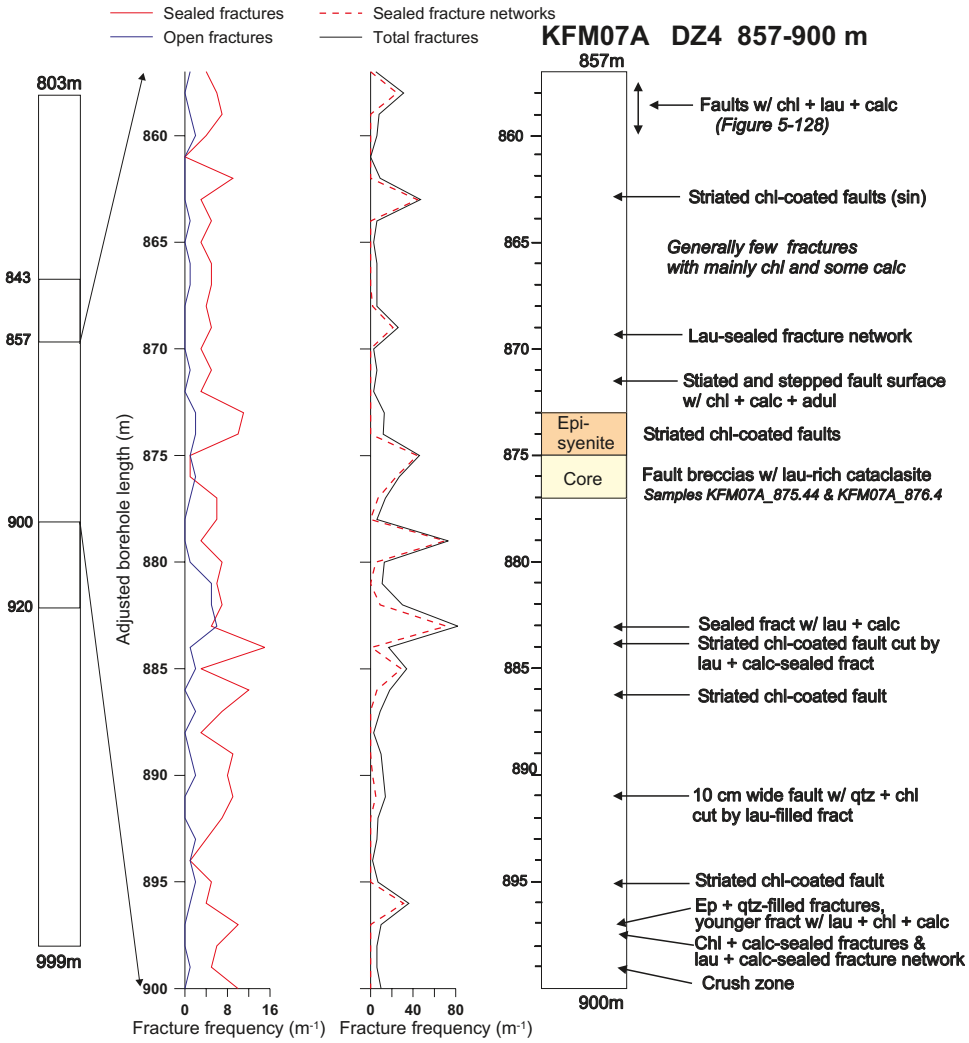

Figure 5-126. *Simplified drawing of KFM07A, DZ4, showing the occurrences of brittle deformation features in the central part of the zone (857–900 m). See text for a more detailed description.*

At 857–860 m, fault rocks with chlorite, laumontite and calcite are present (see Figure 5-130). At ca. 858.3 m there is a 30 cm wide zone of fault rocks with chlorite, laumontite and calcite in addition to altered amphibolite.

At 862–863 m, there are good examples of chlorite striation showing sinistral movement on steeply west-dipping faults. Similar striations with various combinations of minerals (see Figure 5-126) showing strike slip movement are present at 873–875 m and at 897.3–898.2 m. Generally, epidote, quartz and chlorite are post-dated by laumontite and calcite, in cases together with second generation chlorite.

At 875–877 m, there are excellent examples of cemented fault breccias containing variably sized sub-rounded to angular fragments of the host rocks embedded in a fine-grained, brownish red cataclasite (Figure 5-131). In detail, the cataclasite is composed of quartz, feldspar, epidote, clinozoisite, chlorite, and laumontite. Thin laumontite-veins are present (see Figure 5-132). Similar fault breccias are present in a ca. 60 cm long section along the core at about 934 m (see below).

At 877.5–884 m, there are thin laumontite-sealed fractures and fracture networks.

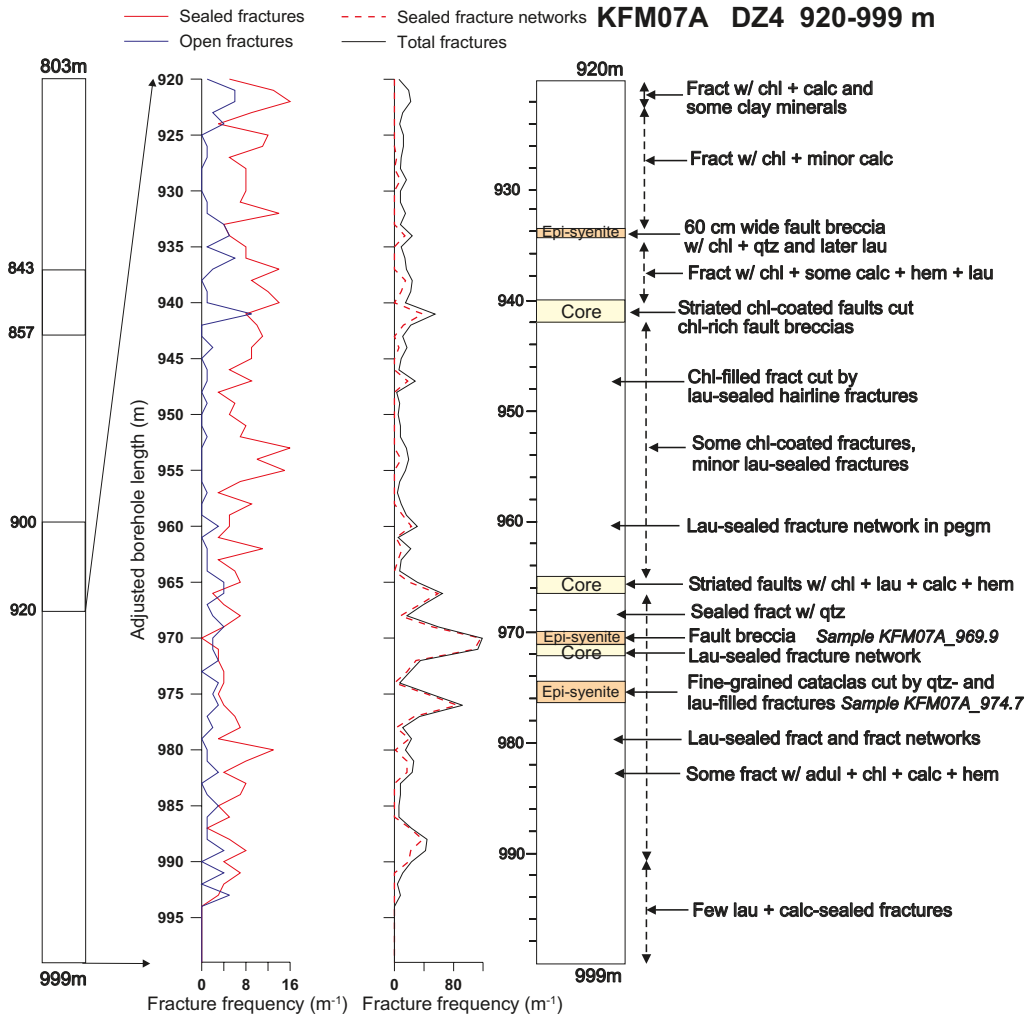

Figure 5-127. *Simplified drawing of KFM07A, DZ4, showing the occurrences of brittle deformation features in the lower part of zone (920–999 m). See text (below) for a more detailed description.*

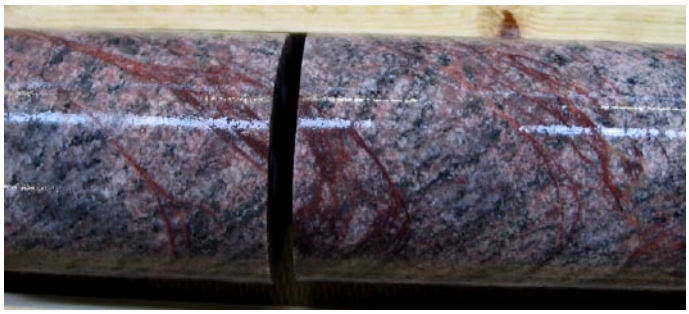

Figure 5-128. *Core from KFM07A_817.7 m, DZ4, up is to the left. Granodioritic gneiss is cut by laumontite-sealed fractures and fracture networks consisting of sub-parallel fractures and narrow zones with crushing of the host rock (see Figure 5-129 for details).*

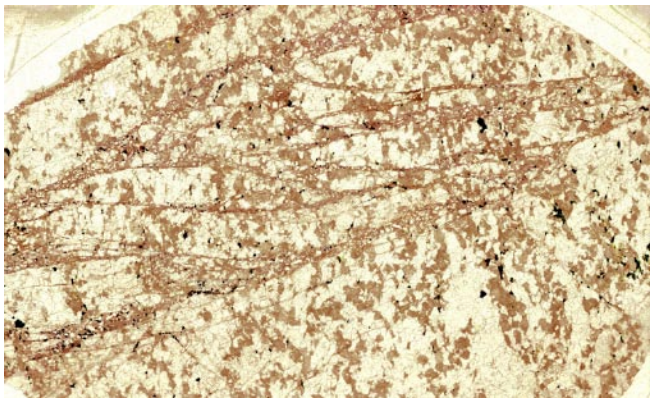

Figure 5-129. *Scanned thin section of sample KFM07A_817.7 m, DZ4. Metagranodiorite with faint foliation is cut by a ca. 1 cm wide zone showing strong fracturing with marked grain size reduction producing angular clasts in a fine-grained groundmass that contain epidote and chlorite. The zone is delimited by two parallel bounding fractures, and between these there are numerous slightly curved fractures intersecting each other at small angles. Reddish dusting (oxides and/or laumontite) along the fractures is prominent. The field of view is ca. 35 mm wide.*

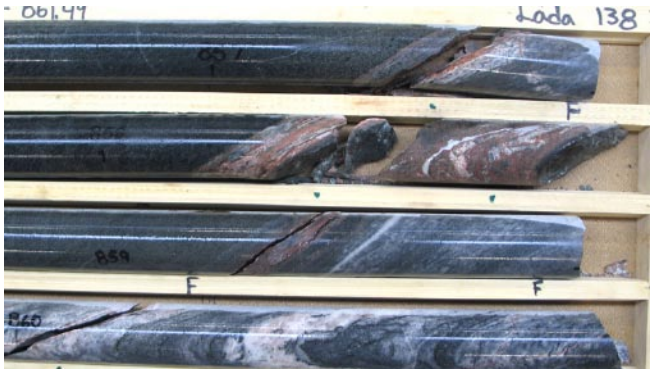

Figure 5-130. *Core from KFM07A in the interval 857–860 m, DZ4. At ca. 858.3 m there is a 30 cm wide zone of fault rocks with chlorite, laumontite and calcite in addition to altered amphibolite. Minor faults are present at ca. 857.2 m and at 859.1 m. These structures are approximately parallel to the strong foliation in the amphibolitic to granitic host rocks. A minor laumontite-sealed fracture can be seen crossing the foliation at ca. 860 m.*

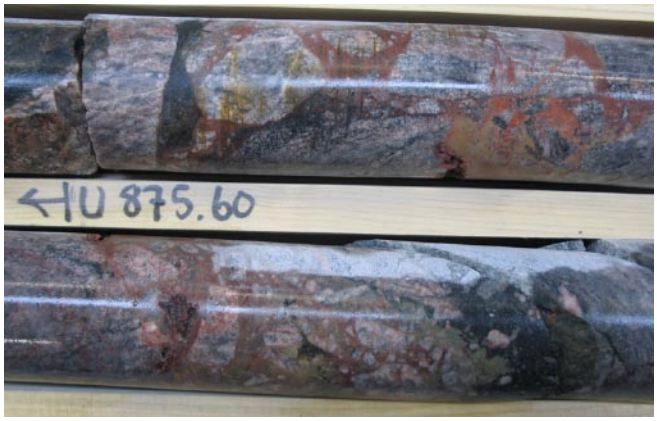

Figure 5-131. *Core from KFM07A in the interval 874–876 m, DZ4. Fault breccias consisting of small and larger fragments of the host rock embedded in fine-grained brownish-red, laumontite-rich cataclasite. Details from the core in the upper part of the figure are shown in Figure 5-132 (below).*

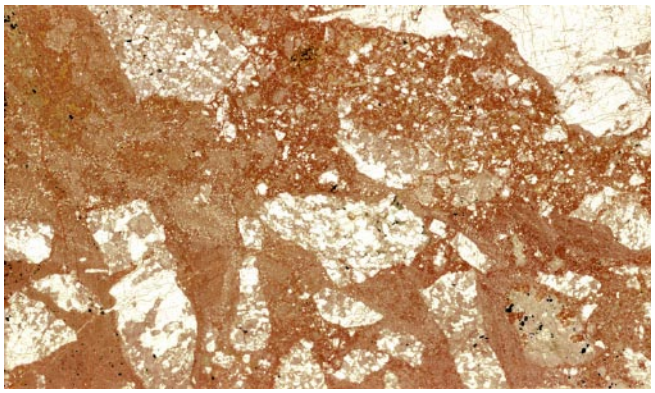

Figure 5-132. *Scanned thin section from core KFM07A_875.44 m. Fragments of host rock, metagranite are present. One big and variably sized small clasts in fine-grained cataclasite to ultra-cataclasite. Note some variation in grain size of the cataclasite. The dark red-brown parts consist mainly of laumontite. A very thin laumontite vein traverses the thin section close to its left margin. The field of view is ca. 35 mm wide.*

At 883.78 m, a steep minor fault (trending 155 degrees) filled with chlorite + laumontite + calcite exhibits excellent striation and steps showing dextral shear sense. This fault is cut by a core-parallel laumontite-sealed, thin vein (Figure 5-133).

At 940–942 m, there are several fractures and small NNW-SSE-trending faults with good striations defined mainly by chlorite (Figure 5-134). The striated faults cut chlorite-rich fault breccias. Numerous striated fractures are also present at ca. 965–966 m. From about this level, there are quite abundant occurrences of laumontite-sealed fractures and fracture networks in the core. Good examples including fault breccias are present between 968 and 979 m (see Figure 5-135 and 5-136 from 969.9 m).

Figure 5-133. *Core from KFM07A at 883.78 m, DZ4. A fault surface exhibits chlorite striation (shown by red mark) and small steps showing sense of shear. A late fracture sealed with laumontite cuts the fault.*

Figure 5-134. *Core from KFM07A at 941.8 m, DZ4. Fault surface with excellent chlorite striation.*

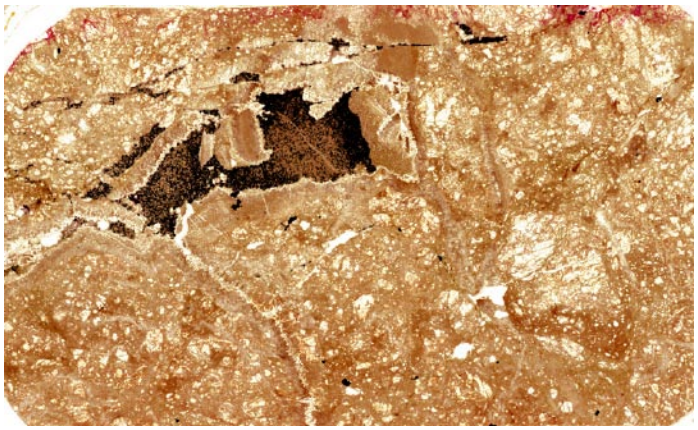

Figure 5-135. *Scanned thin section from core KFM07A_969.9 m. Fragments of host rock metagranite are present as angular small clasts in fine-grained, reddish-brown cataclasite. Pale vein-like features that traverse the cataclasite consist of euhedral quartz that grew epitaxially into open fractures and voids. The dark irregular area is also rimmed by euhedral quartz, and the same is the case for the irregular fracture going across the upper part of the section. The dark fill consists of unidentified sub-microscopic material that has filled open voids following the growth of quartz. The field of view is ca. 35 mm wide.*

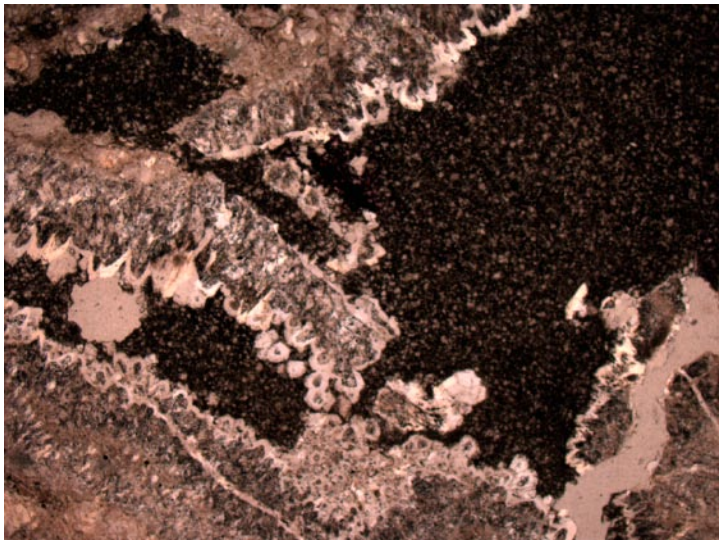

Figure 5-136. *Photomicrograph showing details from Figure 5-135. (KFM07A_969.9 m). The field of view is ca. 1.4 mm wide.*

Figure 5-137. *Core from KFM07A at 975 m, DZ4. Fine-grained cataclasite which in the footwall (right) is post-dated by quartz- and laumontite-filled fractures, in places with some calcite. The section cut from the core was used for thin section study (Figure 5-138).*

At 975 m, a ca. 10 cm wide fault core was collected (Figure 5-137). Boundaries towards the wall rock are sharp, and fault rocks include dark green, fine-grained, greenish cataclasite which in the footwall is post-dated by quartz- and laumontite-filled fractures, in places with some calcite (white inside brick-red laumontite). In thin section (Figure 5-138), the cataclasite is seen to be cut by thin fractures filled with quartz and by less well-defined fractures carrying laumontite. Calcite is found in the core of a pocket of laumontite (Figure 5-138).

60 fault slip data have been measured (stereoplot A of Figure 5-139a). Chlorite is almost ubiquitous and is accompanied by calcite, laumontite, hematite and rarely clay minerals or adularia. For easier reading, the data set has been split into five sub-sets according to their attitude (stereoplots B, C, D, E and F). It appears that this zone is characterized by an important set of 41 NNW-SSE steep strike-slip faults (stereoplots B, C and D). Among the 41 faults with slickensides, 26 have unknown sense of shear, 10 are left-lateral and 5 are right-lateral strike-slip (stereoplots B, C and D, respectively). Also, 4 steeply dipping strike-slip faults of unknown shear sense strike ENE-WSW (stereoplot B). Another sub-set comprises 7 gently-dipping faults, mainly E-W trending and N- or S-dipping with dip-slip or strike-slip slickensides. Only two of the 7 related slickensides show sense of shear with one being dextral reverse and dipping NW, and the other one, dextral plunging 2 degrees to the SSW (numbers 1 and 7, respectively, of stereoplot E). Finally, the last sub-set comprises faults dipping from 50 degrees to nearly vertical and trending NNW-SSE and ENE-WSW to E-W (i.e. similar in trend to the strike-slip faults) with highly oblique to dip-slip striae (stereoplot F), normal movement (numbers 5, 8) or highly oblique sinistral for those of defined sense of shear (numbers 1, 4 dipping north and number 2 dipping south in stereoplot F of Figure 5-139a).

The two upper intervals of DZ4 (803–843 m and 857–900) have mainly NNW-SSE faults. In the deepest interval (920–999 m) faults trending ENE-WSW to E-W are also present (Figure 5-139b).

Figure 5-138. *Photomicrograph from thin section; core KFM07A at 975 m, DZ4. Fine-grained (ultra-)cataclasite with veins sealed by brownish laumontite and calcite. A thin quartz vein also cuts the cataclasite (upper part). The field of view is ca. 1.5 mm wide.*

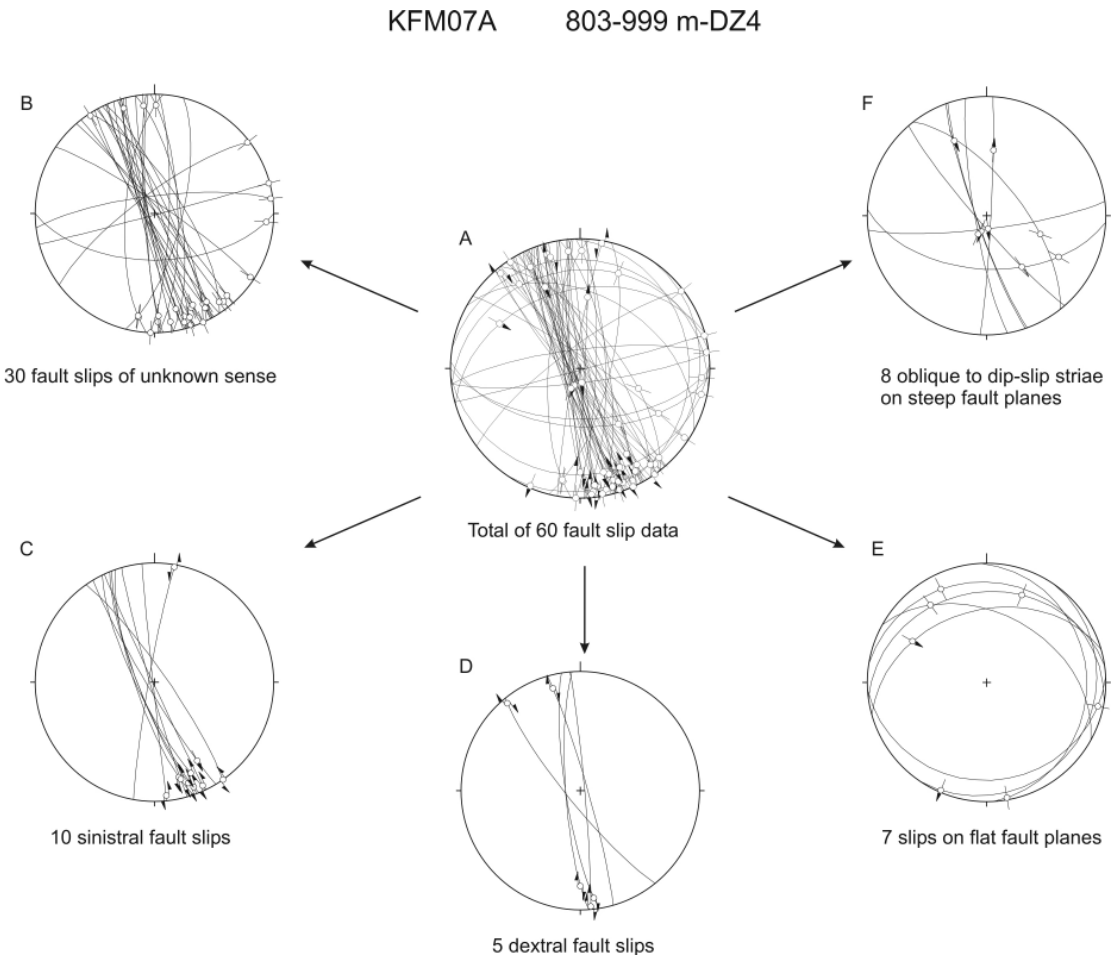

Figure 5-139a. *Stereoplot of fault slip data in DZ4 (KFM07A). The entire set of 60 fault slip data has been split into 5 sub-sets according to the attitude of fault planes and/or slickensides (see the text for description of each).*

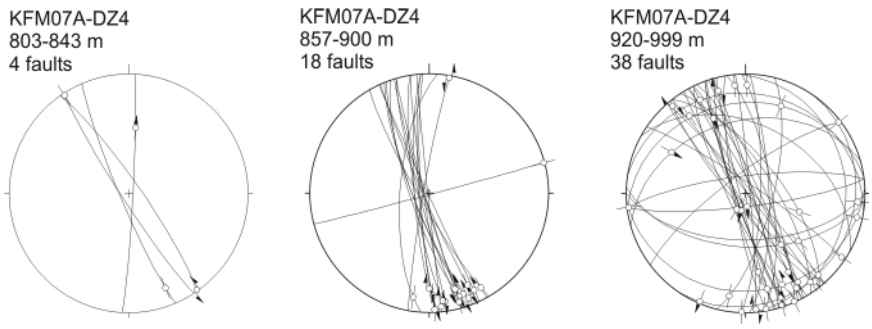

Figure 5-139b. *Stereoplot of fault slip data in DZ4 (KFM07A). The data set has been split into 3 sub-sets according to depth intervals.*

5.2.12 KFM08A

This borehole is located in the north-western part of the investigation area (Figure 5-40). The borehole is oriented 321/61 and has a length of 1,001 m /Carlsten et al. 2005c/. Four deformation zones with a combined length of 239 m were investigated (Table 5-1).

A total of 20 fault slip data were obtained from the drill core (Figure 5-140). Two predominant trends of fault planes are present: NNW–SSE-oriented, steep, left-lateral faults with slickensides plunging 20 degrees SSE, and gently SE-dipping reverse faults.

KFM08A: 172–342 m – DZ1

This zone occurs along a total borehole length of 170 m. The rock types present are strongly foliated, grey, medium-grained and fine-grained metagranite, which locally has reddish staining due to oxidation. Pegmatite occurs as thin veins cutting the core at different angles, and a few pegmatites that are more than 1 m thick along the core. Amphibolites occur as thin sheets but may also occupy longer core sections (e.g. at 251–262 m). Leucocratic granite veins are commonly associated with the amphibolites.

Considering the entire zone, steeply dipping fractures with NE-strike and gently dipping fractures dominate. The average frequency of fractures in the zone is ca. 7.5/m /Carlsten et al. 2005c/. The majority of the fractures are sealed, mainly with calcite, chlorite and laumontite. In parts of the interval, the fracture frequency is relatively low (cf. Figure 5-140). Other sections exhibit a significant increase in mainly laumontite + calcite-sealed fractures (Figure 5-141 and 5-142).

The upper part of the zone down to ca. 270 m borehole length, exhibits sporadic and quite evenly spaced open or sealed fractures with chlorite, laumontite, calcite as infilling minerals. Striations on chlorite-coated surfaces were observed in a couple of cases. At 258.2 m, a narrow cemented fault and thin sealed fractures cut amphibolite (Figure 5-143 and 5-144).

In the interval 274–287 m the core is cut by sealed and open fractures with laumontite (Figure 5-142). Below this level, there are scattered fractures with chlorite, calcite and minor laumontite and pyrite. Based on the high abundance of sealed fractures in addition to a number of open fractures, this section is considered a transition zone with sections of fault core.

A 2 cm wide fault rock cuts the core at 299.95 m. At 335.5 m, there is a 3–4 cm wide fault rock with small, angular fragments of red-stained feldspar embedded in a chlorite-rich matrix (Figure 5-145). A steeply E-dipping fault surface, which is coated with quartz, hematite and specks of pyrite, shows gently N-plunging striation.

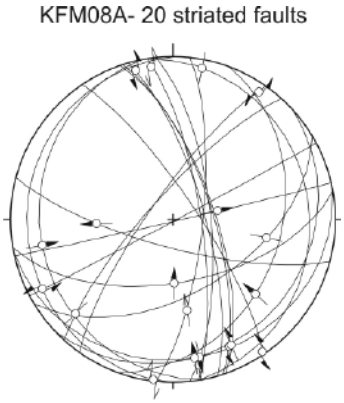

Figure 5-140. *Stereoplot showing all the fault slip data collected along all the studied DZ of drill core KFM08A.*

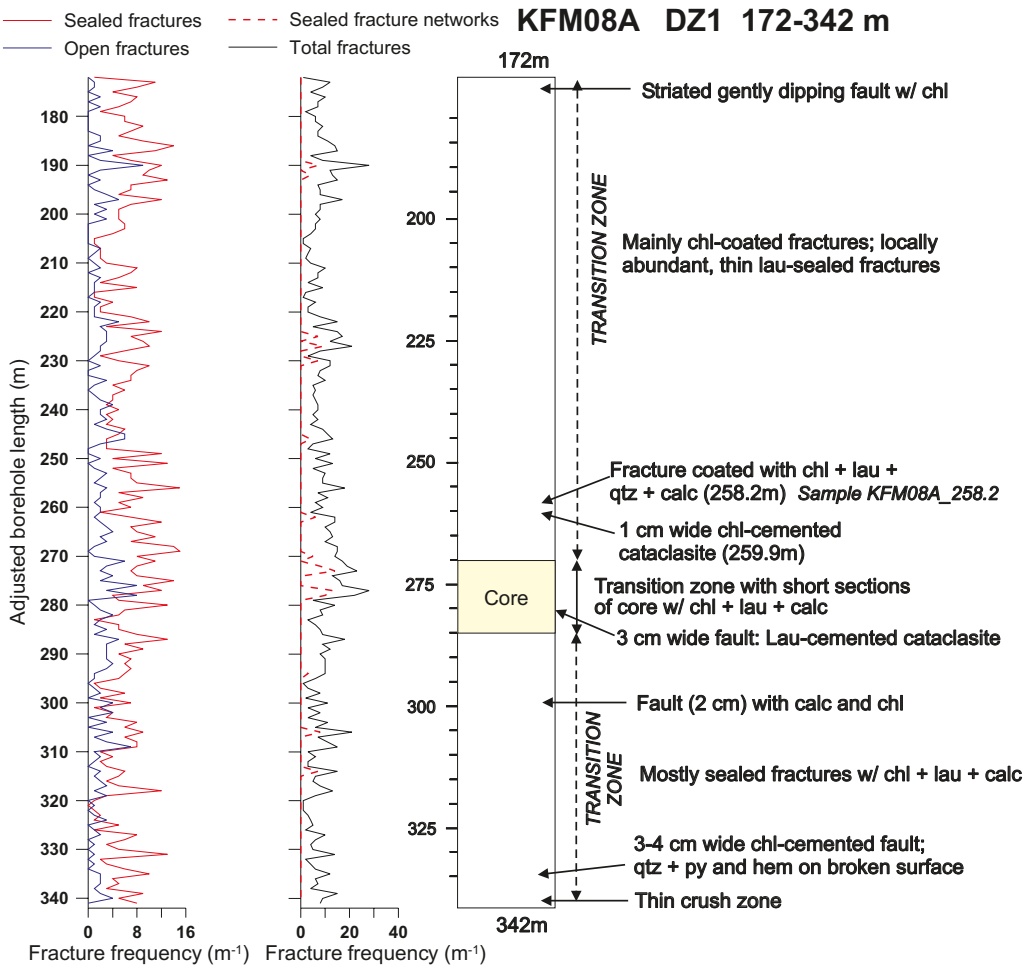

Figure 5-141. *Simplified drawing of KFM08A, DZ1, showing the recorded brittle deformation features. Apart from a section where fault core is developed (274 m–287 m, the interval is defined as a transition zone according to the definition of /Munier et al. 2003/. Photos from the core (Figure 5-142) illustrate selected parts of the borehole.*

Figure 5-142. *Overview of core sections from KFM08A, DZ1. To the left, the section 200–210.5 m illustrates a part of the zone with few spaced, open fractures. To the right, the section 274–287 m is characterized by a relatively high frequency of laumontite-sealed closed and broken fractures, including a 3 cm wide cataclasite sealed with laumontite and euhedral calcite at 281.7 m.*

Figure 5-143. *Scanned thin section from core KFM08A_258.2 m. The host rock is a chloritized amphibolite with altered plagioclase, amphibole, chlorite, opaques and titanite. The amphibolite is transected by a fault and irregular fractures cemented by chlorite, laumontite and euhedral calcite. Early formed euhedral quartz has locally precipitated on fracture walls and along the edges of calcite that fill the fractures. Late thin fracture going across the thin section is partly filled with calcite. The field of view is ca. 35 mm wide.*

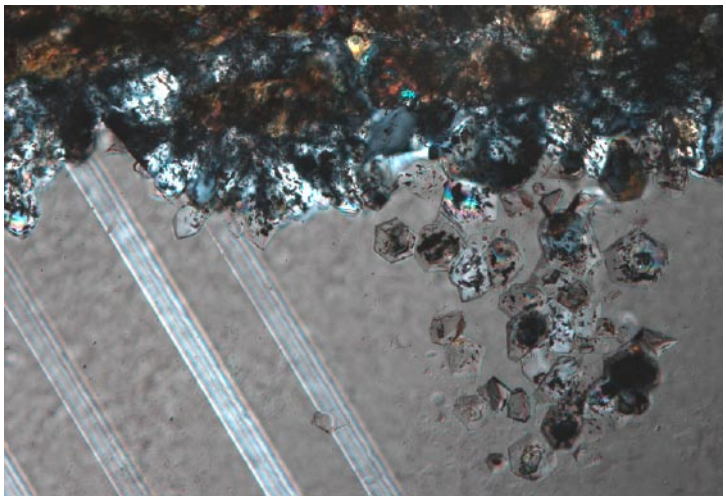

Figure 5-144. *Photomicrograph from thin section from core KFM08A_258.2 m. Small crystals of euhedral quartz have grown along fracture walls and in calcite that fills the fractures. The field of view is ca. 0.5 mm wide.*

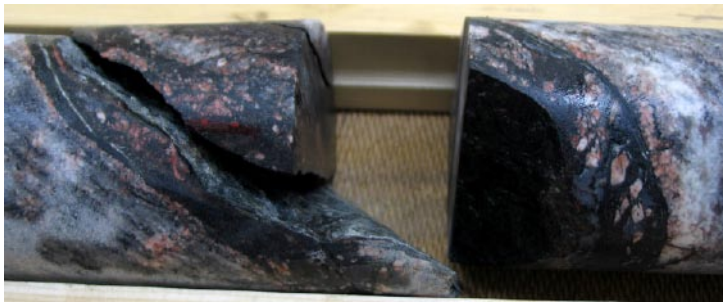

Figure 5-145. *Core section from KFM08A, DZ1, 335.5 m. The metagranite is cut by a 3–4 cm wide fault rock with small, angular fragments of red-stained feldspar embedded in a chlorite-rich matrix. A broken fault surface is coated with quartz + pyrite + hematite.*

Nine faults with slickensides have been measured in this zone. They are predominantly NNW-SSE trending and with gently SSE-plunging striae are defined mainly by chlorite, and in some cases with calcite, laumontite and hematite (Figure 5-146). One fault is coated with quartz + pyrite + hematite. The sense of shear has been determined on some of them as left-lateral strike-slip. Three other faults are observed: (1) a steep NE-SW sinistral fault with calcite (number 3); (2) a sub-horizontal W-dipping dextral fault with chlorite + calcite (number 2) and (3) a 30 degrees SE-dipping fault with dip-slip reverse chlorite striae (number 1 on Figure 5-146).

KFM08A: 479–496 m – DZ2

This is a 17 m wide deformation zone in medium- to coarse-grained metagranite with some amphibolite and pegmatite. The zone has an average fracture frequency of ca. 6/m /Carlsten et al. 2005c/. Minerals filling the fractures are predominantly chlorite and calcite, while laumontite, quartz, corrensite and pyrite occur sporadically. At the top of the zone, there is a fractured pegmatite, and there are some open fractures in the first couple of meters. Few fractures follow down to the base of the zone where there is a minor sealed network with laumontite and subsidiary calcite (Figure 5-147).

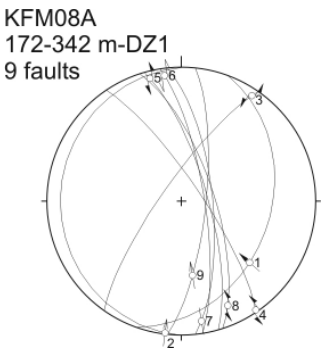

Figure 5-146. *Stereoplot of fault slip data in DZ1 (KFM08A).*

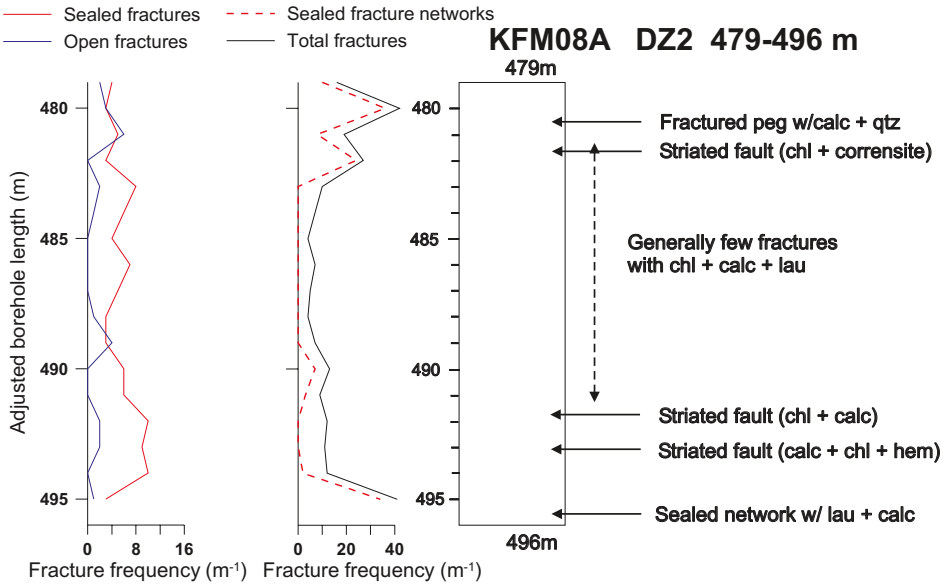

Figure 5-147. *Simplified drawing of KFM08A, DZ2, showing the recorded brittle deformation features.*

Along this zone, the same trend exists as in zone DZ1 (described above): one NNW-SSE fault with gently SSE-plunging strike-slip striae defined by chlorite and clay minerals (number 1 of Figure 5-148) and two NE-SW strike-slip faults with chlorite and calcite, one of which is a well defined left-lateral fault (numbers 2 and 3, respectively, of Figure 5-148).

KFM08A: 672–693 m – DZ4

Deformation zone in medium- to coarse-grained metagranite with some amphibolite and pegmatite. The zone has a fracture frequency of ca. 6/m. Fracture minerals are chlorite, calcite, laumontite, oxides and clay minerals. There are relatively few fractures down to ca. 685 m. From 687 to 689 m, there is a locally dense laumontite-sealed fracture network with some calcite. Some fractures with laumontite, calcite or chlorite continue to ca. 692 m (Figure 5-149).

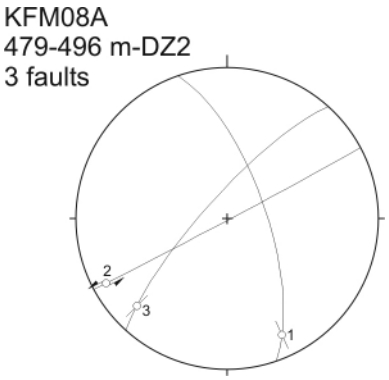

Figure 5-148. *Stereoplot of fault slip data in DZ2 (KFM08A).*

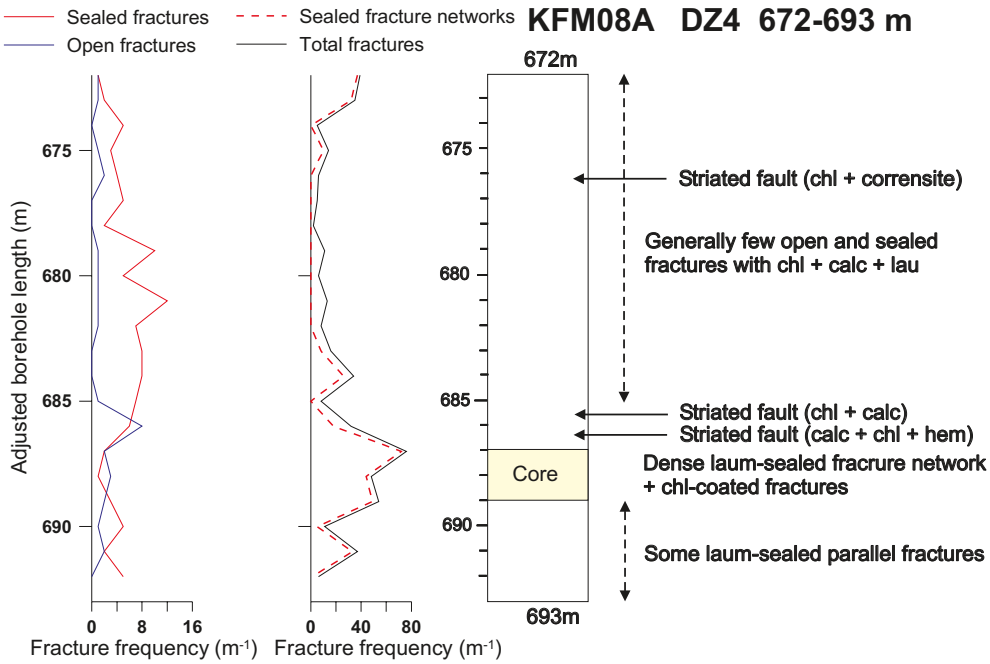

Figure 5-149. *Simplified drawing of KFM08A, DZ4, showing the recorded brittle deformation features.*

The faults of this zone differ from the two other ones described above (i.e. DZ1 and DZ2 of core KFM08A). An ENE-striking vertical fault has laumontite striation plunging steeply to the east (Figure 5-150). Four faults are sub-horizontal with different attitudes. The N-S-striking faults (number 2 and 3) have striations defined by chlorite, hematite and some calcite. On the two sub-parallel ENE-striking faults (number 4 normal with laumontite + calcite, and number 5 reverse with chlorite+calcite+clay minerals), the parallel striae have opposite sense of shear (Figure 5-150).

KFM08A: 915–946 m – DZ6

The rock types in this zone are similar to those in DZ4. Local oxidation with reddish colour occurs. With the exception of some short intervals with highly fractured core, the fracture frequency in the zone is moderate. The average fracture frequency is ca. 8.5/m /Carlsten et al. 2005c/, and most sealed and broken fractures have moderate to steep dips to the south. Some steeply dipping fractures dip NNE and WNW. Minerals filling the fractures include quartz, chlorite, laumontite, calcite, oxides and pyrite.

Near the top of the zone at 915.7 m, there is a more than 10 cm wide fault zone with highly chloritised amphibolite and a striated fault with laumontite, chlorite and calcite. At ca. 918 m there is a network of thin, laumontite-sealed fractures in pegmatite (Figure 5-152). Below a gap in the core at ca. 919 m, there is amphibolite with abundant chlorite-coated and some laumontite-sealed fractures. From 920 m and onwards for about 50 cm, thin laumontite-sealed fractures cut quartz- and calcite-filled veins. A thin sealed fault with quartz, laumontite and calcite occurs at 920.1 m (Figure 5-151 and 5-152).

Below 924 m the fracture frequency gradually drops back with mainly chlorite-coated fractures. Some thin laumontite sealed fractures and fracture networks with calcite occur sporadically. Networks of thin, laumontite+calcite sealed fractures occur at ca. 940–941 m. An example of this was collected at 940.38 m (Figure 5-153). Near the base of the zone, there is a 3 cm wide sealed fault.

The three measured faults are trending E-W to WSW-ENE and dip 50–70 degrees to the south (Figure 5-154). One of them is NE-trending with oblique-slip striation defined by chlorite (number 1, Figure 5-154). There is also a reverse dip-slip fault with steps and striae defined by laumontite, chlorite and calcite (number 2). Finally, there is an oblique normal fault in amphibolite with slickensides (chlorite + calcite) plunging to the west (number 3, Figure 5-154).

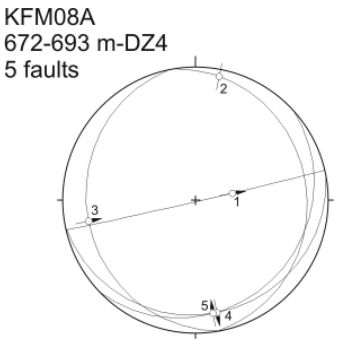

Figure 5-150. *Stereoplot of fault slip data in DZ4 (KFM08A).*

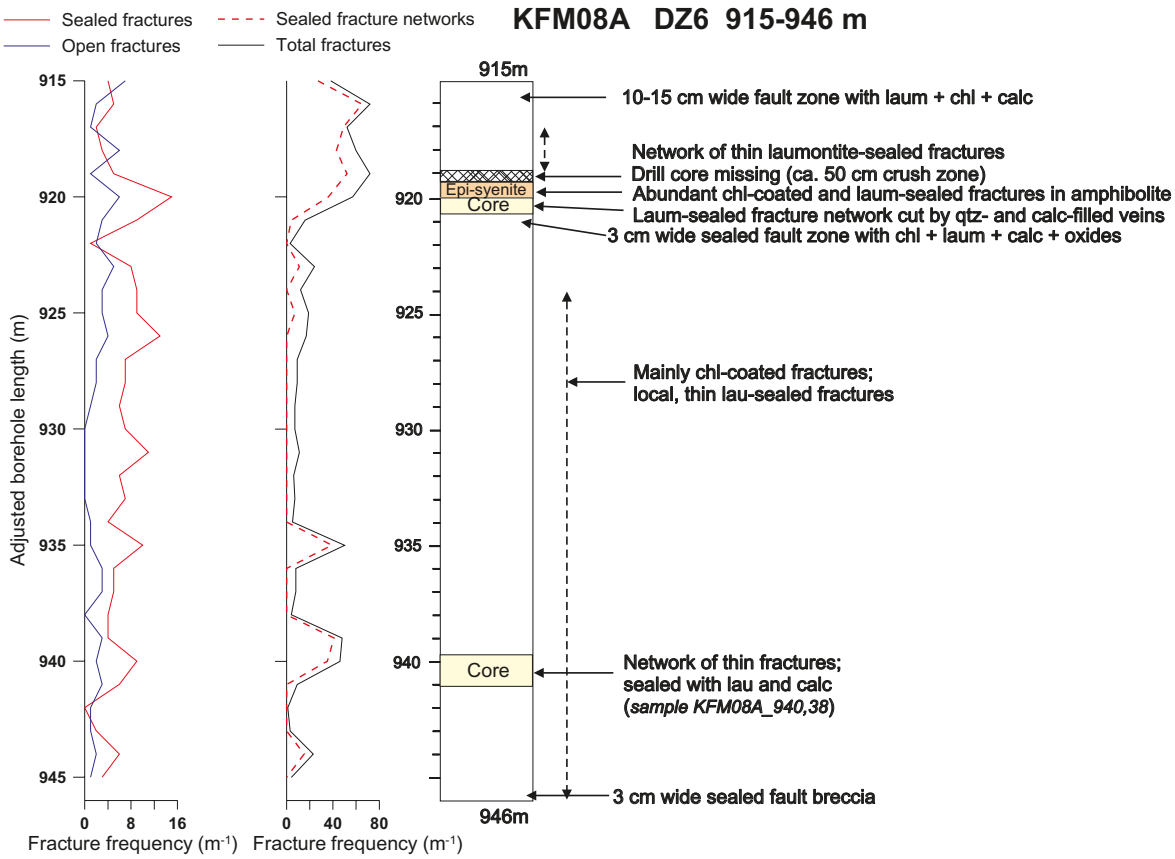

Figure 5-151. *Simplified drawing of KFM08A, DZ6, showing the recorded brittle deformation features. The intervals marked at ca. 920 m and 940 m are considered fault core. The remaining part of the DZ is a transition zone according to /Munier et al. 2003/.*

Figure 5-152. *Core section from KFM08A, DZ6, 917.5–922.5 m. A variety of rock types and deformation products are present (see text for details).*

Figure 5-153. *Scanned thin section from core KFM08A_940.38 m. The fractures cut a pink-grey, biotite-bearing metagranite to metagranodiorite. Strong crushing of the host rock has taken place along the fractures, and some epidote/clinozoisite and laumontite have sealed the fine-grained deformation products. Laumontite (brown) and minor quartz have also grown on fracture walls, whereas coarse-grained calcite is a late mineral filling remaining space along the central part of the fractures. The field of view is ca. 35 mm wide.*

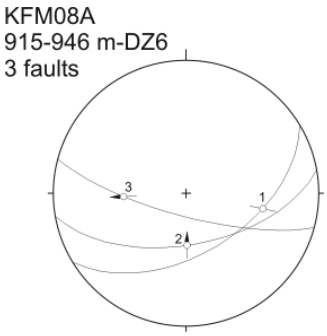

Figure 5-154. *Stereoplot of fault slip data in DZ6 (KFM08A).*

5.2.13 KFM08B

This borehole is located in the north-western part of the investigation area (Figure 5-40). The borehole is oriented 270/59 and has a length of 200.5 m /Carlsten et al. 2005c/. Only one deformation zone was investigated (Table 5-1). A set of NNW–SSE-oriented, steep strike-slip faults are present, i.e. a situation similar to that observed in KFM07A and KFM08A.

KFM08B: 167–185 m – DZ2

A deformation zone occurs along an 18 m long borehole interval in medium- to coarse-grained metagranite with some layers of amphibolite (up to 1.5 m in the core). The average fracture frequency is ca. 8 m /Carlsten et al. 2005c/. However, the upper part of the zone has a relatively low frequency compared to a section with fairly abundant fractures from ca. 175 m and onwards (Figure 5-155). Fractures and some fracture networks are predominantly sealed by chlorite, calcite and laumontite; minor corrensite and oxides are present.

The most interesting fault rocks with good striation on chlorite-coated planes occur near the base of the zone, from 182 m. At ca. 183.5 m, a fault containing brecciated, chloritized amphibolite is sealed by laumontite + calcite (Figure 5-156). A thin section from this fault shows the late growth of platy euhedral calcite (Figure 5-157).

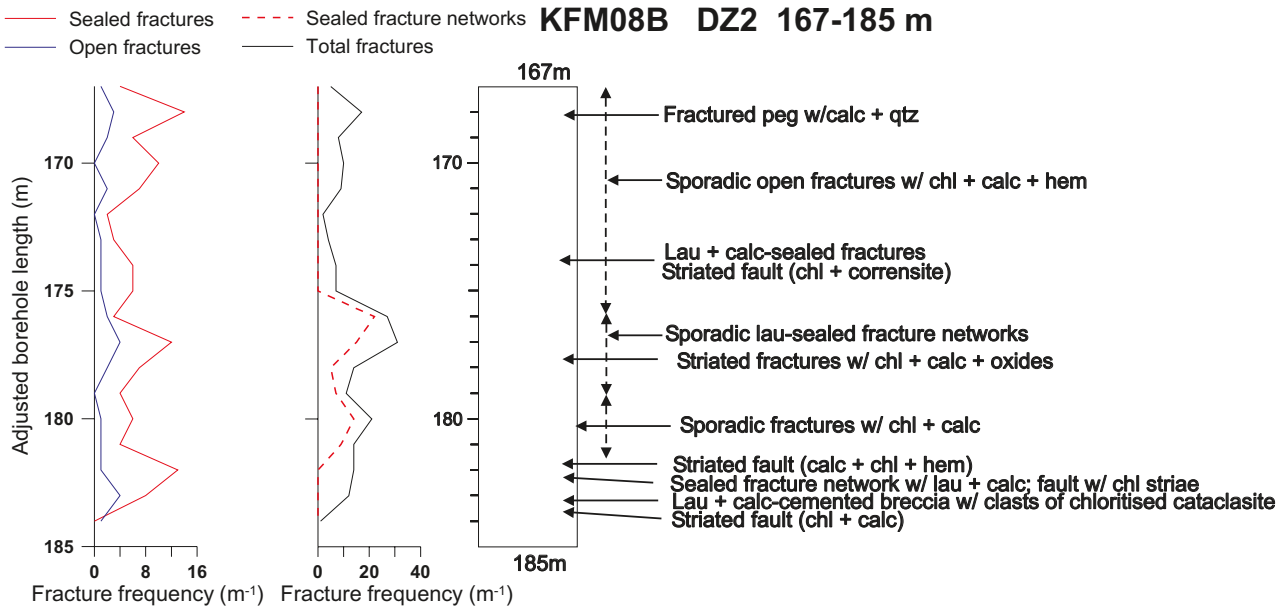

Figure 5-155. *Simplified drawing of KFM08B, DZ2, showing the recorded brittle deformation features. The intervals marked at ca. 920 m and 940 m are considered fault core. The remaining part of the DZ is a transition zone according to /Munier et al. 2003/.*

Figure 5-156. *Core section from KFM08B, DZ2, 183.5 m, up is to the left. Fault containing brecciated, chloritized amphibolite is sealed by laumontite + calcite. Note chlorite-coated surface with good striation in the hanging wall of the fault.*

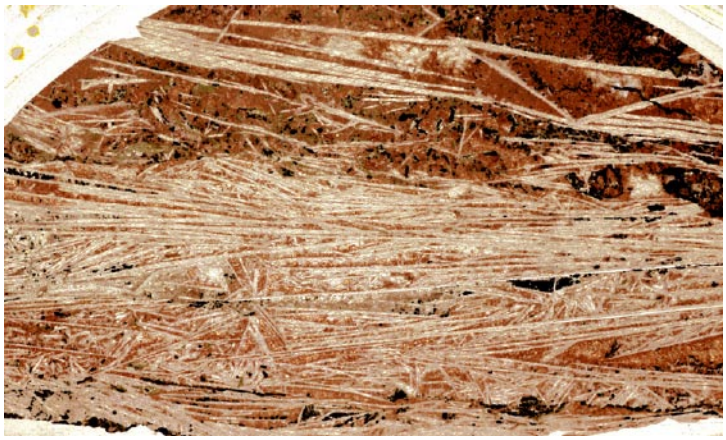

Figure 5-157. *Scanned thin section from core KFM08B_183.5 m. Platy calcite is prominent and postdates laumontite. Other minerals include mainly chlorite, epidote/clinoziosite and opaques representing the altered amphibolitic host rock. The field of view is ca. 35 mm wide.*

The main trend of faults in this zone is NNW-SSE with some of the striae defined by chlorite + calcite clearly indicating a sinistral sense of shear (numbers 4, 5 and 6 of Figure 5-158). An ENE-WSW trending dip-slip reverse fault (chlorite + corrensite) that dips 30 degrees to the south is also observed (number 3 on Figure 5-158).

5.2.14 Summary of the results of the borehole data

Three boreholes (KFM02A and KFM03A and B) are situated in the southeast part of the investigation area (Figure 5-40). Kinematic data were mainly obtained from a population of faults in KFM02A, that strike NE-SW with gentle to moderate SE dips. Slickensides on these faults show reverse dip-slip sense of movement. Important seismic reflectors that dip gently to the southeast were interpreted as thrusts by /Juhlin and Stephens 2006/. Thus, the analysis of kinematic data from the boreholes appears to be consistent with the conclusion of /Juhlin and Stephens 2006/.

Three drill sites (KFM01A/B, KFM04A, KFM05A) are located close to the south-western boundary of the candidate investigation area (Figure 5-40). KFM06A is located some distance to the northeast. Kinematic data were mainly obtained from KFM04A and KFM06A. In the former, the predominant set of fault planes strike NW to NNW with steep dips; i.e. sup-parallel to the EDZ. Slickensides plunge 10 or 80 degrees to the NW. Another set with less abundant faults strike ENE-WSW and may form a conjugate set with faults striking NNE. However, the relative sense of movement along the faults could not be determined. Fault planes yielding kinematic data in KFM06A are largely oriented ENE-WSW with steep dips. Slickensides suggest mainly strike-slip movement and plunge 20 degrees to the WSW. Most of the kinematic data were obtained from the deeper levels of the borehole.

The three boreholes (KFM07A, KFM08A and KFM08B) in the north-western part of the investigation area yielded about 100 faults with kinematic indicators. Steep fault planes trending NNW-SSE are the most common, i.e. similar to borehole KFM04A. The slickensides are gently plunging and both sinistral and dextral sense of movement was recorded. A set of E- to NE-striking faults with variable dip direction and sense of shear was also recorded in these boreholes.

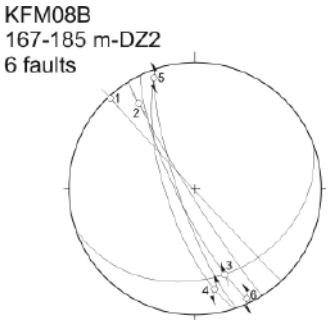

Figure 5-158. *Stereoplot of fault slip data in DZ2 (KFM08B).*

6 References

Braathen A, 1999. Kinematics of brittle faulting in the Sunnfjord region, western Norway. Tectonophysics 302, 99–121.

Braathen A, Gabrielsen R H, 2000. Bruddsoner i fjell – oppbygning og definisjoner. Gråstein, 7, 1–20. Norges Geologiske Undersøkelse, ISSN 0807-4801.

Braathen A, Osmundsen P T, Nordgulen Ø, Roberts D, Meyer G B, 2002. Orogen-parallel extension of the Caledonides in northern Central Norway: an overview. Norwegian Journal of Geology, 82, 225–241.

Braathen A, Osmundsen P T, Gabrielsen R, 2004. Dynamic development of fault rocks in a crustal-scale detachment; an example from western Norway. Tectonics, 23, TC4010, doi:10.1029/2003TC001558.

Caine J S, Evans J P, Forster C B, 1996. Fault zone architecture and permeability structure. Geology, 24, 11, 1025–1028.

Carlsten S, Peterson J, Stephens M B, Gustafsson J, 2004a. Geological single-hole interpretation of KFM01A, KFM01B and HFM01–03 (DS1). SKB P-04-116, Svensk Kärnbränslehantering AB.

Carlsten S, Peterson J, Stephens M B, Mattson H, Gustafsson J, 2004b. Geological single-hole interpretation of KFM02A and HFM04–05 (DS2). SKB P-04-117, Svensk Kärnbränslehantering AB.

Carlsten S, Peterson J, Stephens M B, Mattson H, Gustafsson J, 2004c. Geological single-hole interpretation of KFM04A and HFM09–10 (DS4). SKB P-04-119, Svensk Kärnbränslehantering AB.

Carlsten S, Peterson J, Stephens M B, Thunehed, H, Gustafsson J, 2004d. Geological single-hole interpretation of KFM05A and HFM19 (DS5). SKB P-04-296, Svensk Kärnbränslehantering AB.

Carlsten S, Peterson J, Stephens M B, Thunehed, H, Gustafsson J, 2004e. Geological single-hole interpretation of KFM03B, KFM03A and HFM06–08 (DS3). SKB P-04-118, Svensk Kärnbränslehantering AB.

Carlsten S, Gustafsson J, Mattson H, Peterson J, Stephens M B, 2005a. Geological single-hole interpretation of KFM06A and KFM06B (DS6). SKB P-05-132, Svensk Kärnbränslehantering AB.

Carlsten S, Gustafsson J, Mattson H, Peterson J, Stephens M B, 2005b. Geological single-hole interpretation of KFM07A and HFM20–21 (DS7). SKB P-05-157, Svensk Kärnbränslehantering AB.

Carlsten S, Gustafsson J, Mattson H, Peterson J, Stephens M B, 2005c. Geological single-hole interpretation of KFM08A and KFM08B and HFM22 (DS8). SKB P-05-262, Svensk Kärnbränslehantering AB.

Evans J P, Forster C B, Goddard J V, 1997. Permeability of fault-related rocks, and implications for hydraulic structure of fault zones. Journal of Structural Geology, 19, 1393–1404.

Gudmundsson A, Berg S S, Lyslo K B, Skurtveit E, 2001. Fracture networks and fluid transport in active fault zones. Journal of Structural Geology, 23, 2–3, 343–353. 0191–8141.

Juhlin C, Stephens M B, 2006. Gently dipping fracture zones in Paleoproterozoic metagranite, Sweden: Evidence from reflection seismic and cored borehole data and implications for disposal of nuclear waste. Journal of Geophysical Research, B09302, doi: 10.1029/2005JB003887.

Munier R, Stanfors R, Milnes A G, Hermanson J, Triumf C-A, 2003. Geological Site Descriptive Model. A strategy for the development during site investigations. SKB R-03-07, Svensk Kärnbränslehantering AB.

Nordgulen Ø, Braathen A, Corfu F, Osmundsen P T, Husmo T, 2002. Polyphase kinematics and geochronology of the Kollstraumen detachment, north-central Norway. Norwegian Journal of Geology, 82, 299–316.

Nordgulen Ø, Braathen A, 2005. Structural investigations of deformation zones (ductile shear zones and faults) around Forsmark – a pilot study. SKB P-05-183, Svensk Kärnbränslehantering AB.

Osmundsen P T, Braathen A, Nordgulen Ø, Roberts D, Meyer G B, Eide E A, 2003. The Nesna shear zone and adjacent gneiss-cored culminations, North-central Norwegian Caledonides. Journal of the Geological Society, London 160*,* 1–14.

Petit J P, 1987. Criteria for the sense of movement on fault surfaces in brittle rocks. Journal of Structural Geology 9, 597–608.

Sandström B, Savolainen M, Tullborg E-L, 2004. Fracture mineralogy. Results from fracture minerals and wall rock alteration in boreholes KFM01A, KFM02A, KFM03A and KFM03B. Forsmark site investigation SKB P-04-149, Svensk Kärnbränslehantering AB, 93pp.

Sandström B, Tullborg E-L, 2005. Fracture mineralogy. Results from fracture minerals and wall rock alteration in boreholes KFM01B, KFM04A, KFM05A and KFM06A. SKB P-05-197, Svensk Kärnbränslehantering AB, 151pp.

SKB 2004. Preliminary site description Forsmark area – version 1.1. SKB R-04-15, Svensk Kärnbränslehantering AB.

SKB 2005. Preliminary site description Forsmark area – version 1.2. SKB R-05-18, Svensk Kärnbränslehantering AB.

Twiss R J, Moores E M, 1992. Structural geology. W.H. Freeman & Company, New York, 592 pp.

Appendix 1

List of investigated field localities.

ID	North	East
PFM007085	6700080	1631010
PFM007086	6697398	1631527
PFM007087	6697344	1631571
PFM007088	6697245	1631597
PFM007089	6697272	1631572
PFM007090	6697396	1631520
PFM007091	6697534	1631404
PFM007092	6697791	1631080
PFM007093	6698000	1631040
PFM007094	6698143	1630946
PFM007095	6697997	1631053
PFM007096	6699360	1634355
PFM007097	6700200	1631060

List of samples collected in possible deformation zones.

ID	Adjusted secup	Possible DZ	Samples
KFM01B	23.15	DZ1	Epdote-cemented fractures/breccia
KFM01B	418.5	DZ3	Calcite-cemented breccia
KFM02A	516.0	DZ6	Epidote-filled fractures
KFM04A	212.0	DZ2	Laumontite-sealed breccia
KFM04A	244.1	DZ3	Chlorite-filled fracture cut by laumontite network
KFM04A	407.4	DZ4	Chlorite-rich cataclasite
KFM04A	419.2	DZ4	Calcite-cemented breccia post-date laumontite
KFM05A	419.8	DZ2	Fractured pegmatie with breccia/cataclasite
KFM06A	220.1	DZ2	Fractures with laumontite + calcite
KFM06A	234.8	DZ2	Fine-grained black fault product in pegmatite
KFM06A	262.2	DZ3	Chlorite-filled breccia
KFM06A	330.9	DZ4	Laumontite-cemented breccia with chlorite
KFM06A	794.4	DZ8	Laumontite-sealed fracture network
KFM06A	927.3	DZ10	Laumontite-cemented fault breccia
KFM07A	817.7	DZ4	Fractures in metagranodiorite
KFM07A	875.44	DZ4	Cataclasite
KFM07A	876.4	DZ4	Cataclasite
KFM07A	969.9	DZ4	Reddish brown cataclasite
KFM07A	974.7	DZ4	Fine-grained (ultra-)cataclasite
KFM08A	258.2	DZ1	Cemented fractures in amphibolite
KFM08A	335.5	DZ1	Metagranite cut by 3–4 cm wide fault
KFM08A	940.38	DZ6	Cemented fractures in metagranitoid
KFM08B	182.5	DZ2	Fault in amphibolite cemented by laumontite + calcite